国际木材解剖学家协会（IAWA）中国分会

第七届学术研讨会

The Seventh Annual Meeting of International Association of Wood Anatomists (IAWA) China Group

论

文

摘

要

浙江　杭州　临安

2020 年 11 月 28 日-29 日

目 录

西双版纳地区红椿（Toona ciliata）的径向生长和形成层活动动态研究

Arisa Kaewmano[1,2]　付培立[1]　范泽鑫[1,3]

（1 中国科学院西双版纳热带植物园热带森林生态学重点实验室

2 中国科学院大学生命科学学院；

3 中国科学院核心植物园植物生态中心）

摘 要：热带森林是全球碳循环的重要组成组分，研究热带森林的径向生长动态及其对环境因子的响应有助于预测未来气候变化对热带森林和全球碳循环的影响。西双版纳位于亚洲热带北缘，该区域的植物对气候变化的响应尤为敏感。该文利用生长仪和微树芯的方法对比了该区域土壤水分条件迥异的热带季节雨林和热带喀斯特森林中红椿 2018–2019 年径向生长动态。研究发现红椿形成层活动开始时间为 12 月份到次年的 1 月份，生长结束时间为 10 月–12 月。热带季节雨林的红椿在 2018 和 2019 年的径向生长量均高于喀斯特森林。红椿的径向生长速率与日均降水量呈显著的负相关关系，而与饱和水汽压差呈负相关关系。相关的结果还在进一步的分析当中。

关键词：红椿；径向生长；形成层活动；热带森林

Seasonal radial growth of *Toona ciliata* from tropical forests with contrasting soil water status in Xishuangbanna, SW China

Arisa Kaewmano[1,2]　Pei-Li Fu[1]　Ze-Xin Fan[1,3]

(1 CAS Key Laboratory of Tropical Forest Ecology, Xishuangbanna Tropical Botanical Garden, Chinese Academy of Sciences;

2 Department of Life Sciences, University of Chinese Academy of Sciences; 3 Center for Plant Ecology, Core Botanical Gardens, Chinese Academy of Sciences)

Abstract Tropical forest is a crucial component of the global carbon cycle. Understanding the seasonal radial growth pattern of tropical tree species is important to predict the impact of climate change on tropical forest and global carbon cycle. Xishuangbanan is located at the northern margin of Asian tropical region, and the forests therein are very sensitive to climate change. We monitored the seasonal radial growth of *Toona ciliata* by using both dendrometer and micro core sampling from a tropical karst forest (dry forest) and a tropical seasonal forest (wet forest) in Xishuangbanna for continuously two years (2018-2019). We found that the cambial of *T. ciliata* started to be active during December to next January, and the cell wall thickening ended during October to December. The radial growth rate of *T. ciliata* in rainforest was significantly higher than that of karst forest. The radial growth rate of *T. ciliata* was negatively correlated with VPD and positively correlated with precipitation.

Keywords： *Toona ciliata*, radial growth, cambial activity, tropical forest

祁连圆柏径向生长对极端气候事件的响应

张军周[1,2]，M. Ross Alexander[2]，勾晓华[1]，Annie Deslauriers[3]，Patrick Fonti[4]，张芬[1]，Neil Pederson[2]

（1 兰州大学资源环境学院西部环境教育部重点实验室，甘肃，兰州；

2 Harvard Forest, Harvard University, Petersham, MA, USA;

3 Département des Sciences Fondamentales, Université du Québec à Chicoutimi, Chicoutimi, QC, Canada;

4 WSL Swiss Federal Research Institute, Landscape Dynamics, Birmensdorf, Switzerland）

在气候变化背景下，明确树木径向生长对极端气候的响应对于评估气候变化对树木生长的影响具有重要意义。基于木材解剖的树木形成层活动及径向生长监测研究能够精确确定树木径向生长各阶段发生的时间，是明确极端气候事件对树木径向生长影响的重要手段。通过连续采集微树芯（microcores），我们对分布于青藏高原东北部的 5 棵祁连圆柏的径向生长进行了连续 6 年（2011-2016）的监测研究，并重点关注了 2016 年生长季末期极端气候事件对树木径向生长的影响。监测结果显示，不同于 2011-2015 年，在 2016 年生长季末期有 3 棵监测树木的径向生长出现了年内密度波动（intra-annual density fluctuation，IADF，即伪轮现象）。为了确定 IADF 在祁连圆柏种群中的发生频率，我们在监测树木的周围随机选择了 50 棵树进行了树轮样芯的采集，发现多达 32 棵祁连圆柏在 2016 年的年轮中形成了 IADF。同步的气象观测结果显示，不同于前 5 年，2016 年 8 月初发生了连续 16 天的无降水事件，导致土壤湿度快速下降。但随后的 38 天，恢复的降水使 2016 年 8-9 月的降水高于前 5 年的同期水平，同时保持着比前 5 年更高的温度（直到 9 月 19 日才低于祁连圆柏形成层活动的阈值温度）。

因此，我们认为 8 月中旬干旱事件及其之后的降水恢复以及依然适宜的温度等这一系列极端气候事件导致了 64%的树木发生了 IADF 现象，并使生长季比前 5 年延长了一个多月，额外产生了 17%的径向生物量。

本研究表明，祁连圆柏的径向生长具有非凡的弹性和恢复力，以适应青藏高原寒冷干旱的极端环境。

同质园针叶树木质部特征对干旱的响应差异为树种的选择提供了线索

黄溦溦 [1,2], Patrick Fonti[3], Sven-Olof Lundqvist[4], Jørgen Bo Larsen[2], Jon Kehlet Hansen[2], Lisbeth G. Thygesen[2]

[1] Bamboo Research Institute, Nanjing Forestry University, Nanjing 210037, China

[2] Department of Geosciences and Natural Resource Management, The University of Copenhagen, Rolighedsvej 23, DK-1958 Frederiksberg C, Denmark

[3] Swiss Federal Institute for Forest, Snow and Landscape Research WSL, Zürcherstrasse 111, CH-8903 Birmensdorf, Switzerland

[4] IIC, Rosenlundsgatan 48B, SE-118 63 Stockholm, Sweden

Presenter email: huangww36@gmail.com

气候变化对木质部性状和木材特性起着重要的作用，但是人们对夏季干旱和高温如何长期影响丹麦人工针叶林木质部特征知之甚少。

为了调查不同树种对气候变化（尤其是夏季干旱）的响应方式，我们阐述了丹麦同质园中 6 种外来针叶树种的木质部可塑性。我们分析了受干旱指数和温度影响的木质部功能性状（即管饱壁厚度和管腔面积）以及与材料利用相关的木材特性（密度、硬度和微纤丝角）。

结果表明，木质部性状对夏季干旱（7 月和 8 月）的响应要强于温度，特别是对于生长季后期形成的木质部细胞。其中日本落叶松（*Larix kaempferi* (Lamb.) Carr.）、挪威云杉（*Picea abies* (L.) Karst.）、北美云杉（*Picea sitchensis* (Bong.) Carr.）和冷杉（*Abies alba* Mill.）的气候响应更加强烈，在干旱的夏季它们形成了具有较小内腔和较厚细胞壁的木质部细胞，并且形成具有较高密度、较高硬度和较低微纤丝角的木材。相比之下，欧洲花旗松（*Pseudotsuga menziesii* (Mirb.) Franco）、其次是巨冷杉（*Abies grandis* Lindl.）的木质部显示出更强的抗旱能力，且木质部性状中的气候信号不明显。

本研究比较了在相同条件下生长的不同树种对气候变化的木质部响应。结果表明不同树种在木质部解剖特征和木材特性上的响应不同。据预测，欧洲花旗松的木质部受夏季干旱的影响最小，同时该物种在气候变化下仅显示出年轮宽度的微小变化。

Intra-ring xylem traits responses to drought in conifer common garden hints for species selection

Weiwei Huang[1,2], Patrick Fonti[3], Sven-Olof Lundqvist[4], Jørgen Bo Larsen[2], Jon Kehlet Hansen[2], Lisbeth G. Thygesen[2]

[1] Bamboo Research Institute, Nanjing Forestry University, Nanjing 210037, China

[2] Department of Geosciences and Natural Resource Management, The University of Copenhagen, Rolighedsvej 23, DK-1958 Frederiksberg C, Denmark

[3] Swiss Federal Institute for Forest, Snow and Landscape Research WSL, Zürcherstrasse 111, CH-8903 Birmensdorf, Switzerland

[4] IIC, Rosenlundsgatan 48B, SE-118 63 Stockholm, Sweden

Presenter email: huangww36@gmail.com

The long-term impacts of summer drought and high temperatures on xylem traits of conifers grown in Denmark are scarcely investigated, even though these traits can play an important role in determining xylem functional performance and wood properties under the ongoing climate change.

To investigate how different species are expected to react to climate change, especially summer drought, we elucidated the xylem plasticity of six non-native conifer species from a Danish common garden covering the period 1967-2012. We considered xylem functional traits (i.e. tracheid wall thickness and lumen area) as well as wood properties relevant for utilisation of the material (density, stiffness and microfibril angle) as affected by drought index and temperature.

Results showed that xylem traits responded stronger to summer drought (July and August) than temperature, especially for the part of the ring produced later in the season. The response was stronger for *L. kaempferi*, *P. abies*, *P. sitchensis* and *A. alba*, which formed latewood tracheids with smaller lumen and thicker radial walls, and wood characterised by higher density, higher stiffness and lower microfibril angle. In contrast, *P. menziesii*, and to some extent *A. grandis* showed more drought resistant wood formation with non-significant climatic signal in their xylem traits.

This study comparing the xylem responses of trees growing under the same conditions indicates different anatomical and structural impact among species, whereby the xylem of *P. menziesii* is predicted to be least affected by summer drought of the species considered. This species was already predicted to show only minor changes in growth ring width under climate change.

使用卷积神经网络对木材三切面显微图像进行分类

何鑫[1] 林启招[2] 孙永科[1] 邱坚[2,*]

（1 西南林业大学大数据与智能工程学院；2* 西南林业大学材料科学与工程学院）

摘要：目前木材鉴定主要的方法是制作木材样本三切面(横切面、径切面、弦切面)的染色光学显微图像，再根据 IAWA 阔叶材或针叶材解剖标准进行解剖特征的识别，目前识别过程主要依靠知识丰富的专家人工完成。为实现基于机器视觉的全自动机器判别解剖特征，对三切面图像的分类是一个重要的基础工作。本文对 4 个卷积神经网络算法在三切面图像分类任务进行了评估。制作了包含东南亚 5 属 114 科 600 个树种的 1800 张三切面解剖图像的分类数据集。为降低小数据集对分类网络的影响，按照 60%，20%，20%的比例对三个目录的数据进行训练集、验证集、测试集划分。在训练的过程中，采用旋转、扭曲等 5 种方法对数据集进行了动态增强，获得 7200 张训练数据集。接下来选取了最具代表性的经典卷积神经网络(包括 VGG16、ResNet50、InceptonV3、DensNet121)基于 imagenet 权重进行了迁移训练，结果发现每种网络都能较好拟合了三切面分类数据，其中 DensNet121 分类效果最好，在训练集上达到 99.7%的准确率，接下来 VGG16 达到 97.8%，InceptionV3 达到 95.8%，最低是深度参差网络 ResNet50，在训练准确率 82.5%。并用模型在测试集上进行了测试验证，从预测精度、f1 得分、召回率、混淆矩阵几方面进行了模型评价。最后得出结论：解决木材鉴定中解剖特征图像分裂的智能识别问题，即使是采用未包含木材解剖图像的数据集，进行卷积神经网络迁移训练是可行的。为采用卷积神经网络模型实现实验室智能化木材鉴定、珍稀濒危树种保护、木材区块链溯源等方面打下理论和应用基础。

关键词: 木材解剖；三切面；机器视觉；卷积神经网络；木材数据集

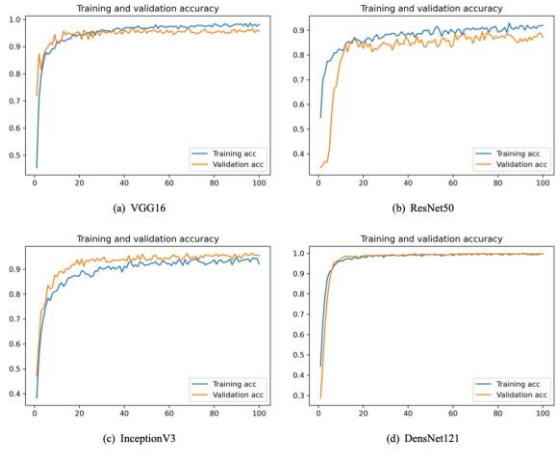

图1 训练集准确率

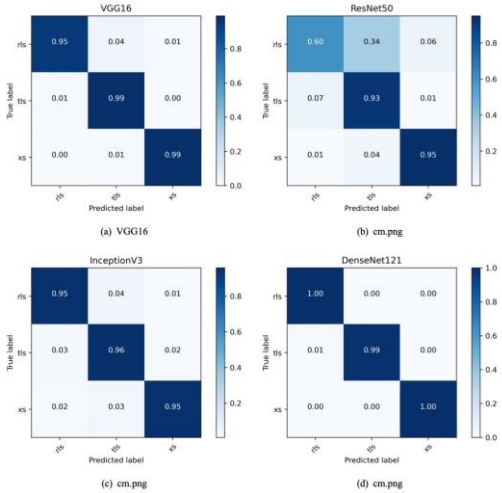

图2 验证混淆矩阵

iWood:木材标本数字化及树种智能识别系统

何拓[1,2]，刘守佳[1,2]，陆杨[1,2]，焦立超[1,2]，郭娟[1,2]，姜笑梅[1,2]，殷亚方[1,2]

（1 中国林业科学研究院木材工业研究所 北京 100091；2 中国林业科学研究院木材标本馆 北京 100091）

摘要：全球约有 180 个木材标本馆，收藏木材标本超过 150 万份，大量的木材标本包含了木材树种的原始地理分布及其分布环境随时间变化的大尺度、可证实的信息。木材标本信息的数字化涉及标本各方面数据的获取、存储、分析和利用，是木材标本馆未来充分发挥其作用的必然趋势。木材标本信息中的图像数据包含了极其丰富的木材构造特征，是木材树种分类的重要依据。为了提高木材标本数字化水平以及树种识别效率，本研究研发了木材构造特征图像采集装置，开发了包含图像采集、图像管理、算法模型和树种识别等功能的智能软件 iWood，为木材标本及其组织切片的数字化提供了硬件和软件支撑，为木材树种在不同场景下的精准快速识别提供新的途径。木材标本数字化及树种智能识别系统研建，为木材信息学研究奠定重要数据基础。

关键词：木材标本，木材构造特征，数字化，树种识别，木材信息学

致谢：感谢中央公益性科研院所基本科研业务专项资金重点项目“木材标本馆升级”（CAFYBB2016MC001）和国家林业和草原局濒危物种行业监管项目“濒危珍稀黄檀属与紫檀属木材识别技术研究”（2020070306）对本项目研究的资助。

iWood: an intelligent system for wood specimens digitalization and wood species identification

He Tuo[1,2], Liu Shoujia[1,2], Jiao Lichao[1,2], Guo Juan[1,2], Jiang Xiaomei[1,2], Yin Yafang[1,2]

1. Research Institute of Wood Industry, Chinese Academy of Forestry, Beijing, 100091

2. Wood Collections of Chinese Academy of Forestry, Beijing, 100091

Abstract: There are approximately 180 wood herbarium collections with more than 1.5 million wood specimens around the world, and a large number of wood specimens contain large-scale, verifiable information on the original geographical distribution of wood species and their distribution environment changes over time. Digitization of wood specimens will be an inevitable trend for xylaria to give full play to its role, which involves the acquisition, storage, analysis and utilization of data from all aspects of the specimen. Among them, the image data of wood specimens contain abundant anatomical features of wood, which is an important scientific basis for wood species identification. In order to improve the efficiency of wood specimen digitalization and wood species identification, this study invented an image acquisition device to collect anatomical images of wood, developed a software i.e. iWood, for image capture, image dataset curation, deep learning models configuration and wood species identification, which will provide technical support for digitalization of wood specimens and their anatomical slides and a new approach to identify wood species accurately and quickly in various scenarios. The intelligent system for wood specimens digitalization and wood species identification will lay the data foundation for wood informatics research.

Keywords: wood specimens, wood anatomical structure, digitalization, species identification, wood informatics

Acknowledgement: This work was financially supported by the projects of Chinese Academy of Forestry (CAFYBB2017ZE003) and National Forestry and Grassland Administration (2020070306).

南方红豆杉鉴定方法的研究

尹文秀[1,2]，张明哲[2]

（1. 浙江农林大学；2. 浙江省检验检疫科学技术研究院）

摘 要： 本研究对南方红豆杉(*Taxus wallichiana* var. *mairei)*、东北红豆杉(*Taxus cuspidata*)、曼地亚红豆杉(*Taxus* × *Media*)、欧洲红豆杉(*Taxus baccata*)、密叶红豆杉(*Taxus fuana*)、喜马拉雅红豆杉(*Taxus wallichiana*)和红豆杉(*Taxus wallichiana* var. *chinensis*)7 种红豆杉属植物的 ITS 序列进行 PCR 扩增和测序，并通过 DNAMAN 软件筛选出多态性位点，设计出南方红豆杉特异性引物和探针。实时荧光定量 PCR 实验表明，该引物探针能特异性扩增南方红豆杉和喜马拉雅红豆杉，且检测灵敏度可以达到 0.001ng/μL，是一种快速、灵敏的鉴定方法。

关键词：南方红豆杉；实时荧光 PCR；ITS；物种鉴定

Identification methods of *Taxus wallichiana* var. *mairei*

Yin Wenxiu[1,2],Zhang Mingzhe

（1.ZhengJing A&F University；2.Zhejiang Academy of Science and Technology for Inspection and Quarantine, Hangzhou 310016, China）

Abstract: In this study，the ITS gene of 7 *Taxus* species(*Taxus wallichiana* var. *mairei*，*Taxus cuspidata*，*Taxus* × *Media*，*Taxus baccata*，*Taxus fuana*，*Taxus wallichiana* and *Taxus wallichiana* var. *chinensis*) were amplified and sequenced. Polymorphic loci were screened by DNAMAN software and specific primers and probes were designed for *Taxus wallichiana* var. *mairei*. The Real-time PCR test showed that the primer and probe can specifically amplify *Taxus chinensis* var. *mairei* and *Taxus wallichiana* ,and the sensitivity can reach 0.001ng/L. It is a sensitive method to identify *Taxus chinensis* var. *mairei* rapidly.

Key words :*Taxus wallichiana* var. *mairei*; Real-time PCR; ITS; species identification.

鞋木和圆盘豆木材解剖学特征研究

于朝阳，胡进波*，苌姗姗，徐东年，刘元

（中南林业科技大学材料科学与工程学院，湖南长沙 410004）

摘要：以产自非洲加蓬具有翼状轴向薄壁组织的含羞草科的圆盘豆（*Cylicodiscus gabunensis*）和苏木科的鞋木（*Berlinia bracteosa*）为研究对象，利用体视显微镜和生物显微镜对两种非洲阔叶材宏观特征、微观构造、纤维形态进行观察和测量分析。结果表明，圆盘豆和鞋木两种木材在构造特征上有诸多相似之处：心边材区别明显；管孔均呈分散型分布，单管孔及径列复管孔（2~3 个），管孔内常含树胶，管间纹孔式互列，导管与射线间纹孔式类似管间纹孔式；都含有丰富的轴向薄壁组织，且呈翼状分布；木射线非叠生；具有中等偏长的纤维。两种木材构造特征也存在差异：圆盘豆心材金黄褐色略带绿色调，具深色细条纹，边材浅粉红色，生长轮不明显；鞋木心材浅红棕色至深红棕色，带有暗紫色或棕色条纹，生长轮明显。圆盘豆木射线 3~7 根/mm，但局部有时呈斜列，多列射线宽 2~4 细胞，高 6~27（多为 15~20）细胞，射线组织同形多列，射线细胞多列部分多为圆形及卵圆形，细胞内树胶丰富。鞋木木射线明显比圆盘豆木射线窄，3~6 根/mm，单列射线占绝大多数，高 5~12 个细胞，2 列射线少，高 10~22 细胞，射线组织同行单列及多列，异形 III 型次之，射线细胞内含菱形晶体。圆盘豆平均纤维长 1579.74μm，宽 26.74μm，长宽比为 59.52，纤维壁腔比为 0.32，单纹孔略具狭缘，分隔木纤维未见；鞋木平均纤维长 1418.27μm，宽 21.75μm，长宽比为 65.91，纤维壁腔比为 0.68，纤维壁较厚，具缘纹孔明显。通过分析圆盘豆和鞋木两种非洲阔叶材解剖学特征，期望为非洲阔叶材的加工利用提供理论基础，同时为进口材种鉴定、商家选材、合理用材提供理论依据。

关键词：含羞草科；苏木科；轴向薄壁组织；纤维形态；微观构造

Wood anatomy characteristics of *Cylicodiscus gabunensis* and *Berlinia bracteosa*

Zhaoyang YU, Jinbo HU*, Shanshan CHANG, Dongnian XU, Yuan LIU

(College of Material Science and Engineering, Central South University of Forestry and Technology, Changsha 410004, Hunan, China)

Abstract: *Cylicodiscus gabunensis* (Mimosaceae) and *Berlinia bracteosa* (Caesalpiniaceae) from Gabon, Africa, which have many aliform parenchyma were examined. The macroscopic characteristics, microstructure and fiber morphology of two African hardwoods were observed and analyzed by means of stereoscopic zoom microscope and biological microscope. The results showed that wood structures are very similar among the two species of wood. The difference between heartwood and sapwood is obvious, they are almost diffuse-porous, with mainly solitary vessels and radial diagonal multiples (usually 2–3 cells). Vessels are usually filled with gum. Intervessel pits were alternated, the pit of ray-vessels was similar to the vessel. All species have rich axial parenchyma, most of which are aliform parenchyma. Wood rays were non-laminated, and there fiber length were medium to long. There are also differences in the structural characteristics of the two species wood: the heartwood of the *Cylicodiscus gabunensis* is golden brown with slightly green, with dark pinstripes, the sapwood is light pink, and the growth ring was not obvious; The heartwood of *Berlinia bracteosa* was light reddish brown to dark reddish brown. With dark purple or brown stripes, and obvious growth rings. The total number of wood rays per millimeter ranged from 3 to 7 in *Cylicodiscus gabunensis*, sometimes oblique, the width of multiseriate rays ranged from 2 to 4 cells with the mean height ranging from 6 to 27 (mostly 15 to 20) cells. The ray tissue had the same shape and multiple rows, most of which were round or oval of the multiple rows, and the cells usually filled with gum. Wood rays of *Berlinia bracteosa* were obviously narrower than the other, 3~6 roots per millimeter, most of which were uniseriate with the height ranged from 5 to 12 cells, few of which were biseriate rays with the height ranged from 10 to 22 cells. Wood rays are uniseriate and multiseriate, followed by Kribs' types Heterogeneous III, and the ray cells usually contained rhombic crystals. The average fiber length and width of *Cylicodiscus gabunensis* were 1579.74μm and 26.74μm, with the ratio of fiber length to width was 59.52, and fiber wall cavity ratio was 0.32. Single pits have slightly narrow edges, with no septate fibers. The average fiber length and width of *Berlinia bracteosa* were 1418.27μm and 21.75μm, with the ratio of fiber length to width was 65.91, and fiber wall cavity ratio was 0.68. *Berlinia bracteosa* had thicker wall of fiber with obvious marginal pits. By analyzing the anatomical characteristics of *Cylicodiscus gabunensis* and *Berlinia bracteosa*, which were two species African hardwoods. It is expected to provide a theoretical basis for the processing and utilization of African hardwoods, and at the same time provide a theoretical basis for the identification of imported trees, the selection of materials for manufacturer, and the rational use of wood materials.

Keywords: Mimosaceae; Caesalpiniaceae; axial parenchyma; fiber morphology; microstructure

胡桃楸(*Juglans mandshurica*)木质部解剖特征对气候变化的响应

朱良军 [1, 2] 刘曙光 [1] 苑丹阳 [2] 王晓春 [2,*]

（[1] 中南林业科技大学生命科学与技术学院，长沙 410004; [2] 东北林业大学森林生态系统可持续经营教育部重点实验室,哈尔滨 150040;）

摘　要：导管(Vessels)是阔叶树传导水分的重要组织，其大小、数量等特征是植物响应与适应气候变化的重要表征。然而，影响温带森林阔叶树导管特征的主要气候因素目前尚不清楚。本研究结合树木年轮学和木材解剖学方法，探究了东北地区重要阔叶树种胡桃楸(Juglans mandshurica)导管特征的时空分布特征及其影响因素。研究结果表明：胡桃楸为半环孔材，年轮宽度(RW)和导管数量(VN) 随形成层年龄增加有明显的下降趋势，25a 以后下降趋势减弱并逐渐趋于平缓；平均导管面积(MVA)则有明显上升趋势，在前 25a 后几十年微弱上升并趋于平缓；导管面积占比(PC)则随形成层年龄增长有逐渐上升的趋势，无存在明显的转折点；TVA 随形成层年龄增加有相对较弱下降趋势。RW 与 VN 显著正相关，与 PC 呈负相关，与 MVA 相关较弱。TVA 主要有 VN 决定而不是 MVA。研究区西南部胡桃楸 VN 和 PC 相对较高,可能与该区暖干的气候有关。胡桃楸径向生长和导管特征主要受温度控制，尤其是前一年生长季温度。胡桃楸 RW、VN 和 TVA 受前一年生长季温度的影响较弱，而 PC 和 MVA 受前一年生长季均温影响较大，研究区北部表现更为明显。研究区西南部胡桃楸 MVA 与当年生长季湿度显著正相关，东北部胡桃楸 PC 与当年生长季湿度显著负相关。导管特征相比传统宽度具有更强的气候代表性，这为我国东北地区的古气候重建提供了新思路。

关键词：导管特征；木质部解剖；胡桃楸；半环孔材；气候响应

染料紫檀与微凹黄檀木材苯醇抽提物及抑菌性能研究

左立转 吕黄飞 岳祥华 曹蕊 徐斌*

（安徽农业大学 林学与园林学院，安徽 合肥 230036）

摘 要：以染料紫檀（*Pterocarpus tinctorius*）和微凹黄檀（*Dalbergia retusa*）心材为原料，选用苯醇抽提法进行抽提得到抽提液，采用滤纸片法研究了其对彩绒革盖菌及密粘褶菌的抑制性能，并运用 GC-MS 对其抽提液进行成分分析，对两者抽提物得率和化学组分以及抑菌性能进行比较研究。结果表明：染料紫檀木材苯醇抽提物含量为 21.21%，颜色呈黄褐色或深黄色；微凹黄檀木材苯醇抽提物含量为 25.47%，颜色接近于黑色；染料紫檀木材苯醇抽提物中分离出 6 类物质，主要组分为烷烃类、醇类、酚类、胺类等物质，其中酚类所占比例最多，为 73.78%，其次是胺类，为 20.98%；微凹黄檀木材苯醇抽提物中分离出 12 种物质，主要有烷烃类、酚类、醇类、酯类、烯类以及芳香族化合物等组分，其中酚类所占比例最多，为 60.18%；两者的苯醇抽提物的抑菌性能在一定的浓度范围表现出了一定的抑菌效果，且对密粘褶菌的抑菌性能均高于对彩绒革盖菌的抑菌性能。

关键词：染料紫檀；微凹黄檀；抽提物；GC-MS；抑菌防腐

刚竹属几种竹材解剖特征比较研究

曹聪 吕黄飞 岳祥华 谢飞 徐斌*

（安徽农业大学 林学与园林学院， 安徽 合肥 230036）

摘要：以刚竹属中篌竹（*Phyllostachys nidularia*）、高节竹（*Phyllostachys prominens*）、假毛竹（*Phyllostachys kwangsiensis*）、早园竹（*Phyllostachys propinqua*）四种竹材为对象，对竹材的解剖特征进行比较研究，结果表明：四种竹材中，纤维长度最长的是假毛竹为 1732.89μm，其次是高节竹为 1626.53μm，纤维宽度均在 13.4μm 左右，纤维长宽比最大的是假毛竹为 130.95，高节竹次之为 120.52。竹子的不同部位的纤维长度、宽度、长宽比有着显著差异，纤维长度集中在 1000～2500μm 之间。四种竹材的维管束密度为 2.43-3.08 个/um,维管束的弦向直径和径向直径分别为 315.59um-578.06um、392.87um-602.75um，弦径比为 0.99-1.75，导管直径为 103.29um-123.66um。

关键词：刚竹属；解剖特征；纤维形态；维管束

Performance and radial variation of wood properties in poplar clones

Yamei Liu[1], Liang Zhou[1], Ying Guan[1], Jianjun Hu[2], Zicheng Zhao[3], Hui Gao[1]*, and Shengquan Liu[1]*

(1. Key Lab of State Forest and Grassland Administration on "Wood Quality Improvement & High Efficient Utilization", School of Forestry & Landscape Architecture, Anhui Agricultural University, Hefei 230036;

2. Research Institute of Forestry, Chinese Academy of Forestry, Beijing 100091; 3. Jiaozuo Academy of Agriculture and Forestry Sciences, Jiaozuo 454001)

Abstract: Wood properties are crucial for the application and development of new clones. In current paper, anatomical and chemical properties were studied in eight new poplar clones (50, Zhonglin46, 108, 36, N179, Danhong, Sangju, and Nanyang) in Henan province, China. This was done to analyze the effects of clones and ages on wood properties and then to select appropriate clones and reasonable rotation age. The results revealed that effects of clones and ages were significant for all wood properties. The poplar clones were ranked as follows in terms of their wood properties: 108, Danghong, and Nangyang > Zhonglin46, 50, and N179 > 36 and Sangju. The quantitative maturity age was between 6-8 years. There was a significant rapid increase and the subsequent reduction or stabilization of ring width, fiber length and diameter, double wall thickness, ray height and width, vessel length and diameter, vessel proportion, fiber proportion, and holocellulose content from the pith to the outer layer. In contrast, the microfibril angle (MFA), vessel frequency, and ray proportion, lignin content, and extractive content initially decreased and subsequently increased or remained relatively constant. All wood properties exhibited turning points across time, with the exception of the double wall thickness and lignin content.

Keywords: poplar, clone, anatomical properties, chemical components, radial variation, rotation age.

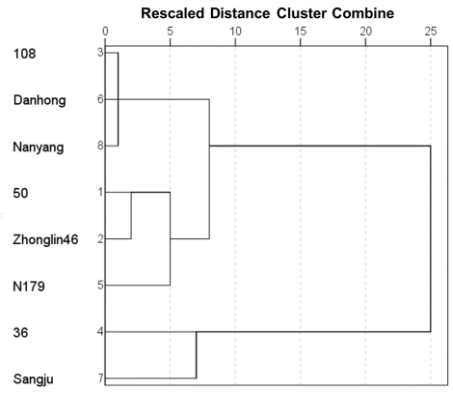

Fig. 1. Dendrogram using average linkage (between groups)

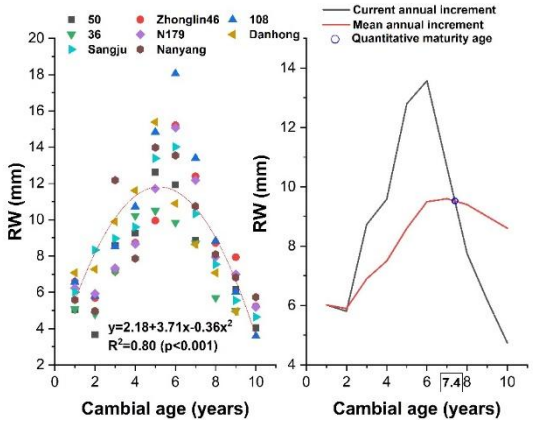

Fig. 2. Average wood ring width in the eight poplar clones versus cambial age. The quantitative maturity age is equal to the intersection point of the current annual increment and mean annual increment curves. RW = ring width.

课题资助：十三五国家重点研发计划课题（2017YFD

福建紫薇（*Lagerstroemia limii*）木材解剖构造研究

张静涵　骆嘉言

（南京林业大学材料科学与工程学院，南京 210037）

摘要：福建紫薇（*Lagerstroemia limii*）是千屈菜科（LYTHRACEAE），紫薇属树种，产于中国福建、江苏、浙江和湖北等地，是中国特有的树种。目前福建紫薇的解剖特征未见报道。本文以取自南京林业大学校园内的福建紫薇木材为研究对象。

宏观下，木材生长轮略可见；散孔材且有半散孔材的趋势；管孔略小，肉眼下不可见，分布不均匀，径列；轴向薄壁组织不丰富，呈带状；木射线极细，肉眼下不可见。未见波痕及胞间道。

通过使用滑走式切片机切片，染色后，用 OLYMPUS BS51 显微镜观察微视情况如下：观察显微特征如下：导管横切面呈圆形及卵圆形；单管孔;径列状排列；平均每平方毫米 40-45 个,最大弦向直径可达 90μm，多数 30—70μm；未见侵填体。单穿孔，穿孔板平行或略倾斜。管间纹孔互列式。木纤维细胞壁薄至厚，具有分隔木纤维。轴向薄壁组织轮界状、切线状以及离管带状，带宽 2-3 个细胞；具有菱形晶体。木射线非叠生；同形单列，高 3—12 细胞或以上。射线-导管间纹孔为同管间纹孔式。未见胞间道。

关键词：木材 福建紫薇 解剖特征

Study on wood anatomical features of *Lagerstroemia limii*

Jinghan Zhang, Jiayan Luo

(college of Materials Science and Engineering, Nanjing Forestry University, Nanjing 210037)

Lagerstroemia limii is a tree from Lagerstroemia of the LYTHRACEAE family, being native to Fujian, Jiangsu, Zhejiang and Hubei, is unique to China. At present, the anatomical structural about *Lagerstroemia limii* were not reported. This article used the *Lagerstroemia limii* wood taken from the Nanjing Forestry University as the research object.

Macroscopic characteristics: Growth ring boundaries indistinct. Wood diffuse to ring-porous or semi-ring-porous. Vessels were slightly smaller, invisible to the naked eye, uneven distribution, radial pattern. Axial parenchyma were not abundant, and their arrangement were marginal bands. The wood rays were extremely thin and invisible to the naked eye. No ripples and intercellular channels were seen.

Slice by using a slide-away microtome, and after staining, observe the microscopic conditions with an OLYMPUS BS51 microscope, the anatomical features are as follows: The shape of vessels in the cross section was round or ovoid; vessels exclusively solitary; the arrangement of vessels was radial pattern; 40-45 vessels per square millimeter, maximum tangential diameter of vessel lumina was 90μm, most 30-70μm; tyloses was not found in vessels. The perforation plates were simple and parallel or slightly inclined. The arrangement of interyessel pits was alternate. Fibers with thin to thick walls, and had separate wood fibers. The arrangement of axial parenchyma were marginal bands, tangent and apotracheal bands with 2-3 cells wide. Rhomboidal crystals frequent in axial parenchyma. Rays homogeneous and storied structural was not found, all exclusively uniseriate and all ray cells procumbent, their heigh were 3-12 cells or more. The vessels-ray pits with distinct borders, similar to intervessels pits in size and shape throughout the ray cell. Intercellular canals were not found.

Keywords: wood *Lagerstroemia limii* anatomical features

杨树立木改性的木材显微构造与微区化学分析

何锐，彭俊懿，夏重阳，刘星，代博仁，石江涛*

（南京林业大学材料科学与工程学院，江苏 南京 210037）

摘 要：速生人工林木材材质较差，对木材进行改性是提高其附加值的必然途径。传统木材改性技术是一种后加工的处理方式，其工序复杂、环境保护性差，而活立木改性作为一种新的探索，可以利用植物自身的蒸腾作用，将改性剂输送至木材各部位中，从而达到木材改性的效果。因此本实验以十年生的意杨活立木为研究对象，采用点滴缓释技术，将改性剂输送到木质部中。改性剂浓度设置为四组：空白对照组（C），1mmol/L 正硅酸乙酯醇溶液（T1）,10mmol/L 正硅酸乙酯醇溶液（T2），100mmol/L 正硅酸乙酯醇溶液（T3）。实验使用显微镜和扫描电镜（SEM）并结合 X 射线能谱（EDS）与 X 射线光电子能谱（XPS）系统地研究了处理前后木材组织的结构和元素组成。研究结果：空白对照组（C）的杨木圆盘心边材区分明显，心材呈灰褐色，边材呈黄白色；立木改性后的杨木圆盘心边材区分不明显，心材呈黄褐色，边材大部分呈黄白色，边材小部分出现黄褐色延伸。立木改性中，木材导管直径变小，导管数量与导管组织比量降低，纤维双壁厚与纤维组织比量增加。正硅酸乙酯浓度为 1mmol/L 时，纤维双壁厚增加幅度最大，新形成木材的纤维平均双壁厚比去年生木材的纤维平均双壁厚多 3.29μm，比空白对照组的纤维平均双壁厚多 0.67μm；导管组织比量下降幅度最大，新形成木材的导管平均组织比量比去年生木材低 19.14%，比空白对照组木材的导管平均组织比量低 15.08%。正硅酸乙酯浓度为 10mmol/L 时，纤维平均组织比量增加幅度最大，新形成木材的纤维平均组织比量比去年生木材的纤维平均组织比量高 17.20%，比空白对照组木材的纤维平均组织比量高 17.77%。正硅酸乙酯浓度为 100mmol/L 时，微纤丝角增加幅度最大，新形成木材的平均微纤丝角比去年生木材的平均微纤丝角大 5.5°，比空白对照组木材的平均微纤丝角大 8.2°。立木改性后，杨木横切面出现黄色内含物，内含物主要存在于木材的导管、纤维、射线中；低浓度下（T1），内含物呈块状并团聚在导管中；较高浓度（T2、T3）下，内含物呈颗粒状并附着在纤维与射线细胞内壁以及纹孔附近。经 EDS 分析，内含物主要元素组成为 C、O、Si、K、Ca；XPS 分析结果表明，改性后新形成木材中检测出 Si 元素。意杨活立木改性后木材结构变得致密，研究结果可以为木材改性以及新型木材制备提供理论基础。

关键词：意杨，活立木改性，正硅酸乙酯，解剖构造，微区化学

The Microstructure and Microchemical Analysis of Modified Poplar Standing Wood

HE Rui，PENG Jun-yi，XIA Chong-yang，LIU Xin，DAI Bo-ren，SHI Jiang-tao

(College of Materials Science and Engineering, Nanjing Forestry University, Nanjing 210037, Jiangsu)

Abstract: Fast-growing plantations have poor wood quality. Modification of wood is a necessary approach to increase its added value.

Traditional wood modification technology is a post-processing method with complex procedures and poor environmental protection. As a new exploration, the modification of living trees can use the transpiration of the plant itself to deliver the modifier to the wood to achieve the effect of wood modification. Therefore, this experiment took ten-year-old Italian poplar living tree as the research object, and used the drip slow-release technology to deliver the modifier to the xylem. The modifier concentration is set to four groups: blank control group (C), 1mmol/L tetraethyl orthosilicate ethanol solution (T1), 10mmol/L tetraethyl orthosilicate ethanol solution (T2), 100mmol/L tetraethyl orthosilicate ethanol solution (T3). The experiment used microscope and scanning electron microscope (SEM) combined with X-ray energy spectroscopy (EDS) and X-ray photoelectron spectroscopy (XPS) to systematically study the structure and element composition of wood tissue before and after treatment. Research results: The sapwood and the heartwood of the poplar disc in the blank control group (C) are clearly distinguished, the heartwood is gray-brown, and the sapwood is yellow-white; The sapwood and the heartwood of the poplar disc after the modification of standing wood are not clearly distinguished, heartwood is grayish brown, most of the sapwood is yellowish white, and a small part of the sapwood is grayish brown extension. In the modification of living tree, the diameter of wood vessel becomes smaller, the vessel quantity and vessel tissue ratio decrease, and the fiber double wall thickness and fiber tissue ratio increase.When the tetraethyl orthosilicate concentration is 1mmol/L, the fiber double wall thickness increases mostly. The fiber average double wall thickness of the newly formed wood is 3.29 μm more than the fiber average double wall thickness of last year's wood, and 0.67 μm more than the fiber average double wall thickness of the blank control group; The ratio of vessel tissue decreased mostly. The average vessel tissue ratio of newly formed wood was 19.14% lower than that of last year's wood and 15.08% lower than that of the blank control wood.When the tetraethyl orthosilicate concentration is 10mmol/L, the average fiber tissue ratio increases the most. The average fiber structure ratio of newly formed wood is 17.20% higher than that of last year's raw wood, and 17.77% higher than that of the blank control wood. When the tetraethyl orthosilicate concentration is 100mmol/L, the microfibril angle increases mostly. The average microfibril angle of newly formed wood is 5.5° larger than the average microfibril angle of last year's wood, and 8.2° larger than that of the blank control wood. After the modification of living tree, yellow inclusions appeared on the cross section of poplar wood, and the inclusions mainly existed in the wood vessels, fibers, and rays; at low concentrations (T1), the inclusions were lumpy and agglomerated in the vessels; At high concentrations (T2, T3), the inclusions are granular and attached to the inner walls of fibers and ray cells and near the pits. After EDS analysis, the main element composition of the inclusions is C, O, Si, K, Ca; XPS analysis results show that Si element is detected in the newly formed wood after modification. The wood structure of Italian poplar becomes dense after living standing wood modification, and the research results can provide a theoretical basis for wood modification and preparation of new types of wood.

Key words: *Populus euramevicana* cv.'I-214'；Modification of living standing trees；TEOS；Anatomical structure；Microzone Chemistry

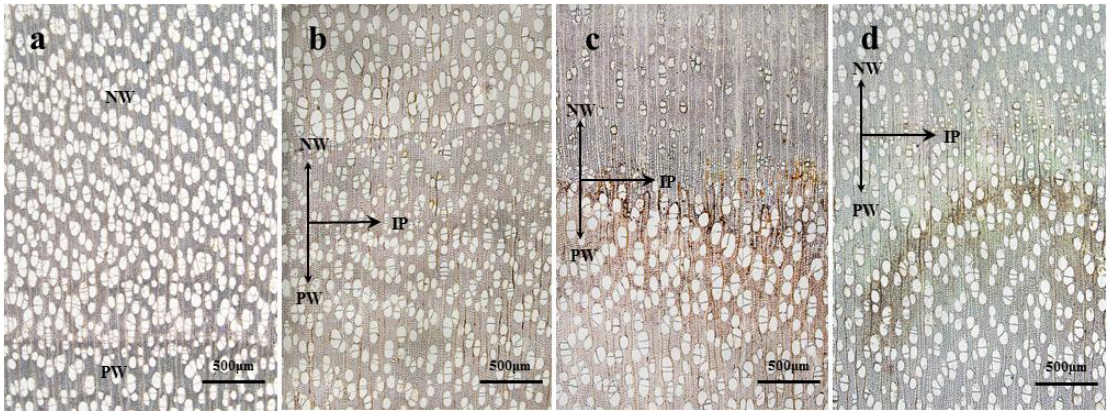

图1 不同处理条件下木材横切面光学图片（4×），新形成木材NW：Newly formed wood，注射点IP：Injection point，往年生木材PW：Previous grown wood.

a：空白对照组（C），**b**：1mmol/L正硅酸乙酯改性处理组（T1），**c**：10mmol/L正硅酸乙酯改性处理组（T2），**d**：100mmol/L正硅酸乙酯改性处理组（T3）

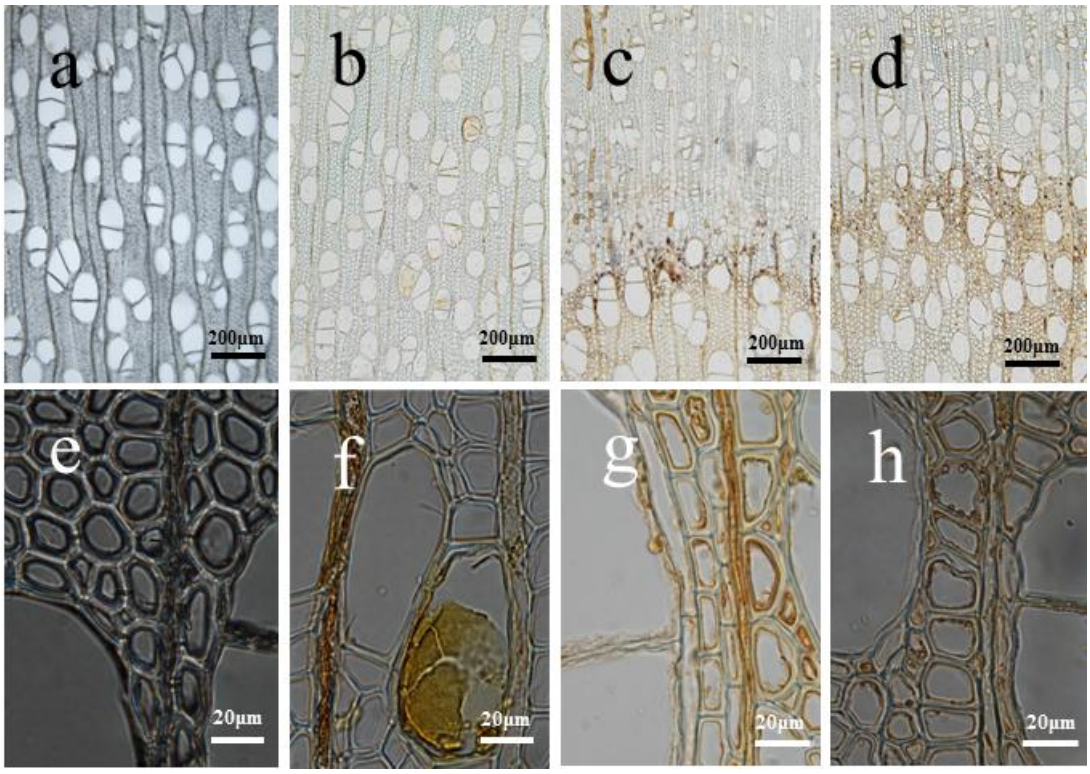

图2 不同处理条件下木材横切面光学图片（10×、100×）

a：空白对照组（C），**b**：1mmol/L正硅酸乙酯改性处理组（T1），**c**：10mmol/L正硅酸乙酯改性处理组（T2），**d**：100mmol/L正硅酸乙酯改性处理组（T3），**e-h**依次为**a-d**的局部放大

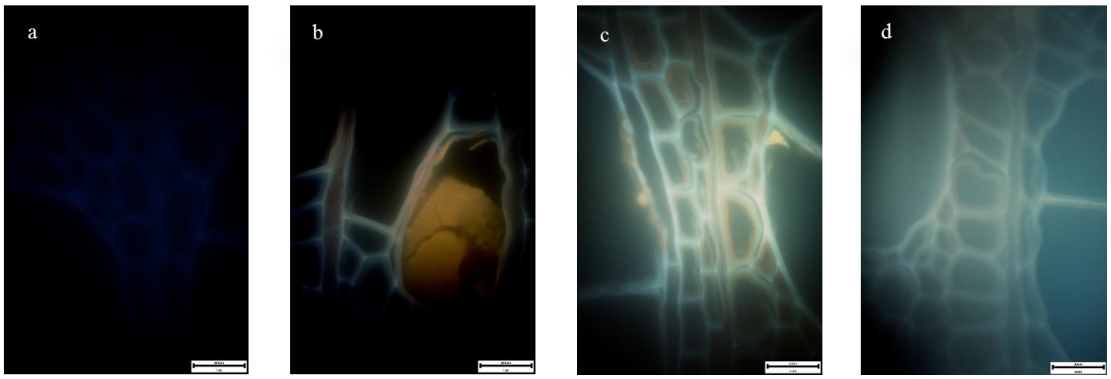

图3 不同处理条件下木材横切面的荧光照片（100×）

a：空白对照组（C），**b**：1mmol/L正硅酸乙酯改性处理组（T1），**c**：10mmol/L正硅酸乙酯改性处理组（T2），**d**：100mmol/L正硅酸乙酯改性处理组（T3）

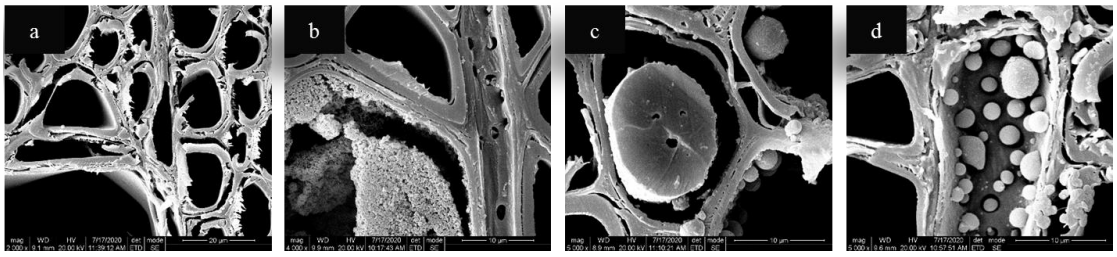

图4 不同处理条件下木材横切面的SEM图片，

a：空白对照组（C），**b**：1mmol/L正硅酸乙酯改性处理组（T1），**c**：10mmol/L正硅酸乙酯改性处理组（T2），**d**：100mmol/L正硅酸乙酯改性处理组（T3）

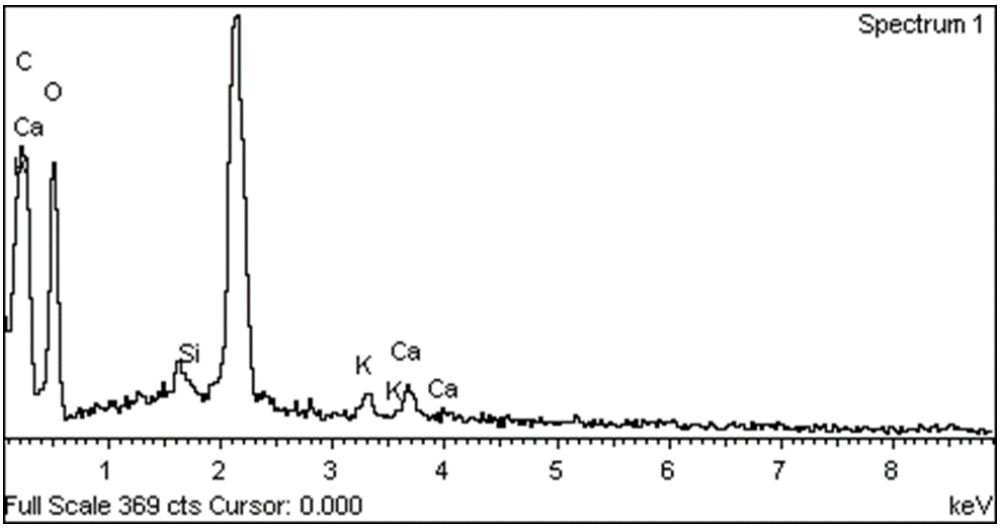

图 5 内含物的 EDS 能谱图

东北东部主要散孔材木质部解剖特征及其对气候变化的响应

苑丹阳[1, 2]

（1 东北林业大学林学院生态研究中心，哈尔滨 150040; 2 东北林业大学森林生态系统可持续经营教育部重点实验室，哈尔滨 150040）

摘要：东北东部山区是我国温带森林的典型分布区域，对维系我国东北乃至整个东北亚地区生态安全至关重要。了解木质部形成与气候的关系是揭示树木对气候变化响应与适应策略的前提，有利于更好地理解宏观生长-气候关系。在气候变暖的大背景下，本研究运用树轮解剖学方法，探究了该区域4个主要散孔材树种木质部解剖特征对气候变化的响应规律，以期为预测该区森林植被动态、生产力与群落演替进程以及准确评估气候变化对森林生态系统影响提供理论基础与科学依据。主要结果如下:

4个散孔材树种无明显早晚材界限，导管大小变化无规则。各树种年轮宽度(RW)与导管数量(NV)及导管总面积(TVA)均显著正相关，与导管面积占比(PC)及导管密度(VD)主要呈负相关。TVA(导水组织大小)大小取决于NV而不是平均导管面积(MVA)，并决定了RW的大小，这也在一定程度上验证了生长过程中的碳水-耦合关系。NV和MVA或MVA与VD的相关性因树种而异，且正负均有。温度对各树种木质部的形成起主要作用，降水次之。降水与各树种年轮宽度呈正相关(尤其是5-7月)，与导管特征主要呈负相关(生长季)；而温度与散孔材(紫椴Tilia amurensis除外)树种RW、NV及TVA主要呈负相关，与MVA、PC及VD均呈正相关。湿度的响应结果与降水类似。部分解剖特征能够记录与传统宽度更强甚至不同的气候信息，这为气候重建提供新思路。快速升温(1980s)后，各树种宏微观生长-气候关系的变化可能与升温所引发的暖干旱现象有关。若气候变暖持续或加剧，相对而言，各散孔材(紫椴除外)对气候变暖的衰退表现的更为明显。东北东部温带森林中主要散孔材树种水力传导的安全性与效率性之间的权衡关系并不明显，其增加MVA和VD，但减少NV的水力策略，导致TVA减少，可能是应对暖干化的后果。

关键词：树木年轮；木质部解剖；散孔材；导管；气候响应

巨紫荆木材解剖构造研究

王明豪 林巧 张静涵 骆嘉言*

（南京林业大学材料科学与工程学院，江苏 南京 210037）

摘要：巨紫荆（*Cercis gigantea*）是豆科（Leguminosae），紫荆属木材，产于湖北、河南、陕西、四川、云南、贵州、广西、广东、湖南、浙江、安徽等省区。生于海拔 600-1900 米的山地疏林或密林中；山谷、路边或岩石上。是集观赏与药用价值于一身的一种优良乡土树种。但目前尚未见对巨紫荆解剖构造的报导。本文以巨紫荆木材为研究对象，材料取自南京林业大学校园内。利用 OLYMPUS SZ2-ILST 体视显微镜观察其宏观构造；使用滑走式切片机切片，利用 OLYMPUS BS51 显微镜观察其微观构造，并利用扫描电镜确定其导管间纹孔的类型。观察特征如下：

（1）宏观下木材有光泽；无特殊气味及滋味。生长轮明显；半环孔材至环孔材。早材管孔通常大，肉眼下可见，常呈单列，有侵填体；晚材管孔多；极小，放大镜下略可见；常埋藏于轴向胞壁组织中呈弦向带或波浪形。轴向薄壁组织发达；宽带状或聚翼状。木射线宽度中，径切面上射线斑纹明显。

（2）微观下导管在横切面上为圆形及卵圆形；单管孔，径列复管孔 2-4 个或以上，管孔团；管孔排列方式为切线状；螺纹加厚明显。穿孔板为单穿孔。管间纹孔式互列，多角形，不具附物纹孔。木纤维细胞壁薄至厚。轴向薄壁组主呈宽带状或聚翼状，稀星散状，并具轮界状；具菱形晶体，分室含晶细胞可连续多至 7 个。木射线非叠生。单列射线数少，宽 10-16 微米；高 5-9 个细胞（68-160 微米）或以上。多列射线宽 2-7 个细胞（22-73 微米），多数 5 个细胞；高 9-37 个细胞（138-567 微米）或以上，多数 15-30 个细胞（254-455 微米）。射线组织异形III型。射线-导管间纹孔式为同管间纹孔式，未见胞间道。

关键词：巨紫荆，宏观构造，微观构造

Study on wood anatomical features of *Cercis gigantea*

Minghao Wang, Qiao Lin, Jinghan Zhang, Jiayan Luo*

(College of Materials Science and Engineering, Nanjing Forestry University, Nanjing,210037, China)

Abstract: *Cercis gigantea* is a tree from the Cercis of the Leguminosae family, being native to Anhui, Guangdong, Guangxi, Guizhou, Henan, Hubei, Hunan, Shaanxi, Sichuan, Yunnan, Zhejiang etc. And grow in open or dense forests, mountain slopes, along valleys near roads, on rocks at the elevation of 600-1900m. It is a kind of better native tree species with ornamental and medicinal value. At present, there is no report on the anatomical feature of *Cercis gigantea*. In this paper, *Cercis gigantea* wood was taken as the research object, and the materials were taken from the campus of Nanjing Forestry University. Macrostructure was observed by OLUMPUS SZ2-ILST stereomicroscope. After slicing by slicing microtome, observation was performed with OLYMPUS BX51 microscope. And the kind of intervessel pits was confirmed by SEM. The structure characteristics are as follows:

Macroscopically, the wood has luster, with no special smell and teste. The growth ring was obvious, from ring-porous to semi-ring-porous material. The early wood pore was usually large, visible to naked eye, often arranged in single row and with thylose. In late wood, the pores were very small, slightly visible under a magnifying glass, and often embedded in the axial parenchyma in the form of wave and band, and the number of it is large. The axial parenchyma was well developed and can be seen by naked eyes, and the type of it was axial parenchyma confluent and banded parenchyma. The wood ray width was middle. The ray speckle is obvious in tangential section.

Microscopically, the shape of vessels in cross section was round or ovoid, the arrangement of vessels was tangential band. Vessels groupings was exclusively solitary, in radial multiples of 2-4 or more and clusters. Helical thickenings were obvious in vessels. The perforation plates were sample. The intervessel pits was alternate, the shape of it was polygonal, and the pits was not vestured pits. The cell wall of fibers was thin to thick. The arrangement of axial parenchyma was confluent, bands more than three cell wide, marginal bands and diffuse, and there were 7 or more rhombic crystals in the parenchyma cells. The wood rays were not storied. The exclusively uniseriate rays were rare, width 10-16μ m, high 5-9 cells (68-160μ m) or more cells. The multi-row rays' width were 2-7 cells (22-73μ m), most were 5 cells, the height of multi-row rays were 9-37 cells(138-567μ m) or more cells, most were 15-30 cells(254-455 μ m). The wood rays was type Ⅲ. The vessel-ray pits with distinct borders; similar to intervessel pits in size and shape throughout the ray cells. The intercellular was not founded.

Keywords: *Cercis gigantea*, Macrostructure, Microstructure

中山杉应压木管胞的分布位置和形态变化

李茜然，毕玉金，潘彪*

（南京林业大学材料科学与工程学院，南京 210037）

【目的】中山杉（*Taxodium* hybrid‘Zhongshanshan’）为落羽杉属(*Taxodium* Rich.)杂交品种，具有早期速生的优良特性，对水淹、干旱、盐碱和大风环境具有一定的适应性。但容易产生应力木是速生材的通病。本试验通过对中山杉应压木的分布及管胞的形态特征进行研究，以期为中山杉应压木对外部环境的响应机制提供理论基础，提高其利用率，为后续加工利用提供理论依据。

【材料与方法】试样 14 年生倾斜生长的中山杉木材，将应压木和对应木木材制作成 12um 切片，使用光学显微镜、荧光显微镜和环境扫描电镜观察应压区的分布和微观解剖特征；使用 Image J 软件测量管胞圆度和双壁厚数据；使用富兰克林离析法解离应压木和对应木管胞，每个试样选取 50 根管胞测定长度，并计算其平均值；使用拉曼成像光谱仪探究应压木和对应木管胞中木质素的微区分布，扫描范围 600-2000cm^{-1}，积分成像范围 1525-1700cm^{-1}。

【结果与分析】1.中山杉应压木管胞的分布：在宏观下可观察到中山杉立木中的应压木分布极不规律，单个生长轮中应压木细胞带分布也较为不规律；在微观下可观察到大多数中山杉在同一生长轮内仅形成一轮应压木（图 1a），偶见在同一生长轮内形成两轮应压木的情况（图 1b）。应压木管胞通常形成于生长轮中部或中后部的早材区，晚材和靠近晚材带的早材管胞不具有应压木管胞特征（图 1c）。

2.中山杉应压木管胞与对应区管胞形态比较：应压区管胞的典型特征具体表现为管胞壁变厚并出现 S2L 层、管胞横截面近似圆形、出现螺纹裂隙和胞间隙、管胞长度变短等。以上特征并不一定在所有应压木管胞中同时呈现。

（1）重度应压木管胞具有高度木质化的细胞壁 S2L 层，轻度应压木管胞的 S2L 层被局限在细胞角隅处，而对应木管胞不具有 S2L 层（图 a2，c2，d2）。

（2）重度应压木管胞呈圆形或卵圆形，圆度值达到 0.778，胞间隙较多；轻度应压木管胞仍具棱角，圆度值为 0.597，胞间隙少；对应区管胞呈现为方形或多边形，无胞间隙。

（3）重度应压木管胞双壁厚平均值达到（10.88±0.18）um，轻度应压木双壁厚为（7.15±0.19）um，对应区管胞双壁厚最薄，仅为（5.94±0.23）um。

（4）重度应压木管胞壁上可观察到明显的螺纹裂隙，与细胞轴夹角呈 33.1~55.0°（图 3 e，f，图 4 a）；轻度应压木管胞中偶可见条纹状的螺纹（图 4 b），对应木管胞内壁未见螺纹裂隙（图 3 g，h，图 4 c）。

（5）应压区管胞的平均长度为（2434.72±32.54）um，长度依次小于应压区起始端早材管胞（2770.09±35.75）um 和对应区早材管胞（3280.12±44.48）um。

3.中山杉应压木中不同区域木质素沉积与管胞形态变化：应压木木质素的分布与对应木不同，具体表现为细胞角隅和复合胞间层的木质素浓度降低，次生壁外层的木质素浓度增高，通常将应压木管胞中高度木质化的次生壁外层称为 S2L 层。综合荧光图片和拉曼成像图分析（如图 2，图 3d2），中山杉对应区和应压区早材均呈多边形，其木质素主要沉积于细胞角隅，复合胞间层的木质素浓度高于次生壁。轻度应压木管胞的木质素的沉积主

要发生在细胞角隅处的次生壁外侧，在 S1 与 S2 层之间具有高度木质化的 S2L 层，管胞棱角明显或略明显，有少量胞间隙，双壁厚度约是正常早材的 1.2 倍，角隅处木质素浓度低于 S2L 层（如图 3 c）。重度应压木管胞的横截面更趋近于圆形，胞间隙多，细胞壁显著增厚，最终细胞壁厚度达到正常早材的 1.8 倍（如图 3a,b）。由此推断，在中山杉应压木管胞的形成过程中，木质素的沉积位置对外部应力的响应比细胞形态更快速。

【结论】中山杉应压木呈带状分布于生长轮中部和中后部的早材区域，生长轮初期的早材和晚材均未见明显的应压木特征。在中山杉应压木管胞的形成初期，大量木质素沉积在次生壁外侧，在管胞棱角处最先形成了 S2L 层，之后 S2L 层逐渐向次生壁四周延伸，最终会形成一层完整的细胞壁 S2L 层。应压木管胞横截面变圆、细胞壁增厚、出现胞间隙和螺纹裂隙等细胞形态的变化要晚于细胞壁 S2L 层的形成。管胞形态是区分应压木与对应木的最显著特征，但对于细胞形态比较相似的轻度应压木管胞和对应木管胞，细胞角隅处 S2L 层的自发荧光是区分两者的唯一明显特征。

关键词：中山杉、应压木、管胞形态、次生壁

The Formation Position and Morphological Changes of Compression wood in Zhongshanshan

Xiran Li, Yujin Bi, Biao Pan

(College of Materials Science and Engineering, Nanjing Forestry university,Nangjing 210037)

Abstract: [objective] As a hybrid species of Taxodium Rich, Zhongshansha is characterized by fast-growing in the early wood and has certain adaptability to water flooding, drought, salinity and strong wind environment. The defect of fast-growing wood is easy to form compression wood. In this experiment, the distribution of compression wood and morphological characteristics of tracheid in Zhongshanshan were studied to provide a theoretical basis for the response mechanism of Zhangshanshan to the external environment and provide a theoretical basis for subsequent processing and utilization.

[Materials and Methods] The sample is a 14-year-old inclined growth of Zhongshanshan. Different regions were observed by optical microscope, fluorescence microscope and environmental scanning electron microscope. The data of roundness and double wall thickness were measured by Image J software. Franklin segregation method was used to isolate the wood to be pressed and the corresponding tracheid, 50 tracheid were selected for each sample to measure the length, and calculate the average value. Raman imaging spectrometer was used to explore the micro region distribution of lignin in compressed wood and opposite wood with a scanning range of 600-2000cm^{-1} and an integral imaging range of 1525-1700cm^{-1}.

[Results and Analysis] 1. Distribution of compression wood tracheid in Zhongshanshan: in macroscopic view, the distribution of compressed wood in Zhongshanshan is very irregular. The distribution of wood - pressing bands in a single growth ring is also irregular. Microscopically, only one round of wood is compressed in one growth wheel (Fig. 1a), and occasionally two rounds of wood are compressed in one growth ring (Fig. 1b). The compressed wood tracheids are usually formed in the early wood area at the middle or middle back of the growth ring. The late wood and the early wood tracheid near the late wood don't have the characteristics of compressed wood tracheid (Fig. 1c).

2. Comparison of the morphology of the compressed tracheid and the corresponding tracheid: the typical characteristics of the compressed wood tracheid are as follows, the cell wall thickened and S2L layer appeared, the tracheid were nearly round in cross section, the cracks and intercellular spaces appeared, and the length of the tracheid became shorter. These characteristics may not be present in all compressible tracheid simultaneously. (1) The severely compression wood has a highly lignified S2L layer of cell wall, while the S2L layer of the lightly compression wood is confined to the corner of the cell. But the opposite wood's tracheid does not have the S2L layer (Fig. a2, c2, d2). (2) The severely compressed wood's cells were round or oval, with roundness value up to 0.778, and there were many intercellular spaces; the slightly compressed wood cells were still angular, roundness value was 0.597, and the cell gap was small. The opposite tracheid are square or polygonal without intercellular spaces. (3) The average double wall thickness of the severely pressed woodshed was (10.88±0.18) um, the average double wall thickness of the lightly compressed wood was (7.15±0.19) um, and the opposite area had the thinnest double wall thickness, only (5.94±0.23)

um. (4) On the cell wall in severe pressure tissues, thread gaps and thread cracks embedded in the inner wall were observed, and the included angle with the cell axis was 33.1~55.0 °(Fig. 3e, f, Fig. 4a). Occasionally striated threads can be seen in the slightly compressed wood (Fig. 4b), and no thread gaps and thread cracks embedded in the inner wall can be seen in the tracheid of the opposite wood (Fig. 3g, h, Fig. 4c). (5) The average length of the tracheid in the compression wood was (2434.72±32.54) um, which was smaller than that of the tracheid in the compression zone (2770.09±35.75) um at the beginning of the compression wood and (3280.12±44.48) um in the opposite wood.

3. Lignin deposition and morphological changes of tracheid during the compaction process of Zhangshanshan: the distribution of lignin in compression wood is different from that in opposite wood. The high lignification of the outer layer of the secondary wall in the compressed tracheid is usually called the S2L layer. Based on the analysis of fluorescence images and Raman imaging (Fig.2, Fig.3d_2), the opposite wood and the early wood in the compression wood of Zhongshanshan are polygonal. Lignin is mainly deposited in the cell corner, and the lignin concentration in the composite intercellular layer is higher than that in the secondary wall. The lignin deposition of slightly compressed tracheid occurred mainly in the lateral secondary wall of the corner of the cell. There is a highly lignified S2L layer between The S1 and S2 layers. The tracheid edges are obvious, with a small amount of intercellular spaces. The thickness of the double walls is about 1.2 times that of the normal early wood, and the lignin concentration at the corner is lower than that of the S2L layer (Fig. 3c).The cross section of the severely pressed wood is more close to round, with more intercellular spaces and significantly thickened cell walls. Finally, the cell wall thickness reaches 1.8 times of the normal early wood (Fig.3a, b). It can be inferred that during the formation of the compressed xylem cells, the response of lignin deposition to external stress is faster than that of cell morphology.

[Conclusion] The compression wood of Zhongshanshan is distributed in the early wood area in the middle and later period in middle of the growth ring in a zonal pattern. There are no obvious characteristics of compression wood in the early and late wood of the growth ring. In the early stage of the formation of the compressed xylem cells, a large amount of lignin was deposited on the outside of the secondary wall, and S2L layer was first formed at the edges of the tracheid, and then the S2L layer gradually extended around the secondary wall, eventually forming a complete S2L layer of the cell wall. The changes of cell morphology, such as roundness of cross section, thickening of cell wall, intercellular space and crevice appeared later than the formation of S2L layer. The morphology of tracheid is the most significant feature to distinguish the wood that should be pressed from the corresponding wood. However, for the slightly compression wood tracheid and opposite wood with similar cell morphology, the spontaneous fluorescence of the S2L layer at the corner of cells is the only obvious feature to distinguish the two.

Key words: Zhongshanshan; Compression wood; Tracheid morphology; Secondary wall

毛竹工艺纤维高温饱和蒸汽-机械分离及其物理力学特性

黄雅茜[1]，袁朱润[1]，石江涛[1]，许斌[1]，王新洲[1*]

（1. 南京林业大学材料科学与工程学院 南京 210037）

摘要：采用高温饱和蒸汽对高含水率新鲜毛竹竹材进行热处理，再通过机械辊轧制备竹材工艺纤维（由多根纤维组成），并运用光学显微、纳米压痕等分析技术研究了提取的工艺纤维的微观结构、化学组分、力学性能及吸湿特性。研究结果表明：高温饱和蒸汽处理可使细胞壁中半纤维发生降解，薄壁细胞由于壁薄更易受到破坏，在机械外力下薄壁细胞和维管束成功分离。纤维细胞壁中无定形物质的降解，木质素相对含量的增加以及纤维素相对结晶度的提高，改善了竹材工艺纤维的吸湿性能和细胞壁力学性能。经过饱和蒸汽处理后，纤维细胞壁的弹性模量和硬度分别增加了 14.7%~29.4%和 14.9%～38.5%。饱和蒸汽处理未对工艺纤维的拉伸性能产生明显影响，分离出的竹材工艺纤维最大拉伸强度和模量分别达到了 765MPa 和 24.8GPa。另外，在不同部位处提取的工艺纤维在性能上存在一定差异：外侧区域分离的工艺纤维尺寸大于内侧，因此在实际应用中可考虑分层提取、分级利用。本文举例分析了竹材工艺纤维对速生木材单板层积材（LVL）力学性能的增强效果，以证明其在工程结构材料中的潜在应用。

关键词：纤维；力学性能；物理性能；化学分析；热处理

基金项目：国家自然科学基金面上项目（31901374）。

通信作者：许斌，博士，副教授，研究方向为竹材加工利用，E-mail: xr9621@njfu.com.cn。

Physical and mechanical properties of bamboo fibers extracted by high-temperature saturated steam and mechanical treatment

HUANG Yaqian[1], YUAN Zhurun[1], SHI Jiangtao[1], XU Bin[1], WANG Xinzhou[1,*]

(1. College of Materials Science and Engineering, Nanjing Forestry University, Nanjing 210037)

Abstract: High-temperature saturated steam was firstly applied to pre-treat fresh moso bamboo (*Phyllostachys pubescens* Mazel ex H. de Lehaie) culms with high moisture content, and then bamboo fibers were extracted from the thermal treated bamboo culms by rolling in this paper. And then the microstructure, chemical composition, mechanical behavior, and hygroscopicproperties of the extracted fibers were analyzed by using optical microscopy, nanoindentation (NI) and so forth. Results indicate that the vascular bundles and parenchymatouscells in bamboo culms has been effectively seperated due to the degradation of hemicellulose after the steam and mechanical treatment. The degradation of hemicelluloses, increaed relative lignin content and cellulose crystallinity (C_rI) upon thermal treatment make a major contribution to the reduced hygroscopicity and increase of reduced elastic modulus (E_r) and hardness (H) of fiber cell walls. The maximum tensile strength and modulus of bamboo fibers are 765MPa and 24.8GPa, respectively, which is not obviously affected by steam treatment. However, there are some differences in the properties of bamboo fibers extracted from different parts in bamboo culms. The dimensions of fibers from outerlayer are larger than that of inner layer. Thus, multilayer extraction and classifiedutilization of bamboo fibers should be considered in its potential application. The bending properties of BFB reinforced laminated veneer lumber (LVL) was further analyzed to verify the potential application of BFB in engineered composites.

Keywords: fibres; mechanical properties; physical properties; chemical analysis; heat treatment

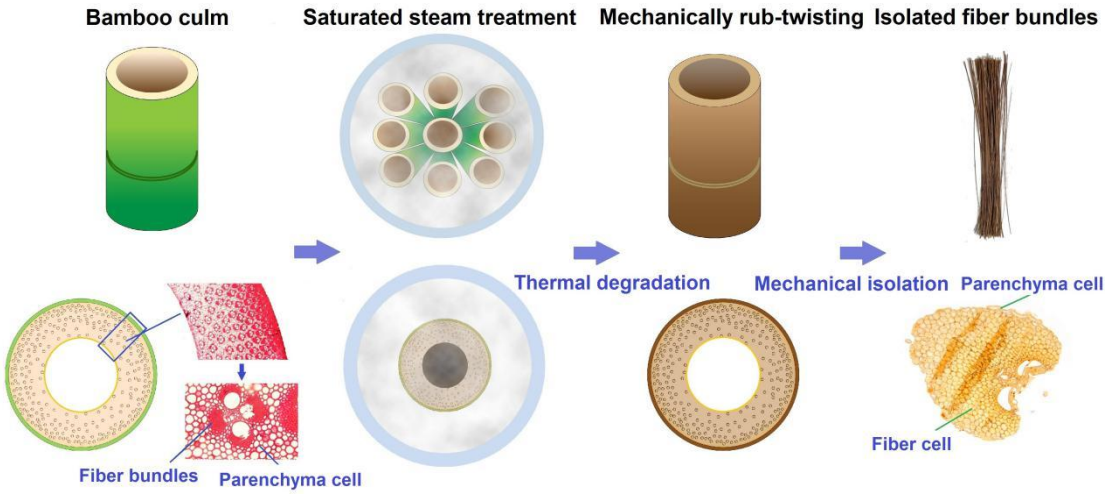

图 1 竹材工艺纤维制备及性能研究示意图

Fig. 1 Schematic diagram showing the extraction of fibers from bamboo culms and characterization of bamboo fibers

不同预处理程度及热压条件下的密实化木材的性能研究

蒯炳斌[1]，张耀丽[1]

（南京林业大学材料科学与工程学院，南京 210037）

摘 要: 木材密实化是一种能够在短时间内有效提高木材力学性能的技术，将木材通过预处理后机械压缩变形，以减少细胞腔的体积，从而提高木材的密度。然而，无论哪种压缩木材的方法，为了获得更好的压缩效果，都需要在压缩木材之前对木材进行软化，软化的过程即为预处理。为了充分利用天然木材资源，本研究使用 $NaOH/Na_2SO_3$ 溶液将木材进行脱木素处理，控制脱木素处理的时间，并调整热压工艺，经机械热压与固定，制得强度高、密度大和尺寸稳定性好的密实化木材可以更好的应用建筑与装饰领域。

本实验使用扫描电镜观察了木材的微观形貌，并且使用美国 NREL 法测定木材的木质素含量，图像表明木材经过 10h 的脱木素处理，木质素含量为 16%，此时通过观察发现密实化后的木材横切面管孔之间几乎完全密实，且排列整齐规则;经过热压机热压处理的木材密度达到 1.202 g/cm3，此时的物理机械性能得到了显著提高，弯曲强度和弹性模量比天然木材分别提高了约 101%和 75%;通过实验对比，木材的尺寸稳定性相比较未处理的木材得到了很大的提升。不过在预处理时间大于 10h 之后，木材的各项性能出现小幅下降。但是这并不影响木材各项性能相较于天然木材有较好的提升与应用。

关键词： 密实化，木质素，$NaOH/Na_2SO_3$ 预处理，尺寸稳定性

Study on the performance of densified wood under different pretreatment degree and hot pressing conditions

Wood densification is a technology that can effectively improve the mechanical properties of wood in a short time. The wood is mechanically compressed and deformed after pretreatment to reduce the volume of the cell cavity, thereby increasing the density of the wood. However, no matter which method of compressing wood, in order to obtain a better compression effect, it is necessary to soften the wood before compressing the wood, and the process of softening is pretreatment. In order to make full use of natural wood resources, this study uses NaOH/NaSO3 solution to delignify the wood, control the time of delignification, and adjust the hot pressing process. After mechanical hot pressing and fixing, the wood has high strength, high density and density. Densified wood with good dimensional stability can be better used in construction and decoration fields.

In this experiment, the microscopic morphology of the wood was observed by scanning electron microscope, and the lignin content of the wood was measured by the American NREL method. The image shows that the wood has been delignified for 10 hours, and the lignin content is 16%. At this time, the compaction is found through observation The pipe holes on the cross-section of the wood are almost completely dense, and the arrangement is neat and regular; the density of the wood after the heat pressing treatment reaches 1.202 g/cm^3, at this time the physical and mechanical properties have been significantly improved, the bending strength and elastic modulus The amount is about 101% and 75% higher than that of natural wood. Through experimental comparison, the dimensional stability of wood has been greatly improved compared with untreated wood. However, after the pretreatment time is greater than 10h, the properties of the wood show a slight decline. But this does not affect the performance of wood compared with natural wood has better improvement and application.

Keywords: densification, lignin, NaOH/Na_2SO_3 pretreatment, dimensional stability

一种毛竹纤维组织比量径向分布规律的研究方法*

徐皓诚[1]　黎静[1,2]　易武坤[3]　马欣欣[1]　王汉坤[1]

(1.国际竹藤中心 国家林业和草原局/北京市共建竹藤科学与技术重点实验室　北京　100102；2.中国林业科学研究院木材工业研究所 国家林业和草原局木材科学与技术重点实验室　北京　100053；3.湖南潇湘大数据研究院　湖南　长沙　410000)

摘要:【目的】通过机器学习算法以及图像分割技术，解决毛竹组织比量计算过程中耗时、耗力、精度低的问题，定量分析毛竹横切面中纤维组织比量的径向分布规律，为梯度材料和仿生材料的开发提供支撑。【方法】以毛竹（*Phyllostachys edulis* (Carr.) H. De Lehaie）为研究对象，通过平板式影像扫描仪获取经精细砂光的竹环横切面图像；采用 Label-Img 软件对扫描图像中的维管束进行坐标化管理，并通过预先训练的 YOLO v3 模型逐一抓取；将维管束各个像素点的像素值作为特征，利用 K-Means 聚类算法，将像素均值大的聚类为白色，均值小的聚类为黑色，引入多点投票聚类机制判定边界点属于哪一类的概率更大，以完成单个维管束的二值化；将单个维管束的二值化图根据坐标全部还原至与原扫描图像同尺寸的空白图像中，从而生成整体的二值化图；统计图中黑色像素点的总个数，并乘以每个像素点代表的实际面积，获得该竹环横切面的纤维鞘面积；采用图像分割技术对横切面二值化图像沿径向均匀分为 10、15、20、25、30、35 层，并获得各层纤维鞘面积，以研究毛竹纤维组织比量径向分布规律。**【结果】**将 K-Means 聚类算法和多点投票聚类机制相结合，获得的二值化图像可以清晰得分辨出纤维鞘与背景；对于壁厚约为 10 mm 的毛竹，横切面径向分层数量优选为 25 层；毛竹纤维组织比量自竹青至竹黄递减，前 30%区域（1-8 层）纤维组织比量减少量占总减少量的 65%，后 30%区域（18-25 层）减少量仅占总减少量的 5%；毛竹纤维组织比量径向梯度分布规律符合二阶衰减指数函数，拟合优度 R 为 0.99。**【结论】**本研究采用的图像处理方法可以快速且准确得获得毛竹纤维组织比量的径向分布。

基金项目：国际竹藤中心基本科研业务费专项（1632020012，1632020011）。

第一作者：徐皓诚，男，硕士研究生，研究方向竹材基础性质。　***通信作者：**王汉坤，副研究员。Email: wanghankun@icbr.ac.cn

淹水胁迫对中山杉次生组织生长的影响

杨季雨，郑欣欣，潘彪*

（南京林业大学材料科学与工程学院，南京 210037）

摘要：以正常生境、淹水 3cm、淹水 30cm 的三年生中山杉树苗为试材，编号 A、B、C 组，7-10 月间每月月初取样观察，每组取 3 棵生长情况相近的试材，取样部位为离基部 3cm 处，对试样进行染色和石蜡包埋，通过显微镜进行观察。对形成层带细胞层数、木质部细胞从年初到取样时生长量和胼胝质数量以及分布进行统计。结果表明：（1）形成层带细胞层数：三组样本存在显著差异，其中 A 组形成层带细胞层数从七月到十月依次为：6.4、4.1、3.0、3.0 层，B 组依次为 7.3、7.6、4.5、3.9 层，C 组依次为 5.3、3.4、2.3、2.4 层。形成层带细胞层数从 7 月到 10 月总体呈下降趋势，三组形成层带细胞层数数量大小关系为：B 组＞A 组＞C 组；（2）木质部细胞从年初到取样时生长量：三组样本存在显著差异，A 组木质部细胞年初到取样时生长量依次为 8.6、10、12.3、14.1 个。B 组依次为 13.5、40.5、69.3、73.7 个。C 组依次为 4.4、6.2、10.8、11.0 个。其中 B 组生长量最大，且与其他组差异显著，A 组相对于 C 组略高但无显著差异。同时在 10 月的 A、B 和 C 切片均观察到晚材，表明 10 月时形成层已趋于休眠；（3）胼胝质数量和分布：样本数据整体呈随时间增加趋势，A 组胼胝质数量从七月到十月依次为 1.9、1.8、2.0、2.7 个。B 组依次为 1.0、1.8、2.2、2.6 个。C 组依次为 1.1、1.5、2.1、2.1 个。其中 C 组胼胝质数量相对 A 组偏少且增加缓慢，B 组胼胝质较 A 组多且增加迅速。从胼胝质分布和数量变化来看，10 月前胼胝质随时间推移缓慢外移且不断增加，7-9 月时同时间段不同组间无明显差异，10 月 C 组胼胝质数量下降明显。形成层带细胞在径向上的数量被认为是评判形成层细胞活跃程度的标准，从形成层带细胞数量和生长量来看，水深 3 cm 左右的淹水处理能够促进中山杉的生长，水深 30 cm 左右的淹水胁迫会对中山杉生长起抑制作用。胼胝质的消失意味着形成层进入休眠，从 C 组胼胝质的数量变化来看，水深 30 cm 左右的淹水胁迫会使得中山杉形成层提前进入休眠。

关键词：中山杉，淹水胁迫，次生组织，胼胝质。

Effects of Flooding Stress on the Growth of Secondary Tissues of *Taxodium* hybrid ‘Zhongshanshan’

Yang Jiyu, Zheng Xinxin, Pan Biao*

（Nanjing Forestry University Materials Science and Engineering)

Abstract: Three-year-old *Taxodium* hybrid 'Zhongshanshan' tree seedlings with normal habitats, 3 cm flooding and 30 cm flooding were used as test materials, numbered in groups A, B, and C. From July to October, samples were taken at the beginning of each month for observation. Each group took 3 plants with similar growth conditions. The sampling site is 3 cm away from the base. The sample is dyed and embedded in paraffin, and observed by optical microscope and fluorescence microscope. The number of cambium belt cell layers, the accumulation and growth of xylem cells and the number and distribution of callose were calculated. The results showed that: (1) cambium belt cell layer number: There are significant differences between the three groups of samples. The number of cambium belt cell layers in group A from July to October are: 6.4, 4.1, 3.0, 3.0, and group B is 7.3, 7.6 , 4.5, and 3.9 floors, group C is 5.3, 3.4, 2.3, and 2.4 floors in sequence. The number of cambium belt cell layers showed an overall downward trend from July to October. The relationship between the number of cambium belt cell layers in the three groups was: Group B>Group A>Group C; (2) Growth of xylem cells from the beginning of the year to the time of sampling: There were significant differences between the three groups. The growth of xylem cells from the beginning of the year to the time of sampling in group A was 8.6, 10, 12.3, 14.1 in sequence. Group B has 13.5, 40.5, 69.3, 73.7 in sequence. Group C was 4.4, 6.2, 10.8, and 11.0 in sequence. Among them, group B has the largest growth and is significantly different from other groups. Group A is slightly higher than group C but has no significant difference; (3) The number and distribution of callose: the overall sample data shows an increasing trend over time, and the number of callose in group A has increased from seven From month to October, the numbers are 1.9, 1.8, 2.0, and 2.7. Group B has 1.0, 1.8, 2.2, 2.6 in turn. Group C has 1.1, 1.5, 2.1, 2.1 in turn. Among them, the number of callose in group C was less than that in group A and increased slowly, and the number of callose in group B was more than that in group A and increased rapidly. From the perspective of callose distribution and quantity changes, callose slowly moved out and increased over time, and there was no significant difference between different groups in the same time period from July to September, and the number of calloses in group C decreased significantly in October. The number of cambium belt cells in the radial direction is considered to be the criterion for judging the activity of cambium cells. From the perspective of the number and growth of cells in the cambium zone, flooding stress with a water depth of about 3 cm can promote the growth of *Taxodium* hybrid 'Zhongshanshan', and a water depth of about 30 cm can inhibit the growth of *Taxodium* hybrid 'Zhongshanshan'. The disappearance of callose means that the cambium enters dormancy. From the change in the amount of callose in group C, the flooding stress of about 30 cm will cause the cambium to enter dormancy in advance.

Keywords: *Taxodium* hybrid 'Zhongshanshan'; flooding stress; secondary tissues; callose;

高温热处理对中山杉木材材色和化学成分的影响

赵洋，郑欣欣，毕玉金，李茜然，勇璐，杨季雨，潘彪*

(南京林业大学材料科学与工程学院，江苏 南京 210037)

摘要：中山杉（*Taxodium* hybrid ‘Zhongshanshan’）既具有早期速生的优良生长特性，又具有抗水湿、抗干旱贫瘠、抗风和抗盐碱的良好能力，所以中山杉是一种极具开发应用潜力的树种。但是，中山杉木材具有易开裂、易蓝变和尺寸稳定性差等缺点。为了更好的利用中山杉，本文以蒸汽为热处理介质，在三个温度水平下对中山杉木材处理处理 2 h。研究处理前后中山杉木材试件材色和化学成分的变化，为优化中山杉木材的热处理工艺提供理论依据。

本试验用 DP-3 型全自动测色色差计测量高温热处理前后中山杉木材的色度学指数，并通过半自动滑走切片机获取高温热处理前后的中山杉木材横切面用于荧光分析，和偏光显微镜观察，通过荧光显微镜分析热处理前后中山杉木材细胞壁木质素的分布；通过偏光显微镜观察处理前后中山杉木材的纤维素相对含量的变化。

1．木材材色变化

1.1.1 表面材色变化

图 1 为中山杉木材经不同温度高温热处理后的表面材色对比。从图中可以看出，未处理中山杉木材为浅黄色；在相同的时间下随着处理温度的升高，中山杉木材材色逐渐加深，同时木材表面的纹理更加清晰，具有良好的装饰效果。当热处理温度为 240℃时，中山杉木材的颜色为深褐色，与珍贵木材颜色相近，具有一种古典的视觉感受。

1.1.2 色度指数变化

采用 DP-3 型全自动测色色差计测量并记录处理前后中山杉木材颜色变化时的 L*、a*、 b*值 。图 2 为中山杉木材经不同温度高温热处理后 L*，a*，b*对比：

从图 2 中可以看出，在相同的处理时间下随着处理温度的升高，木材的 *L**呈现递减的趋势，在 200℃时，试件的 L*为 60.9，比处理前试件下降了 16.53%，随着温度的升高，在 220℃，240℃时分别下降了 28.89%，35.52%。随着处理温度的升高，a*与 L*有相同的变化趋势，但随温度的升高，a*表现为小幅增长，未处理材的 a*为 7.3，当处理温度为 200℃、220℃和 240℃时，中山杉木材的 a*分别增长了 10.83%、15.51%和 19.56%。随着处理温度的升高，b*表现出与 L*不同的变化趋势。b*则先呈现小幅增加趋势，然后逐渐减小。未处理材的 b*为 20.9，与未处理材相比，200℃处理后的中山杉木材 b*增加了 2.44%，在 220℃，240℃时分别下降了 2.14%，7.05%。这里 a*，b*的变化规律与其他学者的研究。

2. 偏光显微镜观察结果

木材细胞壁由于纤维素分子有序排列而形成的结晶区具有双折射性。通过偏光显微镜，可以观察到木材细胞壁内微纤丝结晶区存在与否，从而定性判断纤维素结晶区的分解情况。图 3.a 为处理前中山杉木材的偏光图像;图 3.b 为 200℃处理后中山杉木材的偏光图像;图 3.c 为 220℃处理后中山杉木材的偏光图像;图 3.d 为 240℃处理后中山杉木材的偏光图像。与未处理材相比， 200℃时中山杉木材的偏光亮度变化不明显，这是因为在 200℃时纤维素还没有分解。当处理温度为 220℃和 240℃时中山杉木材细胞壁的偏光亮度减弱，说明在乙酸和

高温热处理的共同作用下，纤维素结晶区被分解。

3. 荧光显微镜观察结果

有些生物体内的物质受激发光照射后可以直接产生荧光，称为自发荧光。木材细胞壁中的木质素在激发光的照射下，可以产生自发荧光。据此，可以通过荧光的强度来判定细胞壁内木质素浓度的高低。通过图 4.a，可以观察到未处理材的细胞壁荧光强度最强的是细胞角隅处，其次是复合胞间层，这是因为管胞的木质化是从细胞角隅开始，且在细胞角隅和胞间层沉积大量木质素。通过图 4.b、图 4.c 和图 4.d 观察到复合胞间层的荧光强度与次生壁的荧光强度差异越来越小，这应该是因为 200℃达到了木质素的玻璃态转变温度，木质素由原来的玻璃态转变为粘流态，粘流态的木质素由复合胞间层和细胞角隅处通过纹孔流到细胞壁的其他区域，导致复合胞间层、细胞角隅处、次生壁的木质素浓度趋于一致。

4. 结论

（1）未处理中山杉木材为浅黄色，随着处理温度的升高，中山杉木材材色逐渐加深，从浅黄色向深褐色转变。

（2）随着处理温度的升高，纤维素结晶区在高温和乙酸的共同作用下分解。

（3）当处理温度达到木质素的玻璃态转变温度，木质素由原来的玻璃态转变为粘流态，粘流态的木质素由复合胞间层和细胞角隅处通过纹孔流到细胞壁的其他区域。

关键词：中山杉；高温热处理；材色；纤维素分布；木质素分布

Influences of High Temperature Heat Treatment on colors and Chemical Composition in *Taxodium* hybrid ‘Zhongshanshan’

Yang Zhao[1], Biao Pan[1]

([1]College of Materials Science and Engineering, Nanjing Forestry University, Nanjing 210037, Jiangsu)

Abstract: In order to make better use of Taxodium hybrid 'Zhongshanshan', Taxodium hybrid 'Zhongshanshan' wood was taken as study object. And Taxodium hybrid 'Zhongshanshan' wood was treated for 2h at three temperature levels(200℃、220℃、240℃).By adopting a process different high temperature heat treatment temperature (200℃、220℃、240℃) for 2 h, this paper analyzed the colors and Chemical Composition in Taxodium hybrid ‘Zhongshanshan’ wood after being treated

The main conclusions of this paper are concluded as follows:

The untreated Taxodium hybrid ‘Zhongshanshan’ wood is light yellow. At the same time, with the increase of treatment temperature, the wood color of Taxodium hybrid ‘Zhongshanshan’ wood gradually deepens, changing from light yellow to dark brown.

Examination with polarized light demonstrated that secondary cell wall of Taxodium hybrid 'Zhongshanshan' cellulose, which occurs in undegraded walls as crystalline units highly ordered in parallel aligned fibrils, lost its typical birefringence, indicating their disintegration.

Examination with fluorescent light demonstrated that lignin concentration in different morphological areas of untreated wood follows the decreasing order: CCML>CML>S2. With temperature increasing the fluorescence intensity of CCML and S2 of fluorescence intensity difference is more and more small, it should be because glass transition

temperature of 200 ℃ to lignin, lignin from glassy state into a viscous flow, viscous flow of lignin by composite intercellular layer and cell corner by grain orifice flow to other areas of the cell wall, causing composite intercellular layer, cell corner place, the lignin concentration of secondary wall consistent.

Keywords: high temperature heat treatment， color, cellulose distribution, lignin distribution

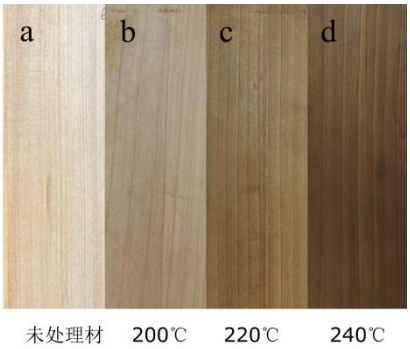

图 1 经不同温度高温热处理后中山杉木材表面颜色的变化

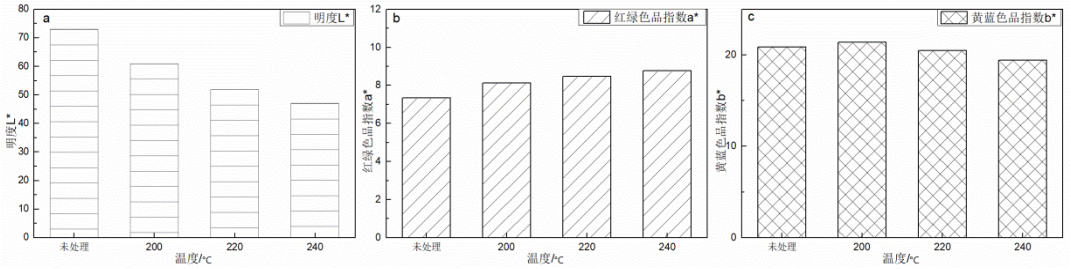

图 2. 热处理温度与 L*、a*、 b*的关系：a. 热处理温度与明度 L*的关系；b. 热处理温度与红绿色品指数 a*的关系；c. 热处理温度与蓝黄色品指数 b*的关系。

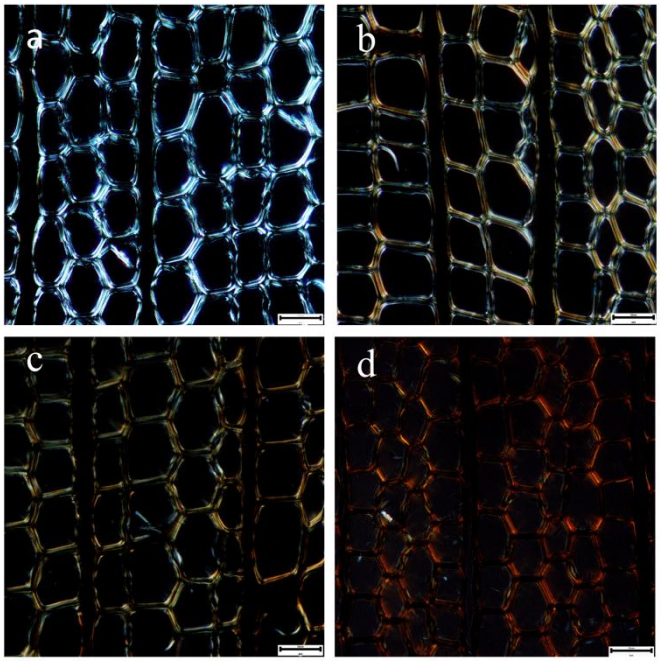

图 3.热处理前后中山杉木材细胞壁偏光图

a 为处理前中山杉木材细胞壁的偏光图；

b 为 200℃处理后中山杉木材细胞壁的偏光图；

c 为 220℃处理后中山杉木材细胞壁的偏光图；

d 为 240℃处理后中山杉木材细胞壁的偏光图

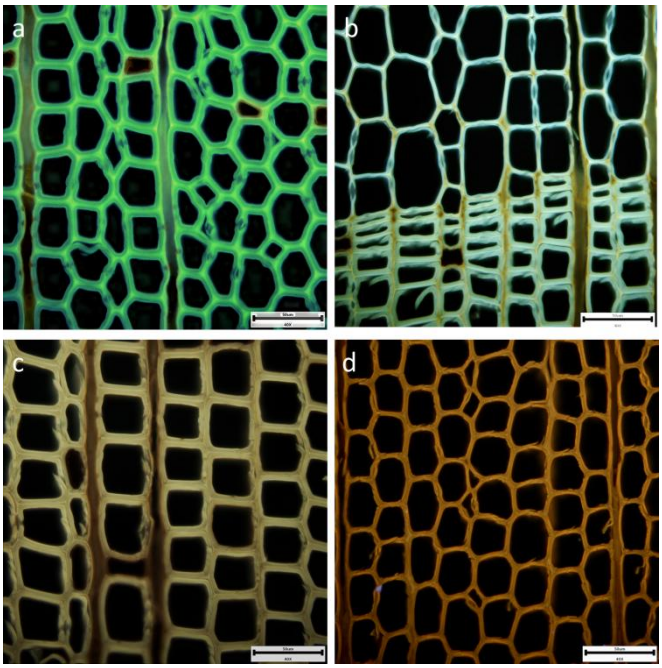

图 3.热处理前后中山杉木材细胞壁荧光图

a 为处理前中山杉木材细胞壁的荧光图；

b 为 200℃处理后中山杉木材细胞壁的荧光图；

c 为 220℃处理后中山杉木材细胞壁的荧光图；

d 为 240℃处理后中山杉木材细胞壁的荧光图

腺瘤豆木材干缩性与解剖构造的关系

刘礼童，于朝阳，徐东年，胡进波，茛姗姗

（中南林业科技大学材料科学与工程学院）

摘要：腺瘤豆（Dabema）隶属于含羞草科腺瘤豆属，本属仅有 1 种，分布于加纳、利比里亚、尼日利亚、刚果等非洲地域。由于它硬度高，耐腐，加工性能良好，所以常使用于重型建筑构件、港口建筑用材、地板、运动器材、车工制品等方面。然而腺瘤豆木材干缩甚大，干燥慢，易开裂、变形严重。这些性质导致对腺瘤豆木材的保存，木材干燥等方面有很大的弊端。本文以非洲木腺瘤豆木材为研究对象，对其解剖构造特性进行研究。观察其宏微观特征，以及研究其密度和干缩特性，并对各项指标进行相关性分析等数理统计方法，以期找出腺瘤豆木材的微观解剖构造与干缩性能之间的关系，为非洲木材的进口加工以及干燥利用提供理论基础。结果如下：

（1）腺瘤豆木材心、边材区分明显，心材金黄褐色，边材灰白色，生长轮不明显，木材光泽强，新鲜材有难闻气味，纹理交错，结构细且均匀，重量中等。

（2）腺瘤豆木材为散孔材，管孔数少，略大，大小略一致，分布略均匀；管孔内含有沉积物或树胶。单穿孔，管间纹孔式互列，系附物纹孔。轴向薄壁组织呈环管状、翼状、少数聚翼状及轮界状。木射线窄至略宽，非叠生；单列射线偶见，多为 5～9 个细胞；多列射线宽 2～5（多数 3~ 5）个细胞，高 10～35（多数 15～24）个细胞，射线组织同形。射线与导管间纹孔类似管间纹孔。木纤维壁薄至厚，单纹孔略具狭缘，分隔木纤维普遍。

（3）根据国家标准对腺瘤豆木材的密度指标进行测量，结果显示，根据木材材性 5 级分级标准，腺瘤豆木材属于III级（中，0.551~0.75 g/cm^3），气干密度、基本密度和全干密度分别为 0.734 g/cm^3、0.604 g/cm^3、0.700 g/cm^3。

（4）根据国家标准测量出腺瘤豆的干缩性。弦向、径向和体积气干干缩率分别为 4.742 %、1.728 %、6.692 %；弦向、径向和体积全干干缩率分别为 9.630 %、4.183 %、13.678 % ，腺瘤豆木材差异干缩值为 2.323，偏大。

（5）通过 SPSS 软件相关系数分析，差异干缩系数与纤维腔径比有微弱的正相关性，差异干缩系数与纤维壁腔比有微弱的负相关性，说明腺瘤豆木材的干缩性与其解剖构造之间有关系。

关键词：腺瘤豆；解剖构造；干缩性；

Relationship between wood shrinkage and anatomical structure of Dabema

Litong Liu　Zhaoyang Yu　Dongnian Xu　Jinbo Hu　Shanshan Chang

(School of Materials Science and Engineering, Central South University of Forestry and Technology)

Abstract: Dabema belongs to the genus Of mimosae, only one species of which is found in Ghana, Liberia, Nigeria, Congo and other African regions.Due to its high hardness, corrosion resistance, good processing performance, so often used in heavy construction components, port building materials, flooring, sports equipment, turning products and other

aspects.However, Dabema bean wood drying shrinkage is very large, slow drying, easy to crack, serious deformation.These properties lead to the preservation of Dabema bean wood, wood drying and other aspects of great drawbacks.In this paper, the anatomical structure characteristics of African wood Dabema
bean wood were studied.By observing its macro and micro characteristics, e 'DE, studying its density and dry shrinkage characteristics, and carrying out correlation analysis and other mathematical statistical methods for each index, the relationship between the microscopic anatomical structure and dry shrinkage performance of Dabema bean wood is expected to be found out, so as to provide a theoretical basis for the import processing and drying utilization of African wood.The results are as follows:

(1) Dabema bean wood heart and sapwood are clearly distinguished, heartwood is golden brown, sapwood is gray white, growth wheel is not obvious, wood luster is strong, fresh wood has unpleasant smell, texture is staggered, structure is fine and uniform, medium weight.

(2) Dabema bean wood is porous, with fewer pipe holes, slightly larger, slightly consistent size, and slightly uniform distribution;The tube bore contains sediment or gum.The intervessel pittings were alternate, and the perforated plates are single, with attachment.The axial parenchyma is circumferential, pterygoid, few pterygoid and wheel boundary.Wood rays narrow to slightly wider, non-overlapping;A single row of rays were seen occasionally, mostly 5 ~ 9 cells;Multiple rows of rays were 2 ~ 5 cells wide (most 3~ 5 cells) and 10 ~ 35 cells high (most 15 ~ 24 cells). The ray tissues were homomorphic.Gamma rays are similar to interductal striations.Wood fiber walls are thin to thick, single grain bore slightly narrow margin, separating wood fiber is common.

(3) according to the national standard of Dabema bean wood density index measurement, the results showed that according to the wood material classification standard level 5, Dabema bean wood belongs to Ⅲ level (0.551 ~ 0.75 g/cm3), air dry density, basic density and dry density were 0.734 g/cm3, 0.604 g/cm3 and 0.700 g/cm3.

(4) The dry shrinkage of Dabema bean was measured according to national standards.The drying shrinkage of chordal, radial and volume gas was 4.742 %, 1.728 % and 6.692 % respectively.The drying shrinkage rate of chordal, radial and volume was 9.630 %, 4.183 % and 13.678 %, respectively. The difference of drying shrinkage value of Dabema bean wood was 2.323, which was too large.

(5) Correlation coefficient analysis by SPSS software showed that there was a weak positive correlation between the coefficient of difference dry shrinkage and the ratio of fiber cavity diameter, and a weak negative correlation between the coefficient of difference dry shrinkage and the ratio of fiber wall cavity, indicating that there was a relationship between the drying shrinkage of Dabema bean wood and its anatomical structure

Key words: Dabema;Anatomical structure;Drying shrinkage;

基于氮气吸附和压汞法对三种木质基材料孔隙表征

杨天舒 胡进波* 汪倩倩 茎姗姗

（中南林业科技大学材料科学与工程学院）

摘要：木质基材料是一种天然可再生资源，具有可循环利用、对环境无污染、经济成本低等生态材料特点，但也存在易腐朽，易燃，强度不高等缺点制约其使用。孔隙结构是影响材料性能的主要因素，可通过对材料孔隙处理达到其使用要求，提高木质基材料的综合利用。因此，开展孔隙结构研究具有重要意义。木质基材料在不同状态下，孔隙结构会产生差异。本研究以针叶材杉木、阔叶材杨木、农林废弃物油茶壳三种木质基材料为研究对象，利用超临界干燥法和常规干燥法对试样进行预处理。采用氮气吸附法对木质基材料中的比表面积、孔体积、孔径分布等孔结构参数进行研究，并通过氮气吸附等温线判断孔隙的形状。采用压汞法对木质基中大孔的孔隙率、孔径分布等参数进行定量测试，分析材料的孔隙结构特征。结果表明：①超临界干燥下，材料的原始孔隙结构得以保持，杉木、杨木和油茶壳的 BET 表面积分别为 5.53m^2 g^{-1}、4.18m^2 g^{-1}、85.65 m^2 g^{-1}，孔体积为 0.015cm^3g^{-1}、0.018cm^3g^{-1}、0.159cm^3g^{-1}，说明油茶壳的孔隙结构较为丰富。杉木孔径在 10.8nm 的孔体积分布密度最大，孔径分布以介孔为主，大孔次之。杨木孔径在 3.4nm 的孔体积分布密度最大，以介孔和大孔分布为主。油茶壳在 7.2 nm 的孔体积分布密度最大，以介孔和微孔为主，提供较大的比表面积。杉木、杨木和油茶壳氮气吸附等温线相类似都属 II 和 IV(b)混合型，杉木、杨木回滞环 H3 型，油茶壳 H2(b)与 H3 混合型，反映出杉木和杨木是一种具有平行壁的狭缝状孔隙，油茶壳具有孔颈相对较宽的墨水瓶状。通过压汞法可知，孔隙率，杨木（77.5%）大于杉木（43.8%）和油茶壳（67.5%），说明杨木内部孔体积较大。杉木、杨木和油茶壳的孔隙分别主要集中在 60nm、226nm、660nm。②常规干燥后，孔隙结构发生了变化。杉木、杨木和油茶壳的 BET 表面积分别为 1.13m^2 g^{-1}、0.32m^2 g^{-1}、0.97m^2 g^{-1}，孔体积为 2.5x$10^{-3}$$cm^3g^{-1}$、5.6x$10^{-4}$$cm^3g^{-1}$、1.5x$10^{-3}$$cm^3g^{-1}$，与超临界干燥相比，比表面积与孔体积均减小，可能是因为干燥过程中巨大的毛细管张力使该部分介观孔隙的隙壁结合在一起，形成大量的氢键网络而导致的。杉木孔径在 11nm 处孔体积分布密度最大，微孔次之。杨木以大孔和介孔为主。 油茶壳在 22 nm 的孔体积分布密度最大，以介孔和大孔为主。孔隙率（杨木 65.2%、油茶壳 49.5%）显著低于超临界状态，内部孔隙收缩，杉木孔隙率 46.2%基本稳定。干燥处理后孔径分布大孔所占比例均减小，微孔、介孔增加。采用氮气吸附法和压汞法可以实现对杉木、杨木及油茶壳全面、定量的孔隙表征分析，有助于准确的了解不同状态下生物质的孔隙结构，对生物质材料的加工利用和提高综合利用率具有重要意义。同时有利于拓宽木质基材料在木陶瓷、生物遗态陶瓷复合材料、超级电容器等方面的应用提供理论基础和依据。

关键词：孔隙结构；氮气吸附法；压汞法

Pore characterization of three kinds of lignin-based materials based on nitrogen adsorption and mercury porosimetry

Tianshu Yang Jinbo Hu* Qianqian Wang Shanshan Chang

(School of Materials Science and Engineering, Central South University of Forestry and Technology)

Abstract: lignin-based material is a kind of natural renewable resource, which has the characteristics of recycling, no pollution to the environment and low economic cost, but it also has some disadvantages such as perishable, flammable, low strength and so on. Pore structure is the main factor affecting the properties of materials, which can meet the requirements of application through the treatment of pores of materials, and improve the comprehensive utilization of wood-based materials. Therefore, it is of great significance to study the pore structure. The pore structure of lignin-based materials will be different in different states. In this study, three kinds of wood-based materials including coniferous Chinese fir, hardwood poplar and agricultural and forestry waste Camellia oleifera shell were studied, and the samples were pretreated by supercritical drying method and conventional drying method. The pore structure parameters such as specific surface area, pore volume and pore size distribution in wood-based materials were studied by nitrogen adsorption method, and the pore shape was judged by nitrogen adsorption isotherm. The parameters such as porosity and pore size distribution of macropores in wood matrix were quantitatively measured by mercury porosimetry, and the pore structure characteristics of the materials were analyzed. The results show that: (1) the original pore structure of the material can be maintained under supercritical drying. The BET surface areas of Cunninghamia lanceolata, poplar and Camellia oleifera shell are 5.53m^2 g^{-1}, 4.18m^2 g^{-1} and 85.65m^2 g^{-1}, respectively, and the pore volumes are 0.015cm^3 g^{-1}, 0.018cm^3g^{-1}, 0.159cm^3g^{-1}, indicating that the pore structure of Camellia oleifera shell is abundant. The pore volume distribution density of Cunninghamia lanceolata in 10.8nm is the highest, the pore size distribution is mainly mesoporous, followed by macropores. Poplar pore diameter has the highest pore volume distribution density in 3.4nm, mainly mesoporous and macroporous. The pore volume distribution density of Camellia oleifera shell in 7.2nm is the highest, mainly mesoporous and micropore, providing a larger specific surface area. The nitrogen adsorption isotherms of Cunninghamia lanceolata, poplar and Camellia oleifera shell all belong to II and IV (b) mixed type, Cunninghamia lanceolata and poplar hysteresis loop H3, oil camellia shell H2 (b) and H3 mixed type, indicating that Cunninghamia lanceolata and poplar are slit-like pores with parallel walls, and oil camellia shells have ink bottles with relatively wide necks. According to the mercury injection method, the porosity of poplar (77.5%) is larger than that of Cunninghamia lanceolata (43.8%) and Camellia oleifera shell (67.5%), indicating that the inner pore volume of poplar is larger. The pores of Chinese fir, poplar and Camellia oleifera shell are mainly concentrated in 60nm, 226nm and 660nm, respectively. (2) after conventional drying, the pore structure changed. The BET surface areas of Cunninghamia lanceolata, poplar and Camellia oleifera shells are 1.13m^2 g^{-1}, 0.32m^2 g^{-1} and 0.97m^2 g^{-1}, respectively, and the pore volumes are 2.5x$10^{-3}$$cm^3g^{-1}$, 5.6x$10^{-4}$$cm^3g^{-1}$ and 1.5x$10^{-3}$$cm^3g^{-1}$, respectively. Compared with supercritical drying, the specific surface area and pore volume are reduced, which may be due to the combination of the mesoscopic pore walls of this part due to the huge capillary tension during the drying process. Caused by the formation of a large number of hydrogen-bonded networks. The pore size distribution density of Cunninghamia lanceolata at

11nm is the highest, followed by micropores. Poplar is mainly composed of macropores and mesopores. The pore volume distribution density of Camellia oleifera shell in 22nm is the highest, mainly mesoporous and macroporous. The porosity (poplar 65.2%, Camellia oleifera shell 49.5%) was significantly lower than that in supercritical state, the internal pores shrank, and the porosity of Cunninghamia lanceolata was 46.2% stable. After drying treatment, the proportion of macropores in pore size distribution decreased, while micropores and mesopores increased. The comprehensive and quantitative pore characterization and analysis of Cunninghamia lanceolata, poplar and Camellia oleifera shell can be realized by nitrogen adsorption and mercury injection method, which is helpful to accurately understand the pore structure of biomass in different states. it is of great significance to the processing and utilization of biomass materials and improving the comprehensive utilization rate. At the same time, it is helpful to broaden the application of wood-based materials in wood ceramics, biological relic ceramic composites, supercapacitors and other fields to provide theoretical basis and basis.
Key words: porosity structure; nitrogen adsorption; mercury porosimetry

翼红铁木木材解剖特征和基本密度的关系研究

姚明，于朝阳，徐东年，胡进波，茛姗姗，刘元

（中南林业科技大学材料科学与工程学院）

摘要：木材的物理特性随着细胞尺寸、种类、和所占比例以及细胞壁厚度等而变化，通过定量分析可以测定其变化的范围和两者之间的相互关系。本研究以翼红铁木木材的细胞结构,纤维形态、组织比量等特征与其基本密度之间的关系为总目标,全面、系统地研究了翼红铁木木材各种构造因子对基本密度所产生的影响。

实验中对木材解剖特征和基本密度进行了测试分析。木材的宏微观构造特征包括心边材、生长轮、木纤维、管孔、轴向薄壁组织、木射线等；采用硝酸离析法对纤维形态特征如纤维长度、纤维宽度、纤维腔径等指标进行测量；利用 ImageJ Pro 软件对木材的组织比量进行测定。基于国家标准对木材基本密度的测定。使用 excel、origin、SPSS 软件对实验数据进行变异系数、标准偏差、相关系数等分析计算，通过作图法和通径系数分析法找出解剖构造与基本密度之间的相互关系。

该研究主要结论如下：（1）翼红铁木木材心边材区别明显，心材红褐色至暗褐色边材粉红色，生长轮略明显；导管呈分散型分布，单管孔及径列复管孔平均 6 个/mm_2,导管分子单穿孔，管间纹孔式互列；轴向薄壁组织带状，内含深色树胶；木射线 3~6 根/mm,多列射线宽 2~3 个细胞，高 11~20 个细胞，射线细胞含丰富树胶，未见胞间道；木材纹理直，结构粗。(2)翼红铁木木材纤维壁甚厚，平均约为 12.89μm。木纤维平均长为 1682.31μm，根据 IAWA 规定的纤维长度分级属于长纤维。纤维腔径比、木纤维和薄壁组织比量在径向变化表现出由髓心向外迅速递增，而后趋于平缓；纤维长宽比和双壁厚在径向表现出先升高在降低；导管比量和木射线比量心材到边材变化规律不明显。（3）翼红铁木木材基本密度为 0.836g/cm3，属于密度较大的类别，结合木材的微观特征观察和纤维形态试验结果来分析，纤维是构成木材的主要结构，该木材的纤维比量达到 59.14%，具有丰富的纤维组织，且该木材纤维腔小壁厚，壁腔比为 5.3，并且导管和射线细胞内具有丰富的树胶和内含物，木材材质致密，从而使得木材基本密度较大。（4）通过相关分析可知纤维形态与基本密度显著相关；利用通径系数分析该木材的微观解剖构造中各因子与基本密度的相互关系，可知影响木材基本密度的主要解剖因子为组织比量，在组织比量中又以木纤维比量影响最大，其次在纤维形态测量数据中，该木材的纤维宽、纤维双壁厚和壁腔比对木材的基本密度具有较大的影响因素。在上述数据中，基本密度与导管比量、木射线比量、纤维宽度、纤维壁厚呈显著正相关，与木纤维比量、薄壁细胞比量呈现显著负相关。说明，基本密度与解剖构造参数之间关系密切。

关键词：翼红铁木；解剖构造；基本密度；相互关系

Study on the relationship between wood anatomical characteristics and basic density of Ekki

Ming Yao，Zhaoyang Yu，Dongnian Xu，Jinbo Hu，Shanshan chang，Yuan Liu

(School of Materials Science and Engineering, Central South University of Forestry and Technology)

Abstract: The physical properties of wood vary with cell size, species, and proportion, as well as cell wall thickness. Quantitative analysis can be used to determine the range of change and the relationship between them. In this study, the

relationship between cell structure, fiber morphology, tissue ratio and basic density was taken as the general objective, and the effects of various structural factors on basic density were comprehensively and systematically studied.

In the experiment, the anatomical characteristics and basic density of wood were tested and analyzed. The macro and micro structural characteristics of wood include heartwood, sapwood，growth ring, wood fiber, pore, axial parenchyma, wood ray, etc.; the fiber morphological characteristics such as fiber length, fiber width, fiber cavity diameter were measured by nitric acid separation method; the tissue ratio of wood was measured by ImageJ Pro software. Based on the national standard, the basic density of wood was determined. Excel, origin and SPSS software were used to analyze and calculate the coefficient of variation, standard deviation and correlation coefficient of the experimental data. The relationship between anatomical structure and basic density was found by drawing and path coefficient analysis.

The main conclusions are as follows: (1) there are obvious differences between heartwood and sapwood, the heartwood is reddish brown to dark brown, the sapwood is pink, and the growth ring is slightly obvious; the vessel is distributed in a dispersed pattern, with an average of 6 / mm^2 for single tube hole and diameter row multiple tube hole; the vessel element is single perforation, and the pit type is interlaced; the axial parenchyma is banded with dark gum; the wood ray is 3~6 roots / mm, There were 2~3 cells in width and 11~20 cells in height. The ray cells were rich in gum and no intercellular channels were found. (2) The wood fiber wall is very thick with an average of 12.89 μ M. The average length of wood fiber is 1682.31 μ m, which is classified as long fiber according to IAWA. The ratio of fiber lumen diameter and the ratio of wood fiber to parenchyma increased rapidly from the pith to the outside, and then tended to be flat; the ratio of fiber length to width and double wall thickness increased at first and then decreased in radial direction; the changes of vessel ratio and wood ray ratio from heartwood to sapwood were not obvious. (3) The basic density of the wood is 0.836g/cm3, which belongs to the category of higher density. Combined with the observation of the microscopic characteristics of wood and the results of fiber morphology test, the wood fiber is the main structure of wood, the fiber ratio of the wood is 59.14%, it has rich fibrous tissue, and the fiber cavity is small and Fiber wall thickness, the wall thickness is 5.3, and the vessel and ray cells have It is rich in gum and inclusions, and the wood material is dense, which makes the basic density of wood larger. (4) The correlation analysis showed that the fiber morphology was significantly correlated with the basic density; the path coefficient was used to analyze the relationship between the factors and the basic density in the micro anatomical structure of the wood. It was found that the main anatomical factor affecting the basic density of the wood was the tissue ratio, in which the wood fiber ratio had the greatest influence, and in the fiber morphology measurement data, the fiber of the wood was the most important Dimension width, fiber double wall thickness and wall cavity ratio have great influence on wood basic density. In the above data, the basic density was significantly positively correlated with vessel ratio, wood ray ratio, fiber width and fiber wall thickness, and negatively correlated with wood fiber ratio and parenchyma cell ratio. It is suggested that the basic density is closely related to the anatomical parameters.

Key words: Ekki; anatomical structure; basic density; correlation

大果紫檀木材花纹形成及分类模型分析

章亮，李文珠*，江文正，李小晴

（浙江农林大学工程学院　杭州临安　311300）

摘要：通过对大果紫檀木材花纹的采集与分类，从宏观构造特征和显微结构特征解析其形成机理，以采用分形维数（FD）量化表达木材纹理的粗糙度为导向，结合高斯-马尔可夫随机场特征参数估计，建立大果紫檀木材花纹图象学模型，为大果紫檀木材的识别和木材花纹分类运用提供理论参考。

关键词：大果紫檀；木材花纹；分形维数；高斯-马尔可夫随机场

Analysis of Wood Pattern Classification and Formation Mechanism of *Pterocarpus macrocarpus* Kurz

Liang Zhang, Wenzhu Li*, Wenzheng Jiang, Xiaoqing Li

(Department of Engineering, Zhejiang A&F University, Linan, Hangzhou, 311300)

Abstract: Based on the collection and classification of the wood pattern of *Pterocarpus macrocarpa* kurz, the formation mechanism of the wood pattern was analyzed from the macroscopic and microscopic structure characteristics. Herein, the fractal dimension (FD) was used to quantify the roughness of the wood texture, and a wood pattern imaging model of Pterocarpus macrocarpa kurz with Gauss-Markov random field characteristic parameter estimation was established, which contributes to provide theoretical references for wood identification, pattern classification and application.

Key words: *Pterocarpus macrocarpa* kurz; wood patterns; fractal dimension; Gauss-Markov

图 1　大果紫檀常见木材花纹类别

（a）虎皮纹；（b）树瘤纹；（c）V 形纹；（d）平行纹；（e）鱼骨纹

大果紫檀的花纹主要有以下几种，如图 1 所示：虎皮纹、树瘤纹、山形纹（V 形纹）、带状纹和鱼骨纹（树丫纹）。

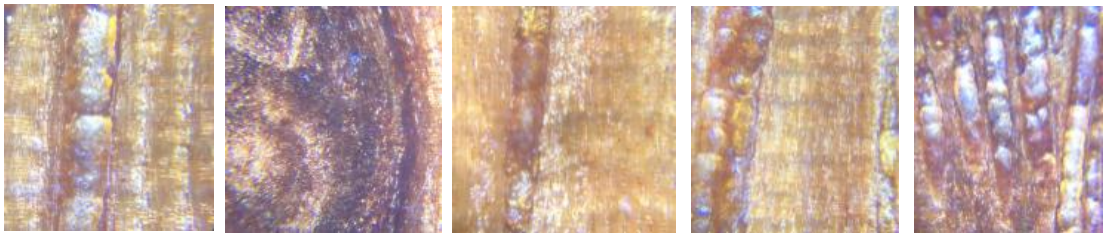

图 2 大果紫檀木材花纹的解剖构造图

（a）虎皮纹；（b）树瘤纹；（c）V 形纹；（d）平行纹；（e）鱼骨纹

从解剖结构分析（图 2），虎皮纹、山形纹、带状纹和鱼骨纹的显微构造特征较为相似，其导管均为轴向管状，呈现长短不一的沟槽沿树干纵向排列；轴向薄壁组织由 2-4 个长方形细胸轴向串联，纵向傍管或离管叠生排列；木纤维两端尖削，腔小壁厚，壁上有具缘纹孔纵向叠生排列，填充于导管和轴向薄壁组织之间；木射线则均为 3-11 个细胞高度。树瘤纹的显微构造明显不同于其他花纹，其导管轴向管状、弯曲状或横向管孔可见，木射线不可见或横向断续状，轴向薄壁组织为轴向串联、弯曲状或横向椭圆形，木纤维轴向细线状、弯曲状或横向椭圆形，均无规律随机排列。

图 3 大果紫檀不同木材花纹的二值化图像

（a）虎皮纹；（b）树瘤纹；（c）V 形纹；（d）平行纹；（e）鱼骨纹

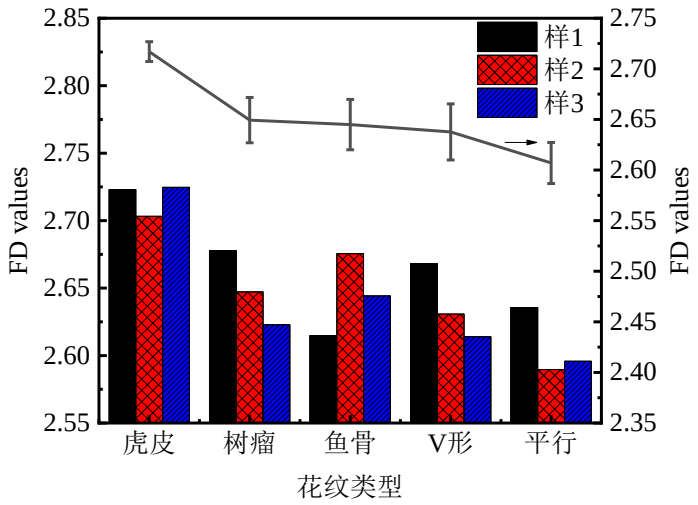

图 4 大果紫檀不同木材花纹的分形维数测试结果

经二值化转换后（图 3）计算，大果紫檀表面特征纹理的 FD 值介于 2.55 至 2.75 间（图 4），高于普通阔叶材树种，不同花纹间的 FD 值差异明显，虎皮纹最高，均值达到 2.72；平行纹最低，均值为 2.61，而同类纹理间 FD 的差异相对较小，FD 从纹理构成的角度上定量地代表了对应的纹理特征，具有一定可行性与准确性。

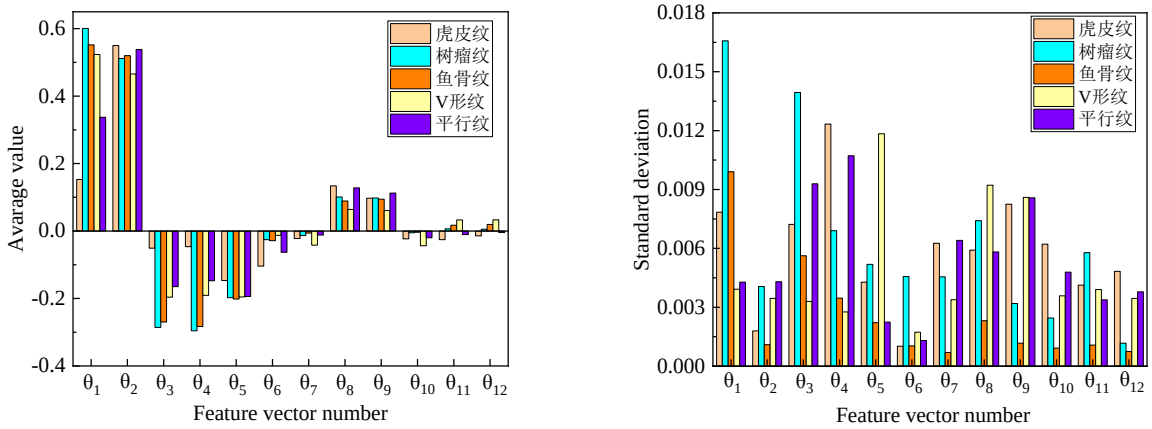

(a) (b)

图 5 大果紫檀表面特征纹理五阶 GMRF 各参数的分布情况:（a）平均值;（b）标准差

大果紫檀表面特征纹理的五阶 Gauss-MRF 参数（图 5）显示各不同特征纹理间存在较大差异，各类特征纹理的随机变异性较强，趋向于形成丰富的视觉感受。各特征纹理的主方向主要集中在 方向，在该方向下纹理的灰度一致性最好，可进一步通过其他参数辅助对不同特征纹理的分类识别；其中树瘤状纹理表面颗粒状凸起造成 方向上的明暗变化差异较大，因而五阶 Gauss-MRF 参数较其他特征纹理波动程度大、范围广。

根据解剖构造与特征，可通过进一步辅助其他参数建立大数据库，对不同特征纹理的分类识别，依托机器语言实现对大果紫檀的鉴定与识别，从而延展到各类名贵红木的的鉴别，从而在识别度较高的情况下简化鉴定程序、降低操作难度。

土壤盐碱胁迫对中山杉木材管胞的影响

夏重阳 彭俊懿 何锐 代博仁 刘星 石江涛*

(南京林业大学材料科学与工程学院，江苏 南京 210037)

摘 要：为了揭示土壤盐碱胁迫对中山杉木材形成组织的影响，以生长良好、长势一致的 2 年生中山杉 302（*Taxodium* 'Zhongshansha302'）无性系幼树为研究对象，对土壤进行不同浓度的混合盐溶液胁迫实验（混合盐溶液的配比模拟沿海滩涂盐渍土的无机离子含量，Na^+浓度分别为 63、189、378mmol Ł$^{-1}$，Cl^-浓度分别为 78.25、234.75、469.5mmol Ł$^{-1}$，SO_4^{2-}浓度分别为 3、9、18mmol Ł$^{-1}$，HCO_3^-浓度分别为 0.5、1.5、3mmol Ł$^{-1}$），在 6 月 14 日至 7 月 28 日期间，每隔两天浇一次混合盐溶液，利用木材解剖技术观察与测定新形成木材组织中管胞的数量、腔径、双壁厚和直径。结果表明：（1）与未处理木材比较，处理后新形成木质部中管胞的数量分别为 6~13、7~11、2~4，其平均细胞数随着盐浓度的增加呈先增多后减少的趋势。（2）在 Na^+浓度为 63mmol Ł$^{-1}$ 和 189mmol Ł$^{-1}$ 处理下新形成的木质部与未处理木材新形成的木质部相比：管胞腔径没有显著差异，管胞双壁厚增大，其差异达到了显著性水平($P<0.05$)，管胞直径没有显著差异；在 Na^+浓度为 378mmol Ł$^{-1}$ 处理下新形成的木质部与未处理木材新形成的木质部相比：管胞腔径减小，其差异达到了显著性水平($P<0.05$)，管胞双壁厚没有显著差异，管胞直径减小，其差异达到了显著性水平($P<0.05$)。（3）与未处理木材新形成的木质部相比：Na^+浓度为 63mmol Ł$^{-1}$ 处理时新形成的木质部第 1 个和第 6 个管胞的双壁厚增大，其差异达到了显著性水平（$P<0.05$），其它管胞的双壁厚没有显著差异；Na^+浓度为 189mmol Ł$^{-1}$ 时，第 1~6 个管胞的双壁厚增大，第 9 个管胞的双壁厚减小，其差异均达到了显著性水平（$P<0.05$），其它管胞的双壁厚没有显著差异；Na^+浓度为 378mmol Ł$^{-1}$ 时，各个管胞的双壁厚没有显著差异。研究说明土壤盐碱胁迫对中山杉木材的形成具有较明显的影响，在较低盐浓度范围内使得新形成木材的管胞数量增加，管胞双壁厚增大；较高盐浓度下使得新形成木材的管胞数量减少，管胞腔径与管胞直径增大。

关键词：中山杉；木材形成；土壤盐碱胁迫

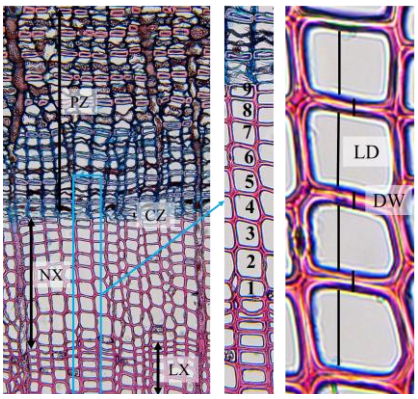

图 1. 盐碱胁迫下中山杉样木的横切面

注：图中 PZ:韧皮部区域，CZ:形成层区域，NX：当年生木质部，LX：去年生木质部，LD：管胞腔径，DW：管胞双壁厚

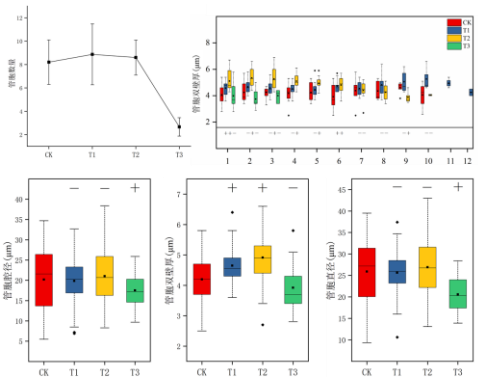

图 2. 盐碱胁迫下管胞数量、腔径、双壁厚与直径的变化

注：图中“－”表示该组与对照组没有显著差异，“＋”表示该组与对照组具有显著差异

*感谢国家自然科学基金面上项目（31971585）支持。

Tracheid changes during wood formation of *Taxodium* 'Zhongshansha' under saline-alkali stress

Chongyang Xia, Junyi Peng, Rui He, Boren Dai, Xing Liu, Jiangtao Shi*

(College of Materials Science and Engineering, Nanjing Forestry University, Nanjing 210037, Jiangsu)

Abstract: In order to reveal the effect of soli saline-alkali on wood formation tissue of *Taxodium* 'Zhongshansha', two-year-old *Taxodium* 'Zhongshansha302' clonal saplings with good and consistent growth were used as the research object, and the different concentrations of mixed salt solution stress experiments were carried out on the soil(The proportion of mixed salt solution simulates the inorganic ion content of the coastal tidal flat, the concentration of Na^+ was 63,189 and 378mmol L^{-1}, respectively, and the concentration of Cl^- was 78.25,234.75 and 469.5mmol L^{-1}, respectively, the concentration of SO_4^{2-} was 3,9 and 18mmol L^{-1}, respectively, the concentration of HCO_3^- was 0.5,1.5 and 3mmol L^{-1}, respectively), the mixed salt solution was poured every two days between June 14 and July 28, the number, lumen diameter, double wall thickness and diameter of tracheids in newly formed wood tissues were observed and measured by wood anatomy technique. The results showed that: (1) compared with untreated wood, the number of tracheids in the new-formed xylem after treatment were 6~13, 7~11,2~4, respectively, and the average number of cells increased at first and then decreased with the increase of salt concentration. (2) Compared with the newly formed xylem of untreated wood under the Na^+ concentration of 63mmol L^{-1} and 189mmol L^{-1}, there is no significant difference in tracheid lumen diameter, but the tracheid double wall thickness increases, and the difference reached the significance level ($P<0.05$), there is no significant difference in tracheid diameter compared with the newly formed xylem of untreated wood; compared with the newly formed xylem of untreated wood under the Na^+ concentration of 378mmol L^{-1}, the tracheid diameter decreased, and the difference reached a significant level ($P<0.05$), there was no significant difference in the double wall thickness of the tracheid, the tracheid diameter decreased, and the difference reached a significant level ($P<0.05$). (3) Compared with the newly formed xylem of untreated wood: the double wall thickness of the first and sixth tracheid of the newly formed xylem increased when the Na^+ concentration was 63mmol L^{-1}, and the difference reached a significant level ($P<0.05$), there is no significant difference in the double wall thickness of other tracheids; when the Na^+ concentration is 189mmol L^{-1}, the double wall thickness of the 1st to 6th tracheids increases, and the double wall thickness of the 9th tracheids decreases, the difference reached a significant level ($P<0.05$), there is no significant difference in the double wall thickness of tracheids in other layers; when the Na^+ concentration is 378mmol L^{-1}, the double wall thickness of each tracheid has no significant difference. The results showed that soil saline-alkali stress had an obvious effect on wood formation, in the lower salt concentration range, the number of tracheid in the newly formed wood increase, and the double wall thickness of the tracheid increase; the number of tracheid forming wood decreases, and the tracheid lumen and tracheid diameters increase.

Keywords: *Taxodium* 'Zhongshansha', Wood formation, soil saline-alkali stress

Comparative culm anatomical characteristics of square bamboo from different regions

Qian-Qian Jiang [1,2], Zhang-Chao Ding [3], Yan Yan [1,4], Chang-Qing Lu [1], Jun-Lan Gao [5], and Sheng-Quan Liu [1,6,*]

[1] Anhui Agriculture University, 130 Changjiang West Road, Hefei 230036, P.R. China

[2] Bozhou University, 2266 Tangwang Avenue, Bozhou 236800, P.R. China

[3] Guizhou Forestry School, 380 Qianjin South Road, Guiyang 550201, P.R. China

[4] International Centre for Bamboo and Rattan, Anhui Taiping Experimental Station, Huangshan 245700, P.R. China

[5] Anhui Academy of Agricultural Sciences, 40 Nongke South Road, Hefei 230001, P.R. China

[6] Key Lab of State Forest and Grassland Administration on "Wood Quality Improvement & High Efficient Utilization", 130 Changjiang West Road, Hefei 230036, P.R. China

*Corresponding authors: Liusq@ahau.edu.cn

Abstract The anatomical structure of the culm is characterized by vascular bundles consisting of xylem, phloem, and sclerenchyma fiber sheaths, as well as parenchymatous ground tissue in which the vascular bundles are embedded. The composition of the culm is considered to be the main factor shaping the anatomical features, for which great variation has been observed in the radial direction. However, in contrast to other circular natural lignocellulosic materials, *Chimonobambusa Quadrangularis (Fenzi) Makino* exhibits square stems, thus we tested the hypothesis that anatomical variation exists in the circumferential direction in cross-section of culm from this species. In this study, we analyzed and compared vascular bundle features of internodes and their associated circumferential and radial variation in cross-sections of *Chimonobambusa hejiangensis* from Guizhou and Huangshan. Microscopic observations were conducted to identify the anatomical features of vascular bundles. Structural parameters of vascular bundles were measured and calculated to assessment and compare different anatomical regions in the circumferential and radial directions. Results indicated that the morphological characteristics of vascular bundles presented as undifferentiated, semi-differentiated, and open in the radial direction. There were significant differences in anatomical elements in both the circumferential ($p < 0.01$) and radial regions ($p < 0.01$) based on variance analysis, thus variance certainly exists both in circumferential and radial regions, while vascular bundles of *chimonobambusa hejiangensis* from Guizhou appear to be larger than Huangshan. Additionally, we explored the circumferential and radial variation patterns of anatomical elements and showed that sharp variation happened in adjacent corners and side regions in circumferential regions and in outer, central, and interior region in radial section. We also confirmed that anatomical structure characteristics of Guizhou and Huangshan are quite different in the circumferential and radial directions, suggesting that the shape of square stems is related to variations of anatomical features of cross-sections.

Keywords: *Chimonobambusa Quadrangularis (Fenzi) Makino*; anatomical characteristics; vascular bundles; Guizhou; Huangshan

杉木无性系幼龄材微观结构与力学性能相关性研究

汪睿[1,2] 贾茹[1,2] 王玉荣[1,2*] 孙海燕[1,2] 赵荣军[1] 任海青[1]

（1. 中国林业科学研究院木材工业研究所 北京 100091；

2.中国林业科学研究院林业新技术研究所 北京 100091）

摘要：本文目的是阐明杉木无性系间幼龄材力学性能差异性，筛选力学性能优良的杉木新无性系，探究影响杉木幼龄材力学性能的微观结构主要特征。试验材料采自福建洋口国有林场一片 10 年生杉木无性系品种比对示范试验林，两个经国家认定的杉木无性系新品种‘洋 020’和‘洋 061’，各取 8 株标准株为样木。应用显微图像分析系统、X 射线衍射、傅里叶变换显微红外成像等技术进行木材样品显微构造、微纤丝角、结晶度和化学组分木质素含量等微观结构观测。木材抗弯强度、抗弯弹性模量、顺纹抗压强度和硬度主要力学性能试件按照国标加工、制备和测定。用单因素方差分析进行数据处理，系统分析了两个杉木无性系幼龄材微观结构与力学性能的相关性。显微构造显示，杉木无性系‘洋 020’与‘洋 061’早材的管胞形态较为接近，但‘洋 020’年轮晚材区较‘洋 061’的宽，管胞壁较厚，管胞腔较小，壁腔比较‘洋 061’约大 25%。‘洋 020’的平均微纤丝角为 12.06°，较‘洋 061’的微纤丝角 14. 97°，约小 18%。 ‘洋 020’ 的平均结晶度为 39.73%，较‘洋 061’结晶度（35.88%）高 11%左右。‘洋 020’的木质素含量特征峰比的平均值约高‘洋 061’的 8%左右。‘洋 020’：‘洋 061’的平均抗弯强度、抗弯弹性模量、顺纹抗压强度和木材平均硬度分别为 51.36MPa ：42.56MPa、10.18GPa ：8.98GPa 、30.27MPa ：27.20MPa 和 1497 N ： 1391 N。‘洋 020’的抗弯强度、抗弯弹性模量、顺纹抗压强度和硬度等力学性能指标分别较‘洋 061’高 21%，13%，11%和 8%；同时‘洋 020’晚材区较宽，管胞壁较厚，壁腔比较大，微纤丝角较小，木质素含量较高， 而‘洋 061’的幼龄材则表现为年轮晚材区较窄，管胞壁较薄，壁腔比较小，微纤丝角较大，木质素含量较低等特征。参试杉木无性系‘洋 020’与‘洋 061’的幼龄材性能，除结晶度外，在解剖构造参数、微纤丝角和木质素等微观结构因子方面均存在显著性差异，‘洋 020’的幼龄材抗弯、抗压性能和硬度等力学性能均高于‘洋 061’。无性系杉木幼龄材管胞壁厚度、壁腔比等解剖构造参数以及化学组分木质素含量与力学性能呈正相关，细胞壁纤维素微纤丝角与力学性能呈负相关关系。杉木无性系幼龄材上述微观结构因子协同作用影响了其力学性能。笔者认为，评价杉木无性系幼龄材木材力学品质性状，解剖构造参数和微纤丝角应是最主要的判断依据。

关键词：杉木无性系；幼龄材；解剖构造；微纤丝角；结晶度；木质素；力学性能

The Relativity of Microstructures and Mechanical Properties of Juvenile Woods of Chinese Fir Clones

Wang Rui[1, 2], Jia Ru[1, 2], Wang Yurong[1, 2 *], Sun Haiyan[1, 2],

Zhao Rongjun[1], Ren Haiqing[1]

（Research Institute of Wood Industry， Chinese Academy of Forestry， Beijing 100091， China; 2. Research Institute of Forestry New Technology， Chinese Academy of Forestry， Beijing 100091， China）

Abstract: To understand the mechanical properties variation on juvenile wood among Chinese fir clones, a serial of standard wood samples were prepared by two new-certificated clones in a ten-years-old growth performance demonstration plantation, for microstructure characteristics analysis on juvenile woods.The microstructure and mechanical properties of juvenile woods of Chinese fir clones were analyzed by microscopic image analysis system, X-ray diffraction technique, Fourier transform-infrared microscopic imaging and the national standards of mechanical properties testing. And data of microstructures observed from ‘Yang 020’ and ‘Yang 061, involving the anatomical structure, microfibril angle, crystallinity and chemical composition lignin, as well as main mechanical properties such as bending strength (MOR), bending modulus of elasticity (MOE), compressive strength parallel to grain and hardness, are to be processed by one-way variance analysis.The tracheid morphology of earlywood was similar between ‘Yang 020’ and ‘Yang 061’, however, a significant differenct on latewood mechanical properties. In compareson with colne ‘Yang 061’, clone ‘Yang 020’ presented with wider latewood zone, thicker tracheid wall, smaller tracheid lumen, and larger wall-lumen ratio by 25%. At the aspect of cell walls, the average microfibril angle for ‘Yang 020’and ‘Yang 061’ was 12.06°, and 14.97°, respectively, it means that smaller microfibril angle would have more fine mechanical properties for ‘Yang 020’;The average crystallinity for ‘Yang 061’ was 35.88%, about 11% lower than 39.73% for ‘Yang 020’; The average lignin content, presented by four groups of characteristic peak ratios on ‘Yang 020’ were 8% higher than on ‘Yang 061’. The average MOR, MOE, compressive strength parallel to wood grain and wood hardness of ‘Yang 020’ vs ‘Yang 061’ was 51.36MPa vs 42.56MPa, 10.18GPa vs 8.98GPa, 30.27MPa vs 27.20MPa and 1497N vs 1391N respectively. Each mechanical property indicators, MOR, MOE, compressive strength parallel to wood grain, and wood hardness of ‘Yang 020’, was higher than ‘Yang 061’ by 21%, 13%, 11% and 8% respectively. Which was indicated that clone ‘Yang 020’ with better mechanical properties, in a wider latewood zones, thicker tracheid wall, larger wall-lumen ratio, smaller microfiber angle and higher lignin content, while ‘Yang 061’ with lower mechanical properties, in a narrower latewood zones, thinner tracheid wall, smaller wall-lumen ratio, larger microfiber angle and lower lignin content.For juvenile woods properties of ‘Yang 061’ and ‘Yang 020’, there were significant differences between the two clones on microstructures, such as anatomical structure parameters, microfibril angle and lignin content, except

the crystallinity. Clone‘Yang 020’had higher tested value on juvenile woods mechanical properties over clone‘Yang 061’, with higher bending, compression resistance and hardness. The juvenile wood mechanical properties of Chinese fir clones was positive correlation of anatomical structure parameters, such as tracheid wall thickness and wall-lumen ratio and chemical composition lignin content, while negative correlation shown between microfibril angle of cell walls cellulose and mechanical property. The tested factors above impacted on juvenile woods mechanical properties of Chinese fir clones synergically，and we suggeste that the anatomical structure parameters and microfibril angle among of them are the most important impact factors on the juvenile woods mechanical properties of Chinese fir clones.

Keywords: Chinese fir clones; juvenile woods; anatomical structure; microfibril angle; crystallinity; lignin; mechanical properties

Acknowledgement: Funded by National Key Research and Development Project of China（2017YFD0600201）

* Corresponding author. Email: yurwang@caf.ac.cn

竹材热解炭化物解剖构造与应用研究

柴伟胜, 张文标*, 周海瑛，赵柯豫

（浙江农林大学工程学院 杭州临安 311300）

摘要：将竹材在不同温度下热解，通过比表面积分析仪（BET）和扫描电镜（SEM）研究温度对竹材炭化物微观结构、孔隙与炭化副产物的影响；将竹炭与聚乙烯（PE）、聚乳酸（PLA）通过熔融共混法制备炭塑复合材料，并通过万能力学试验机、垂直燃烧测试仪、热重分析仪（TG）、电阻测量仪、X 射线衍射（XRD）分析竹炭对炭塑复合材料性能的影响。实验结果表明，对于 PLA，竹炭和次磷酸铝（AHP）的加入可以提高弯曲强度至 74.4MPa，极限氧指数至 29.3 vol%；对于 PE，制备的复合材料对水中甲醛的去除率可达到 63.6%；对于木门加工剩余物与聚丙烯复合材料，竹炭的加入最高可降低 50%的热失重，为竹炭在复合材料领域的利用提供理论基础。

关键词：竹材；竹炭；微观结构；炭塑复合；

The anatomical structure and application of Pyrolysis and charcoalization of bamboo

Weisheng Chai, Wenbiao Zhang, Haiying Zhou, Keyu Zhao

（Department of Engineering, Zhejiang A&F University, Linan, Hangzhou 311300）

Abstract: Pyrolysed bamboo with different temperature, studied the effects of temperature on the microstructure, pores and charcoalation by-products of bamboo charcoal by the Surface Area Analyzer (BET) and Scan Electroscope (SEM). Bamboo charcoal and polyethylene (PE) and poly lactic acid (PLA) are mixed into charcoal plastic composite materials by melting.The effect of bamboo charcoal on the properties of charcoal-plastic composite materials is analyzed by the Universal mechanical testing machine, vertical combustion tester, thermal weight analyzer (TG), resistance gauge and X-ray diffraction (XRD).For PLA, the addition of bamboo charcoal and aluminum hypophosphate (AHP) can increase bending strength to 74.4MPa, the limit oxygen index to 29.3 vol; For PE, the removal rate of formaldehyde in water from prepared composite materials can reach 63.6%. For wood door processing residues and polypropylene composites, the addition of bamboo charcoal can reduce heat weight loss by up to 50%，provides a theoretical basis for the utilization of bamboo charcoal in the field of composite materials.

Keywords: Bamboo; Bamboo charcoal; Microstructure; Charcoal plastic composites

当温度在 400℃以下时，随着热解温度的提高，热解过程以水的蒸发、纤维素与半纤维素的热解、焦油、醋液等可燃性气体的释放为主；升温至 400℃后，由于木质素和纤维素的后期分解，热解产物主要为竹材的完全炭化以及甲烷等烃类可燃气体的释放，此时竹材完全炭化，成为竹炭。

500℃及更高温度下的炭化产物变得更易碎，产物脆化程度更高，竹子中的维管束随着最终炭化温度的升高，结构越来越紧密，木质素和纤维素分解逐渐完全，而且孔隙结构也越清晰，孔内部的有机质物质逐渐被炭化完全。维管束的梅花状孔附近的微孔随着炭化温度提高，也越加清晰通透。可看出，竹炭中存在大量的圆柱

状孔径大小不同的中孔，且在维管束壁上还存在很多微孔。竹炭中的孔径有多种规格，使得其对各类物质均有一定的吸附性，适用于更多种类物质的去除（图 1）。

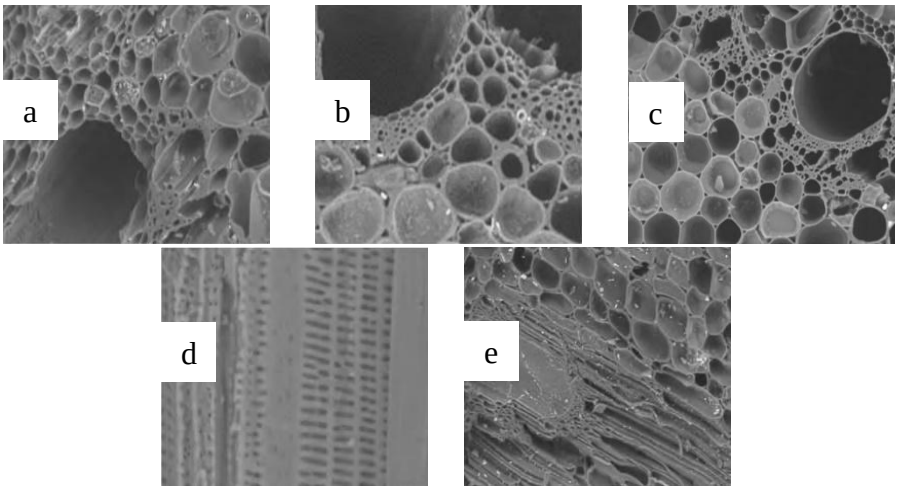

图 1 竹炭的微观结构 其中 a 为 600℃炭化的竹炭 b 为 700℃炭化的竹炭 c 为 800℃炭化的竹炭 d,e 为竹炭纵切面

竹炭的孔径-孔容分布随着炭化温度的变化而发生改变，随着温度升高，微孔容积由 70.4%升高到 82.8%（表 2），而 550℃时大孔容积达到最大值，之后呈下降趋势（表 1）。这个现象的发生，可能是因为竹材在炭化过程中，其几何形状缩小，而且随着炭化温度的变化，炭的外形尺寸收缩率明显，当温度达到 700℃以后其收缩率明显趋小，直至几何尺寸不变化。微孔的增加是由于竹炭的收缩引起其结构的变化，原来封闭的内部微孔被打开。从 750℃起竹炭开始有了石墨化的情形发生，影响了微孔的增加。这一点与竹炭的电阻率变化相吻合，通过电阻测量仪测量竹炭的电阻率，而随着炭化温度的上升，电阻率从 650℃的 $5.6\times10^{4}\Omega$ /cm 降低到 920℃的 0.31Ω /cm，其电阻率的降低除竹炭在高温下石墨化，还与由于竹炭体积缩小在竹炭表面聚集的竹炭灰分中的硅、钾等元素有关。

表 1 热解温度、孔容与比表面积

炭化温度/℃	孔容/($\mu L\cdot g^{-1}$)	比表面积/（$m^2\ g^{-1}$）
450	116.7	213
550	146.7	272
650	178.0	342
750	174.8	346
900	91.1	187

相比木炭 50 m^2/g 的比表面积，竹炭具有更大的比表面积且可以在高温下石墨化，具有优良的吸附性、导电性；将竹炭作为填料与聚合物复合时，可以增大复合材料的接触面积，通过其孔隙以机械互锁的方式提高炭塑复合材料的力学强度并将竹炭的功能与附加在聚合物上，本团队先后将竹炭与木门加工剩余物和 PP、PE、PLA 制备复合材料并研究复合材料的各项性能。

表 2 热解温度与竹炭孔隙分布

Rn/nm	450℃	550℃	650℃	750℃	900℃
<0.9	70.4	71.0	74.2	79.8	82.8
0.9-1.0	6.2	7.7	8.0	3．9	3.1
1.0-1.2	7.5	7.2	5.6	5.5	7.6
1.2-1.4	3.6	5.1	2.9	3.1	1.2
1.4-1.6	2.2	1.5	1.7	1.6	2.8
1.6-1.8	1.7	0.7	1.3	1.1	2.2
1.8-2.2	2.2	0.5	1.8	1.2	1.0
2.2-2.6	1.5	0.4	1.2	0.7	0.1
2.6-3.0	0.8	0.3	0.6	0.4	0.2
3.0-3.4	0.8	0.7	0.6	0.5	0.2
3.4-4.2	1.0	1.2	0.7	0.7	0.4
4.2-5.0	0.5	0.7	0.3	0.3	0.3
5.0-7.0	1.0	1.7	0.6	0.7	0.6
7.0-9.0	0.5	1.0	0.3	0.3	0.4
9.0-11.0	0.2	0.5	0.1	0.2	0.2

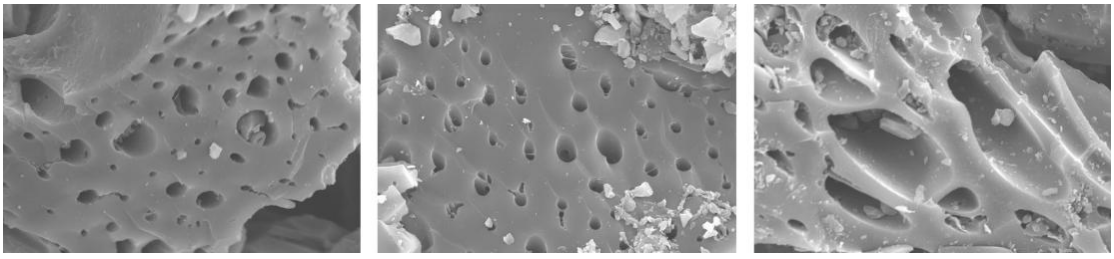

图 2 竹炭吸附甲醛与溶解性有机物分子

实验结果表明，通过添加竹炭，可以使木门加工剩余物与聚丙烯复合材料的力学性能提高，且随着竹炭添加量的提高，复合材料的热失重降低，最高可达 50%，提高了复合材料的热稳定性。以竹炭和高密度聚乙烯制备饮用水净化用炭基滤芯，以甲醛与溶解性有机物分子为处理对象，120 min 去除率达到 63.6%（图 2）。用竹炭和 PLA 制备复合材料，并添加阻燃剂次磷酸铝（AHP）制备三元复合材料，利用万能力学试验机测试复合材料的弯曲强度，结果表明复合材料的弯曲强度提升至 74.4 MPa，通过 XRD 对复合材料进行表征，发现复合材料出现更多的衍射峰，这可能由于 BC 作为填料限制聚合物分子链的运动活性，有助于降低结晶成核的界面自由能，促使晶胚越过位垒形成稳定晶核而加速成核结晶；通过垂直燃烧测试仪测试，得到复合材料的极限氧指数为 29.3%，高于难燃材料规定的 27 vol%。综合以上实验结果，竹炭的加入可以提高聚合物的力学、阻燃等性能，并为聚合物提供原本不具有的功能，炭塑复合材料有着广泛的应用前景与科研潜力，竹炭可以用竹材加工剩余物制备，对原料要求低，提高了竹材利用率，符合绿色可持续发展的方针。

生长速率决定干旱环境下树木年生长量变化

任平[1,3]，梁尔源[1,2,*]

(1 中国科学院青藏高原研究所；

2 中科院青藏高原地球科学卓越中心；

3 安徽师范大学生命科学学院)

摘要：以往的研究认为，生长季长度决定了森林生态系统的固碳量。然而，在气候变暖导致生长季延长的情况下，干旱所引起的生长下降依旧存在。为了探究这一现象背后的原因，我们分析了干旱环境下，生长速率和木质部生产持续时间对年度木材生物量的影响。本研究以位于中国青藏高原东北部的半干旱祁连圆柏（2009-2014年）和美国内华达州南部莫哈韦沙漠极端干旱山地上的美国黄松（2015-2016 年）为研究对象，分析了其木质部分化的年内动态。结果显示，木质部细胞数量（N_{cell}）的变化主要与生长速率（r_m）而非细胞产生持续时间（D_{cell}）相关。在青藏高原区域，上树线和下树线的木质部细胞数量变化分别有 69.9%和 54.7%取决于生长速率。在莫哈韦沙漠地区，生长速率决定了木质部细胞数量 53.9%的变化。此外，我们的研究表明，青藏高原祁连圆柏的生长速度受最低温度和降水量的影响。因此，我们认为生长速率是控制半干旱针叶林木材生物量的主要因子。在暖干条件下，较长的生长季节可能并不会有益于针叶树木质部的形成，相反，升温引起的干旱很可能会通过降低细胞分裂速率来限制固碳。

关键词：针叶树，木材生产，碳汇，生长季长度，生长速率，干旱胁迫

Growth rate rather than growing season length determines wood biomass in dry environments

Ping Ren[1,3], Eryuan Liang[1,2,*]

[1]Key Laboratory of Alpine Ecology, Institute of Tibetan Plateau Research, Chinese Academy of Sciences, Beijing 100101, China

[2]CAS Centre for Excellence in Tibetan Plateau Earth Sciences, Beijing 100101, China

[3]College of Life Sciences, Anhui Normal University, Wuhu 241000, China

[*]To whom correspondence should be addressed. Email: liangey@itpcas.ac.cn

Abstract: A number of studies have suggested that growing season length determines carbon sequestration of forest ecosystems. Given the possibility that drought-induced growth decline will be caused by a prolonged growing season under a warming climate, we investigated the effect of growth rate and duration of xylem production on annual wood biomass in drought-prone environments. We analyzed the intra-annual dynamics of wood formation in Qilian junipers (*Juniperus przewalskii*) from the semi-arid north-eastern Tibetan Plateau, China (2009-2014) and in ponderosa pine (*Pinus ponderosa*) from the hyperarid Mojave Desert in Nevada, USA (2015-2016). Most variability in the number of xylem cells (N_{cell}) was related to growth rate (r_m) rather than duration of cell production (D_{cell}). At the Tibetan sites, 69.9 % and 54.7% of variability in N_{cell} was attributable to r_m for the lower and upper treeline, respectively. Within the Mojave Desert site, 53.9 % of the variability in N_{cell} was related to r_m. The growth rate in the Tibetan Plateau forest is affected by minimum temperature and precipitation. Thus, r_m is a primary control on wood biomass in conifer species of semi-arid forests. Under warmer and drier conditions, a longer growing season will not benefit xylem formation of conifers, and in turn warming-induced drought could limit carbon sequestration by reducing the rate of cell production.

Keywords: conifer, wood production, carbon sequestration, growing season length, growth rate, drought stress

重金属 Cd 对杨树直立生长和倾斜生长下树干部分解剖特征的影响

戎恭,刘盛全*

（安徽农业大学林学与园林学院，合肥 230036）

摘要：以 30 棵一年生人工林 69 杨(*Populus deltoids* cv. I-69/55)为研究对象，在生长季节开展人工倾斜树干试验，将其中的 15 棵苗木人工倾斜 45°，将直立生长和倾斜生长的苗木分别平均分成 5 组（每组 3 棵），分别施加 0，5，20，50，100mg/kg 的重金属 Cd。记为 C_0、C_1、C_2、C_3、C_4。苗木生长 8 个月后开始取样，树干按其纵向上的高度分为顶部、中部和基部，倾斜生长分应拉区和对应区对其微纤丝角、结晶度、纤维长度和导管长度以及双壁厚进行测定分析。结果表明：1）随着土壤中重金属 Cd 浓度的增加，不同生长方式下的杨树微纤丝角的变化不同，倾斜生长下的应拉区微纤丝角小于对应区。方差分析表明不同 Cd 浓度和不同区域对微纤丝角的影响显著。2）随着土壤中重金属 Cd 浓度的增加，不同生长方式下杨树结晶度的变化不同，倾斜生长下应拉区结晶度大于对应区。在树干纵向分布上，结晶度总是呈现出基部＞中部＞顶部的趋势。方差分析表明，不同 Cd 浓度和不同区域对结晶度的影响显著。3）随着土壤中重金属 Cd 浓度的增加，不同生长方式下杨树的纤维长度变化不同，在 C_0 与高浓度处理下（C_4）倾斜生长中应拉区纤维长度小于对应区，而其他浓度处理下（C_1、C_2、C_3）则为应拉区大于对应区。在树干纵向分布上，纤维长度总是呈现出基部＞中部＞顶部的趋势。方差分析表明，不同 Cd 浓度对纤维长度的影响显著，不同区域对纤维长度影响不显著。4）随着土壤中重金属 Cd 浓度的增加，直立生长下的导管长度大于倾斜生长，倾斜生长下应拉区的导管长度大于对应区。在树干纵向分布上，在倾斜生长下导管长度呈现出基部＞中部＞顶部的趋势。方差分析表明，不同 Cd 浓度和不同区域对结晶度的影响显著。5）随着土壤中重金属 Cd 浓度的增加，直立生长与倾斜生长下的双壁厚呈现出不同的变化趋势，低浓度处理下（C_0、C_1）为直立生长小于倾斜生长，高浓度处理中（C_2、C_3、C_4）则与此相反。方差分析表明，不同 Cd 浓度对双壁厚的影响显著，不同生长方式和高度对双壁厚的影响不显著。

关键词：69 杨；直立生长；倾斜生长；应拉木；重金属 Cd;

Effects of Heavy Metal Cd on the Anatomical Characteristics of poplar trunk under Upright growth and Leaning growth

Gong Rong, Shengquan Liu*

(School of Forestry and Landscape A rchitecture, Anhui Agricultural University, Hefei 230036)

Abstract: Taking 69 poplars(*Populus deltoids* cv. I-69/55) of 30 annual plantation as the research object, the artificially inclined trunk experiment was carried out in the growing season. The 15 seedlings were artificially inclined to 45°. The upright and inclined seedlings were divided into 5 groups (3 in each group) on average, and 0,5,20,50,100 mg/kg of heavy metal Cd were added respectively. Note C_0, C_1, C_2, C_3, C_4. Samples were taken after 8 months of seedling growth. The trunk was divided into top, middle and base according to its longitudinal height. The Microfiber Angle, Crystallinity, Fiber length, vessel length and double wall thickness were measured and analyzed in the Tension wood area and Opposite wood area. The results show that:1）With the increase of the concentration of heavy metal Cd in the soil, the microfiber Angle of poplar under different growth modes varied, and the microfiber Angle of tension wood area under inclined growth was smaller than that of opposite wood area. Analysis of variance showed that different Cd concentrations and different regions had significant effects on microfilament Angle. 2）With the increase of Cd concentration in soil, the change of poplar crystallinity was different under different growth modes, and the crystallinity of tension wood area was greater than that of opposite wood area under inclined growth. In the longitudinal distribution of trunk, the crystallinity always showed a trend of base > middle > top. Analysis of variance showed that different Cd concentration and different region had significant effect on crystallinity. 3）With the increase of Cd concentration in soil, the fiber length of poplar was different under different growth modes. The fiber length in the tension wood area was smaller than that in the opposite wood area under the treatment of C_0 and high concentration (C_4), while the fiber length in the tension wood area was larger than that in the opposite wood area under other concentrations (C_1, C_2, C_3). In the longitudinal distribution of trunk, the fiber length always showed the trend of base > middle > top. Variance analysis showed that different Cd concentrations had significant effect on fiber length, but different regions had no significant effect on fiber length. 4）With the increase of the concentration of heavy metal Cd in soil, the length of the vessel under upright growth was greater than that under leaning growth, and the length of the vessel under tension wood area was greater than that in the opposite wood area.

In the longitudinal distribution of the trunk, the length of the vessel showed a trend of base > middle ＞top under leaning growth. Analysis of variance showed that different Cd concentrations and different regions had significant effects on crystallinity. 5）With the increase of the concentration of heavy metal Cd in the soil, the double wall thickness under vertical growth and inclined growth presented different trends. Under low concentration treatment (C_0, C_1), vertical growth was less than inclined growth, while under high concentration treatment (C_2, C_3, C_4), it was the opposite. Analysis of variance showed that different Cd concentrations had significant effects on double wall thickness, while different growth patterns and heights had no significant effects on double wall thickness.

Keywords: 69 Poplar, Upright growth, Leaning growth, Tension wood, Heavy mental Cd

皖南 10 种散生竹材导管分子形态特征研究[2]

何伟　崔浩然　汪佑宏*

（安徽农业大学　林学与园林学院　合肥 230036）

摘要：为了更好的对散生竹材加以利用，采用显微成图像分析系统，对近实心茶秆竹、四季竹、粉酸竹、筚竹、短穗竹、巴山木竹、桂竹、摆竹、长叶苦竹及小叶唐竹共 10 种竹种导管分子形态特征进行了研究。结果显示：10 种竹材导管分子的平均长度、直径及密度平均值依次是近实心茶秆竹：1101.060um、62.712um、1.8 个/mm²；四季竹：795.960um、72.572um、1.6 个/mm²；粉酸竹：919.060um、81.702um、1.35 个/mm²；筚竹：810.278um、50.151um、3.47 个/mm²；短穗竹：841.427um、61.529um、1.92 个/mm²；巴山木竹：1127.187um、70.308um、1.75 个/mm²；桂竹：725.877um、68.434um、3.12 个/mm²；摆竹：924.299um、66.046um、1.92 个/mm²；长叶苦竹：881.096um、109.755um、1.62 个/mm²；小叶唐竹：810.879um、71.568um、1.55 个/mm²。近实心茶秆竹、筚竹、巴山木竹等竹种具有较强的抗旱能力。

关键词：散生竹；导管分子；长度；直径；密度

Vessel Elements Morphological Characteristics of 10 Species of Scattered Bamboo in Southern Anhui Province

He W, Cui H R, Wang Y H*

(college of forestry and landscape architecture, Anhui Agricultural University, Hefei 230036, China)

Abstract: In order to make better use of scattered bamboo, the morphological characteristics of vessel elements of ten bamboo species, i.e. *Pseudosasa subsolida*, *Oligostachyum lubricum*, *Acidosasa chienouensis*, *Qiongzhuea tumidinoda*, *Brachystachyum densiflorum*, *Bashnia fargesii*, *Phyllostachys bambusoides*, *Indosasa shibateoides*, *Pleioblastus chino* var. *hisauchii* and *Sinobambusa parvofolia* were studied with the microscopic image analysis system. The results showed that the average length, diameter and frequency of vessel elements of 10 kinds of bamboos were as follows: The number of *P. subsolida* was 1101.060um, 62.712um and 1.8 pieces/mm^2, the number of *O. lubricum* was 795.960um, 72.572um and 1.6pieces/mm^2, the number of *A. chienouensis* was 919.060um, 81.702um and 1.35 pieces/mm^2, the number of *Q. tumidinoda* was 810.278um, 50.151um and 3.47 pieces/mm^2, the number of *B. densiflorum* was 841.427um, 61.529um and 1.92pieces/mm^2, the number of *B. fargesii* was 1127.187um, 70.308um and 1.75pieces/mm^2, the number of *P. bambusoides* was 725.877um, 68.434um and 3.12pieces/mm^2, the number of *I. shibateoides* was 924.299um, 66.046um and 1.92pieces/mm^2, the number of *P. chino* var. *hisauchii* was 881.096um, 109.755um and 1.62pieces/mm^2, and the number of *S. parvofolia* was 810.879um, 71.568um and 1.55pieces/mm^2 respectively. *P. subsolida*, *Q. tumidinoda* and *B. fargesii* have strong drought resistance.

Key words: Scattered bamboo, Vessel elements, Length, Diameter, Frequency

---

[2]项目资助：国际竹藤中心安徽太平试验中心开放基金项目“中国主要散生竹构造特征的研究”。

作者简介：何伟，硕士研究生，主要从事生物质材料构造方面研究，E-mail: 2737509830@qq.com

通讯作者：汪佑宏，博士，教授。E-mail：wangyh@ahau.edu.cn

近年来，我国木材资源的市场需求量供不应求，导致木材价格的飞涨和乱砍乱伐的现象层出不穷，因此寻找可替代的资源成为急需解决的问题[1]。竹材、藤材作为可再生的绿色材料具有很好的替代价值，尤其是竹材更是被广泛的应用。散生竹材属于禾本科竹亚科绿色植物，生长十分迅速，只要 40~120 天便可达到成竹高度，远高于木材的成长速度[2]。我国的竹材资源十分丰富，全球的竹材植物大约有 70 属 1200 多种，而我国就有 39 属 500 余种，竹林面积高达 641.16 万 hm^2,占到了全球的三分之一[3]。竹子因其具有生命力顽强、弹性佳、韧性好和抗撕裂强度高等优良特性，被广泛应用于家具、板材、建筑等行业[6]；同时，竹子在我国文化史上的崇高地位，具有浓烈的人文关怀属性，用竹材做成的产品又物美价廉，因此，竹材制品被越来越多的人所认可、接受和喜爱[6-8]，具有巨大的经济价值和广阔的市场前景。

因此，试验选择黄山地区近实心茶秆竹（*Pseudosasa subsolida*），四季竹（*Oligostachyum lubricum*），粉酸竹（*Acidosasa chienouensis*），筇竹（*Qiongzhuea tumidinoda*），短穗竹（*Brachystachyum densiflorum*），巴山木竹（*Bashnia fargesii*），桂竹（*Phyllostachys bambusoides*），摆竹（*Indosasa shibateoides*），长叶苦竹(狭叶青苦竹)（*Pleioblastus chino* var. *hisauchii*）及小叶唐竹（*Sinobambusa parvofolia*）共 10 种散生竹为研究对象，通过对其导管分子的长度、直径及密度等特征进行分析，对于更好地了解竹材基本材性、加大对竹材的加工利用，进而缓解木材供求矛盾有着十分重要的意义。

1 材料与方法

1.1 实验材料

10 种散生竹材采自安徽省黄山地区，无病腐、无弯曲、生长适中等其它无严重缺陷的散生竹材。

1.2 实验方法

1.2.1 软化处理

先用微波法将竹材试样软化至下沉，然后放入冰醋酸与双氧水体积为 1:1 的混合溶液中，在 60℃下软化约 4 小时。

1.2.2 制片

依次经切片→番红溶液染色→蒸馏水脱色→50%、75%、95%、100%的乙醇梯度脱水→二甲苯透明→中性树胶封片→30-40℃干燥 3-4 个小时、备用。

1.2.3 离析

将切片后剩余的试样再剖成火柴棒大小，应用富兰克林法离析成单根导管分子、备用。

1.2.4 测试

应用显微成像分析系统，对导管分子长度、直径、密度每组测试不少于 30 个重复。

2 结果与分析

2.1 导管分子长度

10 种散生竹材的导管分子长度数据见表 1。通过对比分析可知，巴山木竹导管分子长度的分布范围为 96.547-2952.800um，其导管分子长度的最大值与最小值是 10 种竹材试样中差异最大的；同时，巴山木竹导管分子的平均长度也是 10 种竹材中最大的，为 1127.187um，其次是近实心茶秆竹为 1101.060um，桂竹的导管分子平均长度是 10 种竹材中最小的，仅为 725.877um。

一般认为：导管分子的长度越短，进化程度越高；导管分子的长度越长，进化程度越低[9-10]。10 种散生竹

导管分子的平均长度为巴山木竹>近实心茶秆竹>摆竹>粉酸竹>长叶苦竹>短穗竹>小叶唐竹>筇竹>四季竹>桂竹；因此，如仅依据导管分子长短推测，10 种竹子进化程度由低到高依次为：巴山木竹、近实心茶秆竹、摆竹、粉酸竹、长叶苦竹、短穗竹、小叶唐竹、筇竹、四季竹和桂竹。

表 1　导管分子长度

Table 1 The length of vessel elements

竹种	最小值	最大值	均值
近实心茶秆竹(*P. subsolida*)	128.627	1909.70	1101.06
四季竹(*O. lubricum*)	472.302	2298.22	795.96
粉酸竹(*A. chienouensis*)	361.649	1559.43	919.06
筇竹(*Q. tumidinoda*)	87.756	1432.488	810.278
短穗竹(*B. densiflorum*)	65.230	1859.89	841.427
巴山木竹(*B. fargesii*)	96.547	2952.800	1127.187
桂竹(*P.bambusoides*	375.907	1189.985	725.877
摆竹(*I. shibateoides*)	400.986	1674.49	924.299
长叶苦竹(*P. chino* var.	335.951	2291.23	881.096
小叶唐竹(*S. parvofolia*)	343.365	2169.55	810.879

2.2 导管分子直径

竹材导管分子直径见表 2。由测试结果可知，长叶苦竹的导管分子平均直径为 109.755um，为 10 种散生竹材中最大的，其次是粉酸竹为 81.702um，最小的是筇竹为 50.151um。根据对矢竹、慈竹等 17 种竹子导管分子的测定，竹材的导管分子平均直径在 85um 左右，10 种散生竹材导管分子直径符合竹材平均直径[11]。

导管直径作为其进化程度的指标之一，导管分子直径越大，进化程度越高；相反，进化程度越低。10 种散生竹材导管分子直径大小为，长叶苦竹>粉酸竹>四季竹>小叶唐竹>巴山木竹>桂竹>摆竹>近实心茶秆竹>短穗竹>筇竹，因此，如仅以导管分子直径为依据推测，10 种竹子进化程度由低到高依次为：筇竹、短穗竹、近实心茶秆竹、摆竹、桂竹、巴山木竹、小叶唐竹、四季竹、粉酸竹和长叶苦竹。

表 2 导管分子直径

Table 2　The average diameter of vessel elements

竹种(bamboo species)	一组(NO.1)	二组(NO.2)	三组(NO.3)	平均值
近实心茶秆竹（*P. subsolida*）	55.261	62.437	70.438	62.712
四季竹（*O. ubricum*）	71.119	64.573	82.025	72.572
粉酸竹（*A. chienouensis*）	86.542	70.32	88.244	81.702
筇竹（*Q. tumidinoda*）	53.544	50.799	46.109	50.151
短穗竹（*B. densiflorum*）	59.574	55.558	69.456	61.529
巴山木竹（*B. fargesii*）	68.183	73.436	69.306	70.308
桂竹（*P.bambusoides f.bambusoides*）	70.889	36.755	97.658	68.434
摆竹（*I. shibateoides*）	67.51	55.805	74.824	66.046
长叶苦竹（*P. chino var. Hisauchii*）	101.996	125.251	102.017	109.755
小叶唐竹（*S. parvofolia*）	76.619	60.99	77.095	71.568

2.3 导管分子的长宽比

通过实验测量后计算导管分子长宽比得图 1 可知：10 种散生竹材中近实心茶秆竹的长宽比最大，为 17.905。

其次是筇竹、巴山木竹长宽比分别为 16.157、15.943。长宽比最小的是长叶苦竹，为 8.028，其次是四季竹、酸粉竹分别为 10.968、11.247。从中可知近实心茶秆竹、筇竹、巴山木竹的长宽比与长叶苦竹、四季竹、粉酸竹、小叶唐竹等竹种的差异性较大，而短穗竹、桂竹及摆竹等竹种不具有明显的差异性。

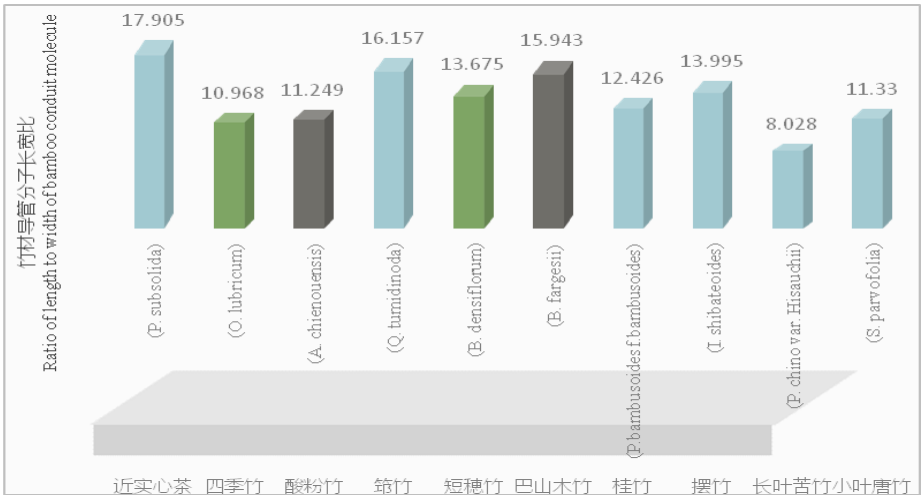

图 1 导管分子长宽比

Fig.1 Ratio of length to width of vessel elements

2.4 导管分子的密度

导管分子分布密度见图 2。对比分析可可知，筇竹、桂竹的导管分子分布相对而言较为密集，对应值分别为 3.483 个/mm²与 3.071 个/mm²；分布较为稀疏的是粉酸竹、四季竹，导管分子分布密度分别为 1.344 个/mm² 与 1.422 个/mm²。

竹壁在宏观条件下由三部分组成，竹皮、髓环组织与竹肉组成，竹肉由维管束与基本组织构成，而导管分子分布在维管束中，包括原生木质部导管分子和后生木质部导管分子，原生木质部导管分子靠近髓腔，后生木质部导管分子在维管束的两侧。维管束分布较多的为竹青，分布较少的为竹黄[12]。竹材输水能力与导管分子的长度、导管分子直径有关[13]，而导管分子密度较大也是其增强输送水分能力的一个因素。竹材导管分子密度大小关系为：筇竹>桂竹>近实心茶秆竹>摆竹>短穗竹>巴山木竹>长叶苦竹>小叶唐竹>四季竹>粉酸竹。

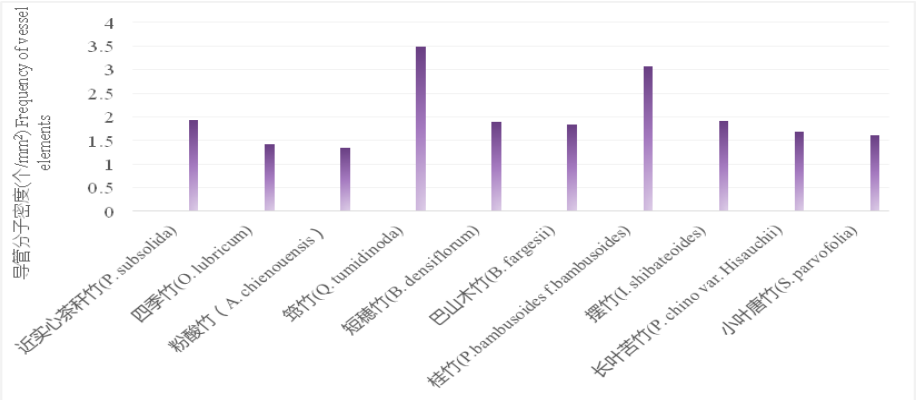

图 2 导管分子密度

Fig.2 The frequency of vessel elements

3 结论与讨论

3.1 在竹材的初生木质部中，导管包括环纹导管、螺纹导管、梯纹导管、网纹导管及孔纹导管[14]。从植物

导管分子演化趋势研究，短导管分子进化程度高于长导管分子，导管分子直径越小，进化程度越低，长/宽比越大，进化程度越低[13]。通过对比分析，在 10 种散生竹材当中，长叶苦竹的长/宽比为 8.028、直径为 109.755um、长度为 881.096um，近实心茶秆竹的长/宽比为 17.905、直径为 62.712um、长度为 1101.060um，长叶苦竹较近实心茶秆竹长/宽比短 9.877um，直径大 47.043um，长度短 219.964um。通过对比分析可以得到在 10 种竹材当中，长叶苦竹是这 10 种散生竹材当中进化程度最高的，近实心茶秆竹是最为原始的。

3.2 从物理学角度看，植物体内运输效率的快慢与其导管分子的端壁斜度的大小、导管分子的直径、长度有着密切的关系，导管分子长度越大，直径越小，端壁斜度越大，则输水阻力越大，运输效率越低。反之，则输水阻力越小，输水效率越高[15]。由于 10 种散生竹材导管分子端壁都是垂直的竹种，端壁的斜度可以忽略不计，从而只要考虑竹材的导管分子长度与直径，即长宽比越大越好。通过实验测得长叶苦竹、四季竹导管分子直径分别为 109.755um、72.572um，导管分子长度分别为 881.096um、795.960um，长宽比分别仅为 8.028 和 10.968，输送水分能力相对较强。除此之外，还有粉酸竹、小叶唐竹等竹种也是有较强的输送能力。而近实心茶秆竹、筚竹、巴山木竹的输送水分的能力相对而言就较弱，导管分子的直径分别为 62.712um、50.151um、70.308 um 及导管分子的长度分别为 1101.060um、810.278um、1127.187 um，导管分子长宽比分别高达 17.905、16.157 和 15.943，从而可以得出近实心茶秆竹、筚竹、巴山木竹等竹种具有较强的抗旱能力。这与李国秀[16]等人认为能够在干旱环境中生长的物种其导管分子直径较小、长度较长的观点是一致的。分析认为导管分子的直径小、长度长虽能提高其内聚力，从而有利于水分运输的存贮性，但不利于导管分子中水分的高效运输，然而导管分子直径较大、长度较长能够保障其水分运输的高效率性。说明植物导管分子自身的生物特性与其进化程度有着相关性，其进化异速性特征间可能存在功能上的平衡[17]-[18]。从而可得出生态环境与植物导管分子有一定的联系，与 Carlquist[19] 提出的木质部进化的生态学途径相一致。

参考文献

[1]. 陈勇. 基于木材安全的中国林产品对外依存度研究[D]. 北京：中国林业科学研究院，2008

[2]. 卢燕华.“竹老大”-毛竹[J]. 广西林业，2015（08）:37-38

[3]. 李延军，许斌，张齐生，等.我国竹材加工产业现状与对策分析[J].林业工程学报，2016,1（01）:2-7

[4]. 江泽慧，岳祥华，费本华. 中国竹类植物图鉴[M]. 北京：科学出版社，2020.10

[5]. 国家林业和草原局. 中国森林资源报告[M]. 北京：中国林业出版社，2019.05

[6]. 李国秀，郑宝江．10 种茶藨子属植物导管分子形态特征及其生态适应性比较研究[J]．植物研究，2014，34（1）：25-31

[7]. 郭豫，邓首哲. 竹纤维性能及发展展望[J]. 中国麻业科学，2008，30（6）：321-325

[8]. 薛孝川. 竹纤维的性能和应用[J]. 化纤与纺织技术，2007（2）：30-33

[9]. Bailey I W. The cambium and its derivative tissues. Ⅱ.Size variations of Cambial initials in gymnosperms and angiosperms [J]. American Journal of Botany,1920,7(9):355-367

[10]. 张立非，姜笑梅，周崟. 阔叶树材导管分子螺纹加厚的电镜观察与探讨[J]. 林业科学，1994，30（1）:64-68

[11]. FUJII T. Application of resin casting method to wood anatomy[J]. Plant Morphology,1993,5(1):3-18.DOI:10.5685/plmorphol.5.3

[12]. 江泽慧. 世界竹藤[M]. 沈阳：辽宁科学技术出版社， 2002.09

[13]. 李红芳，田先华，任毅. 维管植物导管及其穿孔板的研究进展[J]. 西北植物学报，2005，25（2）:419-424

[14]. 刘一星，赵广杰. 木材学[M]. 北京：中国林业出版社，2014，07

[15]. 谷李伟. 黑龙江绣线菊属 15 种植物导管分子形态结构研究[J]. 电子显微学报，2015，34（1）:74-75

[16]. 李国秀，郑宝江．10 种茶藨子属植物导管分子形态特征及其生态适应性比较研究[J]．植物研究，2014，34（1）：25-31

[17]. 晁娟.中国 8 种欠知名竹种基础材性数据采集及比较分析[D] .合肥：安徽农业大学，2018

[18]. 周海燕，赵爱芬．科尔沁沙地黄柳气孔导度和水分状况随季节和地形的变化特征[J]．植物学通报，2000，17(6):543-547

[19]. CARLQUIST S.Wood anatomy of coriariaecae:phylogenetic and ecological implications[J].Syst.Bot.,1985,10(2):174-183

Seasonal dynamic changes of cell polysaccharide granules in cambium active phase of Taxodium ascendens

JieyunTao YoumingXu* Cong Liu Han LinKunxi Wang

College of Forestry and Horticulture, Huazhong Agricultural University, Wuhan China

Objectives: Pond cypress（*Taxodium ascendens Brongn*）is an important timber specie introduced and cultivated in the water grid region of Yangtze River in China. To study the changes of polysaccharide storage in the active phase of cambium is helpful to understand the mechanism of its wood formation and improvement, and to improve its wood economic value.

Methods：Five Pond cypress trees were selected as samples. Samples were taken every 7 days from March to October, and every other month from November to March of the following year. The branches with good healthy growth of 1-3 years were selected and their middle parts was cut into 0.5~1.0cm segments, and paraffin sections were made with a thickness of 10μm, stained with PAS reaction, and photographed by OLYMPAS universal microscope.

Results：The contents in parenchyma of Pond cypress could be dyed purple red granules by PAS reaction, mainly polysaccharide granules (not starch granules). The vascular cambium of Pond cypress was active at the beginning of April. At this time, a large number of purple polysaccharide granules can be seen in various parenchyma, but they were not observed in vascular cambium. After that, the storage of polysaccharides in parenchyma tissue gradually decreased and disappeared at the end of July, which reflected the facts that a large number of daughter cells produced by cambium meristem division need to consume a lot of nutrients. At the beginning of August, a small amount of polysaccharides appeared in parenchyma tissues, at this time, the activity of cambium cells decreased, and the nutrients used for activity decreased. From August to the last ten days of September, the storage of polysaccharides in various parenchyma kept increasing, and the granules were larger; then, the storage of polysaccharides decreased, and the particles became smaller obviously. From September to the end of November, almost no polysaccharide was observed, which indicated that the newly produced daughter cell wall thickening and maturation consumed a lot of nutrients. From late January to early April of the following year, various parenchyma were filled with polysaccharides, which were needed for cambium activities in the coming year.

Conclusion: The cambium division activities of Pond cypress form phloem at first and then xylem. The changes of storage materials in various parenchyma cells of wood are closely related to the division of cambium cells and the growth and maturation of daughter cells. The appearance of new mature phloem is beneficial to hydrolyze part of the stored polysaccharide granules to meet the needs of the cambium division activities and tree growth.

Key words: Pond cypress, Cambium, Parenchyma, Polysaccharides, Seasonal variation

Acknowledgements: This paper is financially supported by National Natural Science Foundation of China (Grants No 31971584 and 31570551).

*E-mail of corresponding author: xuyouming@mail.hzau.edu.cn

建筑用原竹抗菌防裂体系的构建

孙芳利[1*]，姜俊[1]，张文豪[1]，王婕[1]，王慧[1]，张艳[1]

（1. 浙江农林大学工程学院，浙江省杭州市临安区武肃街 666 号）

摘要：随着竹产业、竹建筑和竹文化的融合发展，原竹独特的文化内涵、地域特色、结构和性能优势，使其不仅能“代木”，更能“胜木”，成为乡村振兴和城市建设中引人注目的风景。但是，原竹的霉腐和开裂严重制约了其在建筑领域的应用。

报告将从原竹建筑的应用和存在的问题出发，分析原竹作为建筑用材的霉腐特点、产生原因和解决途径。在此基础上，在竹材中原位构建聚甲基丙烯酸羟乙酯-丙烯酰胺交联共聚物，采用红外光谱和热分析研究共聚物的特性，并将处理材分别置于浸水-干燥和加湿-干燥循环中测试其尺寸稳定性。红外分析显示出甲基丙烯酸羟乙酯和丙烯酰胺形成了共聚物，热分析表明共聚物的热降解温度和玻璃化转变温度均增加。

处理材的扫描电镜观察发现，聚合物主要填充并堵塞纹孔，细胞壁增容明显。浸水-干燥测试和加湿-干燥显示，处理材的抗胀率分别达到 49.4%和 41.7%。以木霉（*Trichoderma viride*）、青霉（*Penicillium citrinum*）和黑曲霉（*Aspergillus niger*）为试菌，对处理材进行室内防霉性能测试。结果表明，交联聚合物处理材霉菌综合感染面积为 13.5%，而对照材在不到一周时间达到 100%。以白腐菌为彩绒革盖菌（*Trametes versicolor*）和褐腐菌密黏褶菌（*Gloeophyllum trabeum*）为试菌，测试处理材的耐腐性。结果表明，接种白腐菌和褐腐菌后，其腐朽后质量损失率比硼盐单独处理竹材分别降低了 52.6%和 37.9%。抗流失试验发现，负载硼盐防腐剂的载药聚合物处理试样，其硼盐流失率比硼盐单独处理材提高 16.8%。可以看出，在竹材内构建载药聚合物网络不仅能提高竹材的尺寸稳定性，还能有效抑制防腐剂的流失，提高竹材的耐腐性。

关键词：原竹，载药聚合物，尺寸稳定性，防霉，防腐

Construction of fungal and cracking resisting systems for raw bamboo as building material

Sun Fangli[1*], Jiang Jun[1], Zhang Wenhao[1], Wang Jie[1], Wang Hui[1], Zhang Yan[1]

（1. School of Engineering, Zhejiang A & F University, Hangzhou, Zhejiang, China, 20000050@zafu.edu.cn）

Abstract: Raw bamboo possesses unique cultural connotation, regional characteristics, structural and performance advantages, accordingly, it can not only "substitute wood", but also "win wood". Raw bamboo enables distinctive structure to be built, which arouses much attention in rural revitalization and urban construction. However, the low resistances of raw bamboo against mold and decay fungi, as well as the risk of splitting and cracking seriously restricted its application in the field of architecture.

Considering the application and existing problems of raw bamboo in building, the report analyzes the characteristics, reasons and solutions for mold, decay and cracking of raw bamboo as building materials. Subsequently, chemical modification of raw bamboo by in situ growth of poly-HEMA and NIPAM (PHN) copolymer was studied. The formation of PHN was confirmed by using Fourier transform infrared spectroscopy and thermogravimetric analysis, which shows the characteristics peaks of both HEMA and PHN, and increased pyrolysis and glass transition temperatures, respectively. After impregnation of PHN pre-polymerization formulation to bamboo, it was observed that PHN filled most of the pits in the bamboo cell wall and formed a tight network. Moreover, the dimensional stability of PHN treated bamboo was significantly improved with an anti-swelling efficiency of 49.4% and 41.7%, respectively, after wetting–drying cycles and soaking–drying cycles. A mold infection rate of 13.5% was observed in PHN-treated bamboo as compared to a 100% infected control group after a 30-day mold resistance test. Furthermore, the resistances of boron loaded PHN treated bamboo against decay fungi was conducted according to the ASTM D1413. Results indicated that the mass loss dropped by 52.6% and 37.9%, respectively, comparing with boron treated bamboo. Besides, the leaching resistance of boron from drug loaded copolymer increased by 16.8% as compared with boron treated one. Obviously, construction of drug loaded crosslinked copolymer in bamboo has the advantage of enhanced dimensional stability, restrained preservative leaching and improved decay resistance.

Keywords: bamboo; drug loaded polymer; dimensional stability; mold resistance, decay resistance

The authors thank the National Natural Science Foundation of China for funding the project (32071853) and Key Natural Science Foundation of Zhejiang Province (LZ20C160004)

高韧性环境友好型固体环氧树脂的改性制备及性能研究

杨佳瑶 何星蔚 刘晓欢 傅深渊*

（浙江农林大学工程学院，浙江 杭州 311300）

摘要：环氧树脂是最重要热固性树脂之一，由于其优异的机械强度、热稳定性和耐化学性，其在粘合剂、涂料和其他特殊复合材料等领域有广泛的应用。与液体环氧树脂相比，固体环氧树脂易于储存和运输，且不需要考虑粘性动力学特性。与固化剂混合后，可得到贮藏时间长、操作简便、不含有机溶剂和挥发性物质，同时具有足够的混溶性和流动性，固化工艺灵活，具有良好的发展前景。开发一种具有高韧性固体环氧树脂体系是至关重要的。因此，本研究通过一步熔融共混的方法，使用环氧化端羟基聚丁二烯(EHTPB)改性制备了一种高韧性、高强度且环保的固体环氧树脂体系。并对整个体系的化学结构、力学性能、固化性能和热性能进行了表征测试。其中 EHTPB 改性环氧树脂具有优异的韧性，断裂伸长率比纯环氧树脂提高 100%。通过断裂面的显微结构表明，橡胶相中的传递应力和耗散能是 EHTPB 增韧的主要机理。EHTPB 对固体环氧树脂的增韧效果优于已有报道的液体环氧树脂。同时，在 EHTPB 添加量为 10% wt%时，EHTPB 改性环氧树脂表现出较高的强度，其中抗弯强度提高 22%，冲击强度提高 101%。此外，在 10% wt% EHTPB 添加时，EHTPB 改性环氧树脂固化反应的活化能从 73.89 kJ·mol^{-1} 下降到 65.12 kJ·mol^{-1}，EHTPB 促进了固化反应的进行。同时，EHTPB 改性环氧树脂具有良好的热稳定性，在 10% wt% EHTPB 添加时，初始降解温度从 249℃升高到 313℃。本研究为高韧性环保型固体环氧树脂的制备提供了一种简便、高效的制备方法。

关键词：固体环氧树脂；环氧化端羟基聚丁二烯；韧性；固化行为；热稳定性

High-toughness, environmental-friendly solid epoxy resins: preparation, mechanical performance, curing behavior, and thermal properties

Jiayao Yang Xingwei He Xiaohuan Liu Shenyuan Fu*

（School of Engineering, Zhejiang A & F University, Hangzhou 311300）

Abstract: Epoxy resin is one of the most important thermosetting resins. Due to its excellent mechanical strength, thermal stability and chemical resistance, it is widely used in adhesives, coatings and other special composite materials. Solid epoxies are easier to store and transport than liquid epoxies and do not require consideration of viscosity dynamics. After being mixed with curing agent, it can be obtained with long storage time, easy operation, free of organic solvents and volatile substances, sufficient miscibility and fluidity, flexible curing process, and good prospects for development. Therefore, it is very important to develop a solid epoxy resin system with high toughness. Herein, we have developed a high-performance environmental-friendly solid epoxy resin modified with epoxidized hydroxyl-terminated polybutadiene (EHTPB) via one-step melt blending. The characterization, mechanical performance, curing behavior, and thermal properties of EHTPB-modified epoxy resin were investigated. EHTPB-modified epoxy resin exhibited excellent toughness with a 100% increase in elongation at break of tensile than that of neat epoxy resin. The transfer stress and dissipated energy in the rubber phase were predominant mechanisms of toughening. The toughening effect of EHTPB on solid epoxy resin was better than that of some of the previously reported liquid epoxy resins. Meanwhile, at 10 wt% of EHTPB loading, the EHTPB-modified epoxy resin displayed high strength and 22% and 101% improvement of flexural strength and impact strength, respectively. Moreover, at 10 wt% of EHTPB loading, the activation energy of EHTPB-modified epoxy resin for curing reaction decreased from 73.89 to 65.12 kJ ṁol-1, which is beneficial for the curing reaction. Furthermore, EHTPB-modified epoxy resin had a good thermal stability and the initial degradation temperature increased from 249oC to 313oC at 10 wt% of EHTPB loading. This work provides a simple-preparation and highly efficient and large-scale approach for the production of high-toughness environment-friendly solid epoxy resins.

Keywords: Environment-friendly solid epoxy resin; Epoxidized hydroxyl-terminated polybutadiene (EHTPB); Toughness; Curing behavior; Thermal properties

燃烧木粉变碳纳米片用于锌离子杂化电容器

楼高波　傅深渊*　陈浩*

(浙江农林大学工程学院，杭州 311300)

摘要：水系锌离子杂化电容器(ZHS)凭借其理论容量高、安全性好、成本低而备受关注。其中，电导率高、电化学稳定性好的碳基材料被认为是一种理想的 ZHS 正极材料。近年来，生物质资源凭借其可再生、环境友好等特点引起了人们的广泛兴趣。各种生物质衍生碳材料被成功应用于超级电容器电极材料。然而，由于生物质资源的复杂结构和多样组成，开发高效、简便的活化方法制备高电化学性能的多孔活性碳材料仍面临诸多挑战。例如：典型的 KOH 和 H_3PO_4 活化被广泛用于制备生物质衍生碳材料，然而 KOH 和 H_3PO_4 的高腐蚀性会造成严重的设备损耗和环境危害。典型的非腐蚀型活化剂如 $ZnCl_2$ 和 K_2CO_3 对环境的影响较小，但不能提供满意的活化效果。因此，开发一种高效、简便的合成方法将生物质转化为可用于 ZHS 电极的高性能碳材料具有重要的意义。

本文通过木材的一步燃烧转化制备了一种 N，O 共掺杂的二维碳纳米片材料，其在锌离子杂化电容器的正极材料应用方面具有良好的前景。该燃烧转化合成法一步即可实现木材的炭化、成孔和杂原子掺杂。在该燃烧转化工艺中，$Zn(NO_3)_2$ $6H_2O$ 为氧化剂和尿素分别作为氧化剂和燃料，它们之间的氧化还原反应释放出大量高温气体，导致木材中的管孔壁发生碳化爆裂，降解成大量的二维碳纳米片。其中 $Zn(NO_3)_2$ $6H_2O$ 除了充当氧化剂的作用，还可以作为锌源，产生锌物质（包括高温下的液态金属锌）。这些锌物质可以穿透并扩散到碳基体中，在除锌过程中可以产生大量的多孔结构。另外，尿素分解释放的 NH_3 和木材中天然存在的含氧物质作为氮源和氧源，在燃烧转化过程中可以同步实现碳纳米片的 N，O 共掺杂。因此，与典型的生物质衍生碳材料的不规则形态不同，制备的 N、O 共掺杂的多孔活性碳材料具有相对均一的二维片状结构和非常高的比表面积（1248m^2 g^{-1}），不仅缩短了电子/离子传输路径，优化了润湿性，而且还提供了丰富的界面活性位点，改善了离子吸附性能，从而提高了电化学活性。得益于这些优点，N、O 共掺杂的碳纳米片在锌离子杂化电容器中展现出了优异的比容量（111.0 mAh g^{-1}）、高的倍率性能（30 倍电流增长后保持 57.6%容量）、以及出色的能量密度（109.5 Wh kg^{-1}），并且具有超长的循环寿命，50000 次循环后容量保持率为 92.7% 。

关键词：锌离子杂化电容器；燃烧反应；木材衍生碳；纳米片

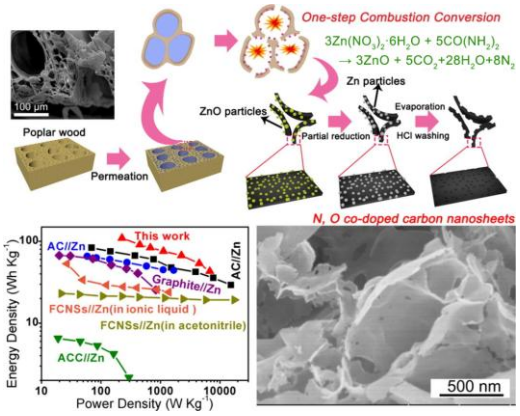

图 1 一步燃烧反应转化木粉制作碳纳米片的合成示意图及由其制作的 ZHS 的能量-功率密度图

Fig1 Synthesis of carbon nanosheets from wood powder by one-step combustion reaction and energy power density diagram of ZHS

Combustion Conversion of Wood to N, O co-doped 2D Carbon Nanosheets for Zinc-ion Hybrid Supercapacitors

LOU Gao-bo FU Shen-yuan* CHEN Hao*
(School of Engineering, Zhejiang A&F University, Hangzhou 311300, China)

Abstract: The aqueous Zn-ion hybrid supercapacitor (ZHS) has attracted great interest because of its high capacity, excellent safety, and low cost. Carbon-based materials with low environmental impact, good conductivity, and excellent electrochemical stability have been regarded as competent cathode materials for ZHSs. Recently, biomass-derived carbons are attracting tremendous research interest owing to the renewable, low-cost, and environment-friendly merits of biomass resources. Up to now, various kinds of biomass have been used to produce porous activated carbons for supercapacitor electrodes, including starch, rice straw, cornstalk, chitosan, peach gum, peanut shells, cotton, and so on. However, due to the complex structures and compositions of biomass resources, there are still many challenges in developing efficient and simple activation methods to prepare porous carbons with high electrochemical performances. For example, typical KOH and H_3PO_4 activations have been widely used to prepare biomass-derived carbon materials. Nevertheless, the high corrosivity of KOH and H_3PO_4 can cause serious equipment damage and environmental hazards, which limit their application. Typical non-corrosive activators (e.g. $ZnCl_2$ and K_2CO_3) have a small impact on the environment, but they are unable to provide satisfactory activation. Therefore, it will be of critical significance to develop an efficient and simple synthetic method to convert biomass into high-performance carbon materials for ZHS electrodes.

Here, an N, O co-doped two-dimensional (2D) carbon nanosheet material is successfully fabricated via a one-step combustion conversion of wood for the excellent usage as the cathode material in zinc-ion hybrid supercapacitors. In this CS process, the $Zn(NO_3)_2$ $6H_2O$ and urea served as oxidizer and fuel, respectively. The redox reaction between them released a large amount of high-temperature gases, which caused the carbonized walls of poplar wood hollow tubes to burst and degrade into numerous 2D carbon nanosheets. Unlike other typical metal nitrates used for the CS, $Zn(NO_3)_2$ $6H_2O$ was utilized not only as an oxidizer of CS in this work, but also as a zinc source to produce some zinc species (including liquid metal Zn at the high temperature), which can penetrate and diffuse into the carbon matrix. The removal of these zinc species produced an ample porous structure for the resultant carbon nanosheets. Furthermore, the NH_3 gas released from the urea decomposition and the oxygen-containing species in the original poplar wood served as nitrogen and oxygen dopants, respectively, to complete the N, O co-doping of the resulting carbon material. Due to the superior electrochemical properties endowed by 2D sheet structure, high specific surface area (1248 $m^2\ g^{-1}$), and N, O co-doping feature, the ZHS based on this N, O co-doped 2D carbon nanosheet material exhibited a superior specific capacity of 111.0 mAh g^{-1} at 0.1 A g^{-1}, high rate capability of 57.6% capacity retention at a 30-fold higher current, and impressive energy density of 109.5 Wh kg^{-1} at 225 W kg^{-1}. Most gratifyingly, it displayed ultralong cycling life with 92.7% capacity reservation after 50,000 charge-discharge cycles.

Keywords: Zinc-ion hybrid supercapacitor; combustion synthesis; wood-derived carbon; nanosheets.

水热法制备碳掺杂的氮化碳用于光催化降解甲基蓝

张平　蔡泰龙　段新朋　王喆*　金春德*

（浙江农林大学工程学院，临安，311300）

摘要：现在世界上水污染比较严重，影响着人们的身体健康，并且世界上的淡水仍处于紧缺状态，对污水进行治理是关系到人们未来身体健康的重要举措。目前，有多种方法来解决这个问题，比如吸附，生物降解，光催化等。其中，光催化技术因其高效、低成本和无污染等优点受到人们的广泛关注，此外光催化能够将污水中的污染物降解成二氧化碳和水，相比于用吸附材料只能吸附污染物并不能降解具有更大的优势。全球每年产生约50 亿吨生物质废渣，其中大部分被焚烧，产生许多有害物质，对环境造成破坏。如果能够有效利用农作物废渣，将会是保护环境、节约资源的重要举措。木聚糖是自然界中除纤维素外最丰富的多糖，它来源广泛,比如像稻草、玉米杆、玉米穗等农作物废渣。如果从农作物废渣中提取出来的木聚糖能够得到有效利用，将进一步提高生物资源的保护和利用。本研究中以木材纤维为碳源，采用水热法制备了碳掺杂类石墨相氮化碳的复合材料，该材料具有吸光能力强、电子和空穴分离效率高且不污染环境等优点。我们以三聚氰胺为原料，在马弗炉中以5℃/min 的升温速率升温到 550℃，然后反应 4 个小时得到淡黄色的类石墨相氮化碳。然后分别用 0.01g、0.02g、0.04g、0.08g 从玉米芯提取出来的木聚糖和 1g 类石墨相氮化碳和 50ml 的水混合在一起在 80℃恒温下搅拌 2 小时，然后放入 180℃的反应釜中反应 4h，90℃干燥 12 小时后取出，样品按木聚糖含量由少到多的顺序分别命名为 C1/g-C3N4、C2/g-C3N4、C3/g-C3N4、C4/g-C3N4。通过对 g-C3N4，C3/g-C3N4 进行 X 射线衍射,扫描电镜，透射电镜，傅里叶红外,X 射线光电子能谱，紫外可见漫反射等进行表征，发现 g-C3N4, C3/g-C3N4 被成功合成，并且紫外-可见漫反射图谱显示 C/g-C3N4 具有很强的吸光能力，其中 C3/g-C3N4 的吸光能力最强。光致发光光谱显示了 C3/g-C3N4 的峰要远低于 g-C3N4, 说明了 C3/g-C3N4 的空穴和电子的复合率要比纯的 g-C3N4 要低很多，更多的电子和空穴用于把污染物降解成二氧化碳和水，也进一步证明 C3/g-C3N4 的光催化性能相比于纯的 g-C3N4 已经提高不少。本文研究表明，此光催化剂对亚甲基蓝具有较强的吸附和光催化降解能力，其中 C3/g-C3N4 对甲基蓝的吸附降解率为 99.97%，远高于纯 g-C3N4。这种现象是由于碳掺杂类石墨相氮化碳后比表面积提高，对甲基蓝溶液有很强的吸附作用，增加了对可见光的吸收。另外掺杂碳元素后形成了离域的键，导致光电子与空穴的复合也减少了。因此，C3/g-C3N4 在染料的吸附和降解方面有很好的应用。

关键词：木聚糖;g-C3N4;碳掺杂;吸附;光降解;

Hydrothermal preparation of carbon-doped carbon nitride for photocatalytic degradation of methyl blue

Ping Zhang , Tailong Cai , Xinpeng Duan , Zhe Wang* , Chunde Jin*

（School of Engineering, Zhejiang A & F University, Lin’an, 311300, PR China）

Abstract: Now the world's water pollution is relatively serious, affecting people's health, and the world's fresh water is still in short supply, so the treatment of sewage is an important measure related to people's future health. Currently,

there are many methods to solve this problem, such as adsorption, biodegradation, photocatalysis, etc . Among them, photocatalysis technology has attracted wide attention due to its high efficiency, low cost and pollution-free advantages. In addition, photocatalysis can degrade pollutants in sewage into carbon dioxide and water. Compared with adsorbent materials that can only adsorb pollutants degradable has a greater advantage . The world produces about 5 billion tons of biomass waste residue every year, most of which are incinerated, producing many harmful substances and causing damage to the environment. If the crop residues can be effectively used, it will be an important measure to protect the environment and save resources. Xylan is the most abundant polysaccharide in nature except cellulose. It has a wide range of sources, such as straw, corn stalks, corn ears and other crop residues. If the xylan extracted from crop residues can be effectively used, the protection and utilization of biological resources will be further improved . In this study, xylan was used as the carbon source, and a carbon-doped graphite-like carbon nitride composite material was prepared by hydrothermal method. This material has the advantages of strong light absorption, weak recombination of electrons and holes, and no pollution to the environment. First, we use melamine as the raw material, then heat it up to 550℃ at a heating rate of 5℃/min in a muffle furnace, reacting for 4 hours to obtain light yellow graphite-like carbon nitride. 0.01g, 0.02g, 0.04g, 0.08g of xylan extracted from wood fiber material, 1g g-C3N4 and 50ml of water, mix together, stir at a constant temperature of 80℃ for 2 hours, and then put them in an autoclave heated to 180℃and maintained for 4 hours, then dried at 90℃for 12 hours and then taken out. The samples were named C1/g-C3N4, C2/g-C3N4, C3/g-C3N4, C4/g-C3N4 in order of xylan content. g-C3N4, C3/g-C3N4 were characterizied by XRD, SEM, TEM, FTIRetc ,which is found that g-C3N4, C3/g- C3N4 was successfully synthesized, and the ultraviolet-visible diffuse reflectance spectrum showed that C/g-C3N4 has a strong light-absorbing ability, and C3/g-C3N4 has the strongest light-absorbing ability. The photoluminescence spectrum shows that the peak of C3/g-C3N4 is much lower than that of g-C3N4, indicating that the recombination rate of holes and electrons of C3/g-C3N4 is much lower than that of pure g-C3N4, and more Electrons and holes are used to degrade pollutants into carbon dioxide and water, which further proves that the photocatalytic performance of C3/g-C3N4 has been improved a lot compared to pure g-C3N4. The research in this paper shows that this photocatalyst has strong adsorption and photocatalytic degradation capacity for methylene blue, and the adsorption degradation rate of MB by C3/g-C3N4 is 99.97%, which is much higher than pure g-C3N4. This phenomenon is due to the increased specific surface area of carbon-doped graphite-like carbon nitride, which has a strong adsorption effect on the solution and increases the absorption of visible light. In addition, the delocalized bonds are formed after carbon doping, which reduces the recombination of photoelectrons and holes. Therefore, C3/g-C3N4 has a good application in dye adsorption and degradation.

Keywords: xylan , g-C3N4 , carbon doping , adsorption , photodegradation

聚多巴胺辅助铜纳米粒子装饰的超疏水和抗菌木材

段新朋 刘淑敏 黄尔卓 沈潇源 王喆* 李松* 金春德*

（浙江农林大学工程学院，临安，311300）

摘要：作为一种天然的可再生资源，木材在社会经济建设和人类基本生活环境中发挥了重要作用。纤维素和半纤维素作为木材的主要成分，具有大量的亲水基团，会导致木材对湿气和水分的吸收。木材吸水吸湿后会出现尺寸变形，细菌侵蚀恶化甚至降解等缺陷，严重影响木材的使用范围和使用寿命。为了克服木材吸水产生的缺陷，提出了一种由微纳米结构的粗糙度和低表面自由能组成的超疏水涂层的制备，以提高木材的疏水性。

本文采用一种简便有效的方法，在木单板表面制备了具有超疏水和抗菌功能的铜涂层。通过将盐酸多巴胺溶解在 Tris 溶液（pH 8.5）中制备盐酸多巴胺（DA）溶液（0.01 M）。然后将清洁过的木材样品放入新鲜获得的 DA 溶液中，并在 25℃下搅拌（400 rpm）24 小时。得到的样品漂洗并在 60℃的温度下干燥后，得到涂有聚多巴胺（PDA）的木材（wood @ PDA）。然后将 wood @ PDA 浸入由五水合硫酸铜（0.05 M），乙二胺四乙酸二钠（0.05 M），硼酸（0.1 M）和二甲基胺硼烷络合物（DMBA）（0.1 M）组成的溶液中。用氢氧化钠溶液（1M）调节溶液（pH 7.0）。反应过程在 30℃下持续 2 h。使用乙醇和水冲洗后，制得具有 Cu 涂层的 wood @ PDA-Cu（wood @ PDA-Cu），然后将其在烘箱中干燥。最后，通过将 0.5mL 的 FAS-17 溶解在 100mL 的乙醇中，获得 0.5%（V / V）的三甲氧基十七氟癸基硅烷（FAS-17）溶液。将 Wood @ PDA-Cu 放入溶液中，在 25℃下搅拌 5 h，然后干燥。FAS-17 修饰后的 wood @ PDA-Cu 标记为 wood @ PDA-Cu-F。

通过扫描电子显微镜（SEM）观察木材样品的表面结构。能量色散 X 射线光谱法（EDS）用于表征木材表面的表面组成和元素分布。傅里叶变换红外光谱（FT-IR）用于评估木材表面的化学基团。木材表面的结晶相通过 X 射线衍射（XRD）证实。使用 X 射线光电子能谱（XPS）观察了木材表面的化学元素。利用接触角系统在环境温度（25℃）下从五个测量结果的平均值测量木材样品的表面润湿性。通过抑菌环法进行抗菌测试，使用大肠杆菌（ATCC 25922，革兰氏阴性细菌）和金黄色葡萄球菌（ATCC 25923，革兰氏阳性细菌）评估木材样品的抗菌活性。

通过多巴胺的自聚合，铜纳米颗粒的化学沉积以及使用氟硅烷的疏水改性，可以制备具有超疏水和抗菌性能的木单板。所获得的铜涂层的水接触角和滚动角分别达到 155.7°和 4°。同时，所制备的涂层显示出对不同 pH 值的酸碱溶液，不同温度老化和机械损伤的耐久性，并且还表现出良好的自清洁能力。此外，超疏水涂层成功显示出优异的抗菌能力。抗菌测试的结果表明，针对大肠杆菌和金黄色葡萄球菌的抑菌环的直径分别达到 7.6mm 和 5.6mm。这项工作为赋予木单板超疏水和抗菌性能，促进其多功能应用提供了一种新颖的方法。

关键词：木单板；铜纳米粒子；聚多巴胺；超疏水；抗菌活性

Superhydrophobic and antibacterial wood enabled by polydopamine-assisted decoration of copper nanoparticles

Xinpeng Duan, Shumin Liu, Erzhuo Huang, Xiaoyuan Shen, Zhe Wang*, Song Li*, Chunde Jin*

（School of Engineering, Zhejiang A & F University, Lin'an, 311300, PR China）

Abstract: As a natural renewable resource, wood has played an important role in social economic construction and

human basic living environment. As the main components of wood, cellulose and hemicellulose possess a large number of hydrophilic groups, which leads to the moisture and water absorption of wood. After absorbing water, wood exhibits some defects such as dimensional deformation, deterioration of bacterial erosion and even degradation, which seriously affects use range and service life of wood. In order to overcome the defects generated by water absorption of wood, the preparation of superhydrophobic coatings composed of roughness of micro-nano structure and low surface free energy is proposed to improve the hydrophobicity of wood.

In this paper, a Cu coating owned superhydrophobic and antibacterial capabilities on wood veneer was fabricated by a facile and valid method. Dopamine hydrochloride (DA) solution (0.01 M) was prepared through dissolving DA in Tris solution (pH 8.5). Then the cleaned wood samples were put into the freshly obtained DA solution and stirred (400 rpm) at 25 ℃ for 24 h. The polydopamine (PDA) coated wood (wood@PDA) was obtained after being rinsed and dried at a temperature of 60 ℃. Then the wood@PDA was immersed in a solution composed of CuSO4·5H2O (0.05 M), EDTA·2Na (0.05 M), H3BO3 (0.1 M) and borane dimethyiamine complex (DMBA) (0.1 M). The solution (pH 7.0) was adjusted by NaOH solution (1 M). The reaction process lasted 2 h at 30 ℃. The wood@PDA with Cu coating (wood@PDA-Cu) was fabricated after being rinsed using ethanol and water, then the wood@PDA-Cu was dried in an oven. Finally, 0.5 % (V/V) trimethoxy(1H, 1H, 2H, 2H-heptadecafluorodecyl)silane (FAS-17) solution was obtained by dissolving 0.5 mL of FAS-17 in 100 mL of ethanol. The wood@PDA-Cu was placed into the solution to be stirred at 25 ℃ for 5 h and dried. The modified wood@PDA-Cu by FAS-17 was marked as wood@PDA-Cu-F. The surface structures of wood samples were observed by scanning electron microscopy (SEM). Energy dispersive X-ray spectrometry (EDS) was utilized to characterize the surface composition and element distribution of wood surfaces. Fourier transform infrared spectroscopy (FT-IR) was used to evaluate the chemical groups of wood surfaces. The crystalline phase of wood surfaces was manifested via X-ray diffraction (XRD). The chemical elements of wood surfaces were observed using X-ray photoelectron spectroscopy (XPS). A contact angle system was utilized to measure surface wettabilities of wood samples with the average values from five measuring results at ambient temperature (25 ℃). The antibacterial test was executed by the bacteria-inhibiting ring method, Escherichia coli (ATCC 25922, Gram-negative bacterium) and Staphylococcus aureus (ATCC 25923, Gram-positive bacterium) were used to evaluate the antimicrobial activities of wood samples.The wood veneer with superhydrophobic and antibacterial properties was prepared by self-polymerization of dopamine, chemical deposition of Cu nanoparticles, and hydrophobic modification using fluorosilane. The water contact angle and sliding angle of obtained Cu coating reached 155.7° and 4°, respectively. Meanwhile, the as-prepared coating showed resistance to acid or base solutions with different pH values, different temperatures aging and mechanical damages, and also displayed a good self-cleaning ability. In addition, the superhydrophobic coating successfully revealed excellent antibacterial abilities. The consequences of antibacterial tests displayed that the diameter of bacteriostatic ring against E. coli and S. aureus reached 7.6mm and 5.6 mm, respectively. This work supplied a novel way to endow the superhydrophobic and antibacterial properties on wood veneer, and promote its multifunction application.

Keywords: Wood veneer, Cu nanoparticles, Polydopamine, Superhydrophobic, Antibacterial activity

仿生木材结构穿孔纤维板吸声性能

贾世芳 刘静怡 林贤铣 孙伟圣 郭玺

（浙江农林大学工程学院，杭州 311300）

摘要：以中密度纤维板为基材，通过设计穿孔结构及打孔方式，达到拓宽木质穿孔板吸声频带和提高声学性能的目的。利用分层加工工艺制备了带侧孔结构的穿孔纤维板，采用阻抗管传递函数法对穿孔纤维板吸声性能进行了测试。通过正交试验方法，研究了主孔直径、穿孔率、倾斜角度对穿孔纤维板吸声性能的影响，并获得了较优的制备工艺，随后利用控制变量法研究了侧孔深度对穿孔纤维板吸声性能的影响。试验结果表明：影响穿孔纤维板吸声系数峰值的因素主次顺序为倾斜角度＞主孔直径＞穿孔率；穿孔纤维板获得良好吸声系数峰值的优选工艺参数为主孔直径 3 mm、穿孔率 3.14%、倾斜角度 30°；增加侧孔结构后，穿孔纤维板在中低频、中高频均表现出良好的吸声特性；侧孔深度对穿孔纤维板中高频共振频率和吸声系数影响较大，当侧孔深度为 4 mm 时，仿生木材结构穿孔纤维板在中高频段共振频率为 3 632 Hz，吸声系数峰值可达 0.67。本研究为穿孔吸声板的结构设计提供参考，解决了复杂孔型加工的技术难题，对多频段吸声木质穿孔板的工业化应用具有重要意义。

关键词：吸声；穿孔纤维板；仿生；木材结构；侧孔

Sound absorption performance of bionic wood structure perforated fiberboard

JIA Shifang, LIU Jingyi, LIN Xianxian, SUN Weisheng, GUO Xi

（School of Engineering,Zhejiang A&F University,Hangzhou 311300,China）

Abstract: Noise pollution has become a widespread topic as same as water pollution, air pollution and waste pollution. So the prevention and control of noise by using sound absorption material has attracted lots of researchers, this material can absorb sound waves within different frequency band and then decrease the damage of noise. Wood perforated panel is a kind of resonant sound absorbing structural material, but the existing wood perforated panel just has absorption effect on the low frequency which can not satisfy the demand of some special acoustic environment. So the research of wooden perforated board with a multi-band sound-absorbing function has a high value. In this study, perforated sound absorption panel was prepared with the inspiration of wood multilevel pore structure and using the medium density fiberboard as the matrix. The sound absorption broadband and acoustic intensity performance of the wood perforated panel were greatly improved. The complex hole structure of perforated fiberboard was carried out by using layered processing technology and the sound absorption properties of the perforated fiberboard were tested by the impedance tube transfer function method. The effects of main hole diameter, perforation rate and inclined angle on the sound absorption properties of perforated fiberboard were investigated by the orthogonal test method, and the better preparation process was obtained. Then the influence of side hole depth on the sound absorption properties of perforated fiberboard was studied by using the control variable method. The results showed that: the order for affecting the peak sound absorption coefficient of the perforated fiberboard were inclined angle > diameter of the main hole > perforation rate; the preferred processing parameters of perforated fiberboard were 3 mm hole diameter, 3.14% perforation rate and 30 °inclined angle; the sound absorption properties of perforated fiberboard at the low and medium high frequencies were both improved after the addition of side hole; the depth of the side hole had a great influence on the sound absorption property of perforated fiberboard at high frequency resonance frequency; three resonance absorption peaks were observed over the whole frequency band (64~6 300 Hz) when the side hole was deeper than 1mm. The bionic perforated fiberboard showed the best sound absorption coefficient (0.67) at 3 632 Hz when the side hole depth was 4 mm. This study could provide a novel perforated sound absorbing panel by using layered processing method which was important for realizing the industrial production of wood perforated panel.

Keywords: sound absorption, perforated fiberboard, bionic, wood structure, side hole

热致变形的柔性相变储能木材的制备与性能研究

林贤铣[1]，贾世芳[1]，刘静怡[1]，李小科[2]，郭玺[1]*，孙伟圣[1]*

1 浙江农林大学工程学院，杭州 311300，中国；

2 湖州衡鼎产品检测中心，湖州 313000，中国；

摘要：随着能源危机的日益严重，相变储能材料作为一种新型节能材料引起了学者们的广泛关注。 本文以具有高孔隙率的脱木素木材为柔性基底，聚氨酯为相变材料，石墨烯为导热材料，通过一步真空浸渍法，制备热致变形的柔性相变储能木材。通过电子扫描显微镜（SEM）和傅立叶变换红外吸收光谱仪（FTIR）对复合相变材料的微观形貌和化学结构进行了表征，同时利用差式扫描量热仪（DSC），热重分析仪（TG）和激光导热仪对其热性能进行了研究分析。结果表明：（1）在相变过程中，柔性相变储能木材展现了良好的柔韧性；（2）石墨烯与聚氨酯成功进入木材空隙内部，木材的孔隙得到了良好的填充。(3)复合材料的最大结晶潜热为 70.26 J/g，熔融潜热为 64.29 J/g，最高熔融温度为 36.3 ℃，最低结晶温度为 28.1℃；（4）石墨烯的添加极大的提升了复合材料的导热系数， 最大导热系数为 0.417 ($W*m^{-1}*K^{-1}$)，较素材提升了 414%。同时，极大的提高了复合材料的吸光能力，有助于改善其光热转换效率。本文所制备的热致变形的柔性相变储能木材具有优异的柔韧性、较高的导热系数以及良好的热能存储能力，为新型建筑节能材料以及可穿戴储能材料的开发、应用提供了参考。

关键词：木材；相变储能材料；热能存储；热致变形

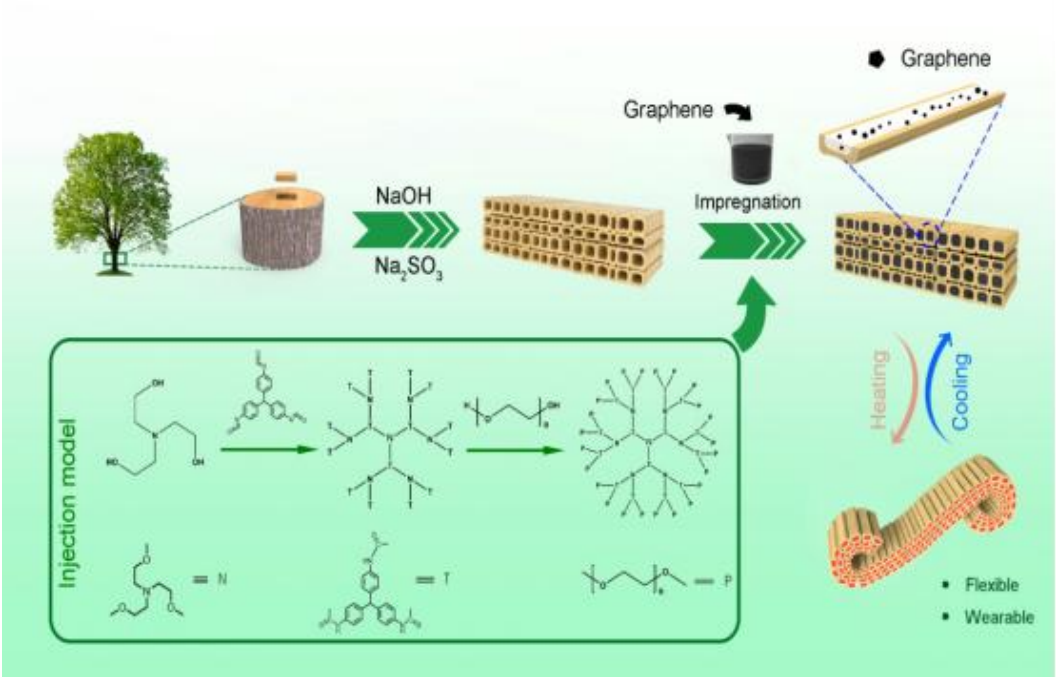

图 1 热致变形的柔性相变储能木材的制备

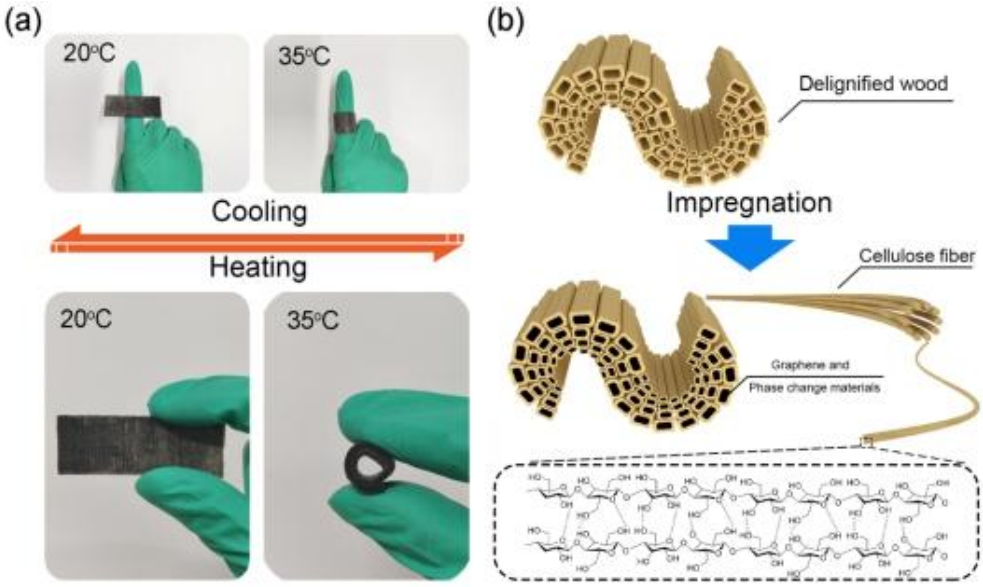

图 2 相变储能木材的热致变形过程

Thermally induced flexible wood based on phase change materials for thermal energy storage and management

Xianxian Lin [a], ShifangJia [a], Jingyi Liu [a], Xiaoke Li [b], Xi Guo* [a], Weisheng Sun* [a]

[a]College of engineering, Zhejiang agricultural and Forestry University, Hangzhou 311300, China

[b]Huzhou hending products testing center, Huzhou 313000, China

Abstract： The applications of composite phase change materials were limited due to their poor energy utilization efficiency, low thermal conductivity and strong rigidity. In this work, thermally induced flexible wood based on phase change material was fabricated by impregnating delignified wood (DW) with graphene and a novel kind of hyperbranched polyurethane. The wood composite showed excellent softness and flexibility during the heating process of hyperbranched polyurethane. It also displayed suitable phase change temperature (28.1 ^{o}C and 36.3 ^{o}C) and acceptable latent heat (64.29 J/g and 70.26 J/g). Thermal conductivity of the composite reached to 0.417 (W*m^{-1}K^{-1}) after adding graphene, which enhanced approximately 414 % than pure wood. The light-harvest efficiency of the composite was also improved after the addition of graphene. Therefore, the thermally induced flexible wood based on phase change material has great potential for building energy conservation and wearable energy storage devices due to its excellent flexibility, high thermal energy storage capacity and outstanding temperature regulating performance.

Keyword: wood; phase change material; thermal energy storage; thermally induced flexibility

木材表面 Pt 负载的 NiFe-LDH 纳米片的合成用于气态甲醛降解

蔡泰龙[1] 王喆[1*] 孙庆丰[1*]

（浙江农林大学工程学院）

摘要：随着美观、舒适、智能的室内设施的全面发展，各种新材料涌入室内，使室内环境污染日益严重。气态甲醛长时间污染室内空气，从而引起眼鼻刺激、头痛、慢性支气管炎甚至癌症等各种问题。传统的去除气态甲醛的方法往往伴随着高能耗和二次污染。本研究通过水热反应和浸渍-化学还原的方法，成功地研制了一种以 Pt 负载 NiFe-LDH 纳米片装饰的新型木单板基复合材料。NiFe-LDH 纳米片作为吸附剂可以通过大量的羟基捕获甲醛分子。Pt 纳米颗粒作为催化中心均匀分布在 NiFe-LDH 表面，激发固定在 NiFe-LDH 上的 O 原子并吸附氧，进一步攻击吸附的甲醛分子生成 CO_2 和 H_2O。木单板不仅使催化剂具有良好的分散性，增加了催化剂的活性面积，而且为反应物和产物提供了便捷的通道。该合成木单板复合材料在模拟室温暗环境下具有良好的催化活性，当初始浓度为 0.2 mg m^{-3}， 30 min 内可有效降解几乎所有的气态甲醛，10 次循环后仍能保持≥ 97%的高催化活性。本文提出了一种可行的节能环保木单板基复合材料在室温下有效降解气态甲醛，作为一种有前景的装饰材料在室内空气净化中发挥重要作用。

关键词：木材；NiFe-LDH；甲醛；催化氧化；室温

Synthesis of Pt-loaded NiFe-LDH Nanosheets on Wood Surface for Gaseous Formaldehyde Degradation

Tailong Cai[1] Zhe Wang[1*] Qingfeng Sun[1*]

（School of Engineering, Zhejiang A & F University）

Abstract: With the comprehensive development of beautiful, comfortable and intelligent indoor facilities, various new materials are flooding into the interior, making indoor environmental pollution increasingly serious. Gaseous formaldehyde can continually release formaldehyde to pollute the indoor air in a long time, thus causing various troubles such as eye and nasal irritation, headaches, chronic bronchitis, and even cancers. Traditional methods of removing gaseous formaldehyde are often associated with high energy consumption and secondary pollution. In this study, a new wood veneer based composite decorated with Pt-loaded NiFe-LDH nanosheets is successfully developed by hydrothermal reaction and impregnation-chemical reduction. NiFe-LDH nanosheets as an adsorbent can capture formaldehyde molecules through abundant hydroxyl groups. Pt nanoparticles as catalytic centers are evenly distributed on the surface of NiFe-LDH to excite the O atoms fixed to NiFe-LDH and absorbed oxygen, which will further attack the absorbed formaldehyde molecules to generate CO_2 and H_2O. And the wood veneer not only increases the active area of the catalyst by endowing it with good dispersion, but also provides convenient channels for reactants and products. In a simulated dark environment at room temperature, this synthetic wood veneer based composite exhibits admirable catalytic activity, which can effectively degrade almost all gaseous formaldehyde with the initial concentration of 0.2 mg m-3 in 30 min and maintain a high catalytic activity of ≥ 97% after ten cycles. This paper presents a feasible strategy of synthesizing an energy-efficient and ecofriendly wood veneer based composite for efficient gaseous formaldehyde degradation at room temperature, which may play an important role in indoor air purification as a promising decorative material.

Keywords: wood, NiFe-LDH, formaldehyde, catalytic oxidation, room temperature